
PhD Thesis

# TEST PARTICLES AND ELECTROMAGNETIC FIELDS IN GRAVITATIONAL WAVE SPACETIMES

PhD Student: MARIA HANEY
Supervisor: Dr. Donato Bini

UNIVERSITÀ DEGLI STUDI DI ROMA "SAPIENZA"

Rome, October 2013

CONTENTS

# 1. INTRODUCTION

The production of gravitational waves as well as of electromagnetic pulses is expected to occur in many violent astrophysical processes, like the merging of compact binaries and high energy phenomena involving strong magnetic fields and accelerating sources of the electromagnetic field. Gravitational and electromagnetic waves are also believed to interact in a variety of ways. There are many exact solutions of Einstein's field equations that describe colliding plane gravitational and electromagnetic waves on a flat Minkowski background [1]. Furthermore, several studies in the literature have shown how gravitational radiation affects the propagation of electromagnetic signals by modifying their direction, amplitude, wavelength and polarization either in vacuum or in the presence of conductive plasmas, leading also to the possibility of resonances between gravitational and electromagnetic sources which could be used either as more efficient gravity-wave detection methods or as a general relativistic mechanism of amplifying large-scale magnetic fields (see, e.g., [2] and references therein).

In the present work we consider the propagation of massive neutral test particles and electromagnetic waves on the background of radiation fields of finite duration that are generated either by an exact gravitational wave or an exact electromagnetic wave in the framework of general relativity.

The features of the scattering of massive particles are analyzed and compared; depending on the nature of the background the particles emerging from the interaction will be scattered along geodesic world lines or will experience a deviation from geodesic motion due to the application of an external radiation force.

To study light scattering by these radiation fields we develop the optical

medium analogy of the associated background, allowing for a comparison of the distinct optical properties of the equivalent optical media. We are able to identify certain detectable observational consequences arising from our analysis, e.g., the deflection and delay of photon beams, the response of a Michelson interferometer to gravitational waves beyond the linear approximation, etc.

Finally we discuss some interesting physical effects of light propagation in the background of colliding strong gravitational waves. Given the complexity of the nonlinear interaction of two gravitational waves in the framework of general relativity, the optical medium analogy of the curved background proves a helpful tool to analyze the propagation of electromagnetic waves in the collision region of these spacetimes. [1]

In order to introduce the problem of radiation fields generated by gravitational or electromagnetic waves in the framework of general relativity, we at first briefly outline the linearized theory of gravitational waves as an approximative solution to Einstein's field equations for weak fields and slow motion in Chapter 2, and then consider the fully nonlinear theory of general relativity and introduce certain exact solutions of the field equations that clearly represent gravitational waves. Here we summarize a more detailed discussion of the problem of exact gravitational waves to be found in "Gravitation" by Misner, Thorne and Wheeler [3], and other textbooks [4, 5, 6]. The background curvature created by electromagnetic waves in four-dimensional spacetime is also discussed in Chapter 2. In Chapter 3 we present the classical Poynting-Robertson effect which describes a deviation from geodesic test particle motion due to the interaction of the particle with a radiation field of electromagnetic nature; we then give a short overview of the recent generalization of the Poynting-Robertson effect to a general relativistic formalism, which is the approach that we will later use to model the scattering of massive test particles by a radiation field in the curved background generated by an

[1] Unless otherwise specified, hereafter units were used such that $G = 1$ and $c = 1$, $G$ being the Newtonian constant and $c$ the speed of light in vacuum. Greek indices run from 0 to 3 and Latin indices run from 1 to 3. The metric signature is chosen to be +2.

electromagnetic wave. Finally, in Chapter 4, we discuss the optical medium analogy of an arbitrary gravitational field which we will later employ as a useful method to study light propagation on a curved background.

# 2. EXACT GRAVITATIONAL WAVE SPACETIMES

The theory of general relativity understands gravitation as a curvature of four-dimensional spacetime. It is implied in general relativity that a time-dependent distribution of mass causes local changes of the gravitational field that travel away from the source at the speed of light. In analogy to electrodynamics, these freely propagating variations of spacetime geometry are called gravitational waves. The structural changes in local geometry during the passage of a gravitational wave should theoretically be measurable by considering the separation of test masses. However, due to the rigidity of spacetime these structural changes are so small that only compact cosmic objects and processes with high accelerations are considered as observable sources of gravitational waves. These sources include supernovae, coalescing compact binary systems of neutron stars and/or black holes, rotating neutron stars, supermassive black holes and the cosmic background radiation. Since gravitational waves, in contrast to electromagnetic waves, are virtually unaffected by the presence of matter between the source and the observer, gravitational wave astronomy is expected to open a new window to the universe.

The dynamic coupling of matter and spacetime geometry is central to general relativity. On the one hand, matter curves the surrounding spacetime; on the other hand, the geometry of a spacetime region determines the motion of matter contained within. Accordingly, general relativity doesn't understand gravitation as a force, but rather as an aspect of a four-dimensional spacetime continuum. As a consequence of the dynamic coupling of matter and spacetime in general relativity all inertial frames are equivalent; due to the dynamical geometry coordinate systems are only events in four-dimensional spacetime. To formulate the coupling of spacetime geometry to the sources

contained within, we require equations which are invariant to the choice of any coordinate system and which, for weak sources and nonrelativistic velocities, recall the Newtonian theory of gravity in a flat Minkowski spacetime. The most general equations satisfying above requirements are the so-called Einstein's field equations

$$G_{\mu\nu} = R_{\mu\nu} - \frac{1}{2} R g_{\mu\nu} = 8\pi T_{\mu\nu}\,, \qquad R = R^{\mu}_{\mu}\,. \tag{2.1}$$

They couple the spacetime geometry represented by the Einstein curvature tensor $G_{\mu\nu}$ to the energy-momentum tensor $T_{\mu\nu}$ which expresses the distribution of energy and matter in a four-dimensional spacetime, analogous to the distribution of mass in the Newtonian theory of gravitation. $R_{\mu\nu}$ denotes the Ricci curvature tensor that is constructed from the components of the metric tensor $g_{\mu\nu}$ of the curved spacetime; $R$ is the so-called scalar curvature. At first sight Einstein's field equations are a system of 16 coupled nonlinear differential equations; with the algebraic symmetries of the curvature tensor the number of degrees of freedom is reduced to 10. By taking into account also differential symmetries of the curvature tensor, the (contracted) Bianchi identities

$$G^{\mu\nu}_{\ ;\nu} \equiv 0\,, \tag{2.2}$$

the field equations can finally be reduced to a set of 6 independent partial differential equations, coupling spacetime and matter. However, even for known initial conditions the general equation (2.1) does not permit an unambiguous determination of the spacetime geometry for a given distribution of energy and matter. (The under-determined nature of the system of equations thus ensures the free choice of coordinates.) An exact solution of the full set of Einstein's field equations is possible only for special, usually highly symmetric cases.

## *2.1 The linearized theory of gravitational waves*

In the limit of weak gravitational fields, i.e., when observing the gravitational field at a great distance from the source, an approximate solution suffices.

The linearized theory of gravitation for weak fields is employed to obtain field equations which resemble the electromagnetic wave equations in flat Minkowski space. In the weak-field limit a local spacetime curvature is introduced as a first-order metric perturbation $h_{\mu\nu}$ of the flat background $\eta_{\mu\nu}$, so that

$$g_{\mu\nu} = \eta_{\mu\nu} + h_{\mu\nu}\,, \qquad |h_{\mu\nu}| \ll 1\,, \tag{2.3}$$

leads to the Ricci tensor

$$\begin{aligned} R_{\mu\nu} &= R_{\mu\nu} - \frac{R}{2}\eta_{\mu\nu} \\ &= \frac{1}{2}(h_{\mu\nu}{}^{,\alpha}{}_{,\alpha} + h^{\alpha}{}_{\alpha,\mu\nu} - h^{\alpha}{}_{\nu,\mu\alpha} - h^{\alpha}{}_{\mu,\nu\alpha} \\ &\quad -\eta_{\mu\nu}h^{\beta}{}_{\beta}{}^{,\alpha}{}_{,\alpha} + \eta_{\mu\nu}h^{\alpha\beta}{}_{,\alpha\beta}) + \mathcal{O}(h^2)\,, \end{aligned} \tag{2.4}$$

where all nonlinear perturbation terms resulting from the metric tensor have been neglected and where all indices are raised and lowered with $\eta_{\mu\nu}$. For simplification purposes we introduce the notation

$$\bar{h}_{\mu\nu} = h_{\mu\nu} - \frac{1}{2}\eta_{\mu\nu}h\,, \qquad \bar{h}^{\mu}_{\mu} = -h^{\mu}_{\mu}\,, \tag{2.5}$$

and find the linearized nonvacuum field equations

$$(\bar{h}_{\mu\nu}{}^{,\alpha}{}_{,\alpha} + \eta_{\mu\nu}\bar{h}^{\alpha\beta}{}_{,\alpha\beta} - \bar{h}^{\alpha}{}_{\nu,\mu\alpha} - \bar{h}^{\alpha}{}_{\mu,\nu\alpha}) = -16\pi T_{\mu\nu}\,. \tag{2.6}$$

By choosing a suitable gauge (i.e., a coordinate transformation) that satisfies a gauge condition $\bar{h}^{\mu\nu}{}_{,\nu} = 0$ (analogous to the Lorentz gauge $A^{\mu}{}_{,\mu=0}$ in the theory of electromagnetism) some of the terms of the field equations can be made to disappear and (2.6) reduces to

$$\Box\bar{h}_{\mu\nu} = \bar{h}_{\mu\nu,\ \alpha}{}^{\alpha} = -16\pi T_{\mu\nu}\,, \qquad \bar{h}^{\mu\nu}{}_{,\nu} = 0\,, \tag{2.7}$$

representing ordinary inhomogeneous wave equations. This linearized approximation to the system of Einstein's field equations is already decoupled.

Further infinitesimal coordinate transformations and gauge changes

$$x'^{\mu} = x^{\mu} + \xi^{\mu}(x^{\nu})\,, \qquad \bar{h}'_{\mu\nu} = \bar{h}_{\mu\nu} - \xi_{\mu,\ \nu} - \xi_{\nu,\ \mu} + \eta_{\mu\nu}\xi^{\alpha}{}_{,\alpha}\,, \tag{2.8}$$

preserve the gauge condition in (2.7) if the sourceless wave equation

$$\Box\xi_{\mu} = \xi_{\mu,\ \alpha}{}^{\alpha} = 0\,, \tag{2.9}$$

is satisfied.

For a spacetime without sources the field equations of linearized theory (2.7) reduce to the wave equations

$$\Box\bar{h}_{\mu\nu} = 0\,, \qquad \bar{h}^{\mu\nu}{}_{,\nu} = 0\,, \tag{2.10}$$

of a propagating vacuum gravitational field. The gravitational wave is connected to the source of gravitational radiation through the inhomogeneous wave equations (2.7) whose general retarded solution

$$\bar{h}_{\mu\nu}(\mathbf{x}, t) = 4\int_{V} \frac{T_{\mu\nu}(\mathbf{x}', t - |\mathbf{x} - \mathbf{x}'|/c)}{|\mathbf{x} - \mathbf{x}'|} d^3x'\,, \tag{2.11}$$

describes gravitational waves radiated by isolated source of stress-energy $T_{\mu}\nu$. (Observed in the far-field of slow moving sources the gravitational waves represent radiation generated by a mass quadrupole.) For more details on the linearized theory of gravitational waves as well as their generation and detection, see e.g. [7].

## 2.2 Nonlinear effects in gravitational waves

The linearized theory of gravitational waves describes only local changes in spacetime geometry, it does not take into account the large-scale background curvature. In the full nonlinear theory of general relativity the energy and momentum carried by a gravitational wave contribute to the curvature of the background spacetime. Although it does not appear as a source term in the field equations (the gravitational wave still has to satisfy vacuum equations),

the stress-energy carried by the wave does enter the physical picture through the nonlinearity of the full vacuum equations.

Other nonlinear effects in gravitational waves not taken into account by the linearized theory are related to the source of the wave and to the presence of matter in the universe.

The energy of the gravitational wave source decreases as radiation energy is carried away by the source, resulting in a dampening of the gravitational wave which makes an exactly periodic gravitational wave signal impossible. (Consider, f.e., the decreasing orbital period observed in double pulsars due to the energy loss through gravitational radiation, which is regarded as an indirect detection of gravitational waves.) A presence of matter between the gravitational wave source and the observer results in local curvatures and subsequently influences the shape of the wave fronts and its wavelength (gravitational redshift). Such local curvatures (or even the background curvature induced by the wave itself) cause the wave to backscatter and produce "tails" behind the propagating wave.[1]

Beyond the linearized theory of gravitational waves a variety of approximation methods have been developed and applied to physical scenarios in which nonlinear effects cannot be neglected; such as the post-Newtonian (PN) expansion employed by gravitational wave astronomy to describe deviation from flat background geometry due to a slowly moving, weakly self-gravitating source of gravitational radiation.

In the following section, we return to the fully nonlinear theory of general relativity and consider certain exact solutions of Einstein's field equations that clearly represent gravitational waves.

It has to be noted that any exact gravitational wave solution to Einstein's field equations in a closed mathematical form will be highly idealized (characterized, e.g., by completely flat wavefronts) and that these mathematically exact solutions can't be connected to a particular source distribution.

[1] A "tail" denotes a region behind the gravitational wave for which the wave region induces an ordinary nonradiative gravitational field.

## 2.3 Exact plane gravitational wave solutions and the sandwich wave scenario

Exact solutions of Einstein's field equations which admit a constant null vector field $\mathbf{k}$ with $k_{a;b} = 0$ are called *pp*-waves; these spacetimes represent plane-fronted gravitational waves with parallel rays. They were discovered by Brinkmann in 1925 [8] and are a subclass of Kundt's class of exact solutions which are characterized by a nonexpanding, shear- and twist-free null congruence $\mathbf{k}$ [5]. The metric of *pp*-wave spacetimes can be written as [5, 10]

$$\mathrm{d}s^2 = 2\mathrm{d}\zeta\mathrm{d}\bar{\zeta} - 2\mathrm{d}u\mathrm{d}\phi - \left(f + \bar{f}\right)\mathrm{d}u^2\,, \quad f = f\left(u,\zeta\right)\,, \quad \bar{f} = \bar{f}\left(u,\bar{\zeta}\right)\,, \tag{2.12}$$

where $f$ is an arbitrary function of $u$ and analytic in $\zeta$. These solutions are either of Petrov type N (with one multiple principal null direction $\mathbf{k}$), or (in the limit $f_{,\zeta\zeta} = 0$) conformally flat.

The simplest solution 2.12 representing homogeneous *pp*-waves is given by $f(u,\zeta) = d(u)\zeta^2$. With the transformation [9, 10]

$$\zeta = \frac{Fx + iGy}{\sqrt{2}}\,, \quad \phi = \frac{t + z + FF'x^2 + GG'y^2}{2}\,, \quad u = t - z\,, \tag{2.13}$$

the metric of these "plane" gravitational wave spacetimes

$$\mathrm{d}s^2 = -2\mathrm{d}u\mathrm{d}v + F^2\mathrm{d}x^2 + G^2\mathrm{d}y^2 \tag{2.14}$$

is characterized by the two real functions $F = F(u)$ and $G = G(u)$, which are solutions to

$$F'' + d(u)F = 0\,, \qquad G'' - d(u)G = 0\,, \tag{2.15}$$

where the prime denotes a differentiation with respect to $u$.

The relative motion of test particles in $x$ and $y$ direction is then solely determined by $F$ and $G$, respectively. The motion of test particles in $z$ direction is aligned with the wave's direction of propagation, and the plane gravitational wave is transversal. The coordinate $u$ is representing a re-

tarded time, whereas the arbitrary function $d(u)$ describes the profile of the wave. For shock waves this profile is characterized by a step-function; in the case of impulsive waves the (distributional) profile is proportional to a delta-function. In both cases the metric functions $F(u)$ and $G(u)$ may still be smooth, thereby ensuring a continuity of relative test particle motion in these gravitational wave spacetimes.

In the sandwich wave scenario, the gravitational wave is considered to be sandwiched in a finite region of $u$ between two flat Minkowski regions before and after the passage of the wave. A standard example of such a sandwich wave is characterized by a "square" profile [11]

$$d(u) = \begin{cases} 0 & u < 0 \\ a^{-2} & 0 \leq u \leq a^2 \\ 0 & u > a^2 \end{cases} \tag{2.16}$$

where $1/a$ represents the overall curvature of the wave region. There also exist other more general sandwich wave solutions which do not exhibit a stationary $d(u)$ in the wave region. One such nonstandard sandwich wave has a "wedge" profile of the form [10]

$$d(u) = \begin{cases} 0 & u \leq -a \\ \frac{b}{a}\,(a+u) & -a \leq u \leq 0 \\ \frac{b}{a}\,(a-u) & 0 \leq u \leq a \\ 0 & u \geq a \end{cases} \tag{2.17}$$

whith real, positive constants $a$ and $b$. Other possible nonstandard sandwich waves are those with a nonsymmetric "saw" profile or an "asymptotic profile" (where the regions before and after the passage of the wave are flat only asymptotically, for $u \to \pm\infty$). For more details on nonstandard sandwich waves see [10].

In the following we will limit our discussion to sandwich waves with a standard (stationary) profile $d(u)$ in the wave region. In particular, we want to consider one possible class of homogeneous *pp*-wave solutions (2.14) that is characterized by the line element [12, 13, 3]

$$\mathrm{d}s^2 = -\mathrm{d}u\mathrm{d}v + L_B^2 \left(e^{2\beta_W}\mathrm{d}x^2 + e^{-2\beta_W}\mathrm{d}y^2\right) , \tag{2.18}$$

in a null coordinate system $(u, v, x, y)$, where the null coordinates $u$ and $v$ are related to standard temporal and spatial coordinates $t$ and $z$ by

$$u = t - z\,, \qquad v = t + z\,. \tag{2.19}$$

The metric functions $L_B = L_B(u)$ and $\beta_W = \beta_W(u)$ describe the profile of the gravitational pulse: $\beta_W(u)$ is the so-called "wave factor" associated with the short-scale ripples of the gravitational wave, whereas $L_B(u)$ is called the "background factor" connected to the large-scale bending of the background geometry by the effective stress-energy of the wave. Both metric functions are determined by the field equations. In the null coordinate system considered only one component of the Ricci tensor is nonzero,

$$R_{uu} = -\frac{2}{L_B}\left[L_B'' + (\beta_W{}')^2 L_B\right] , \tag{2.20}$$

where a prime denotes differentiation with respect to $u$. Einstein's field equations in vacuum reduce to the single equation

$$L_B'' + (\beta_W{}')^2 L_B = 0\,, \tag{2.21}$$

thereby relating the curvature of the background to the wave.

For the weak-field approximation (the second-order) $(\beta_W{}')^2$ vanishes and the field equation is $L_B'' = 0$. The weak-field limit of the exact gravitational wave solution (2.18) is thus characterized by the spacetime metric

$$\mathrm{d}s^2 = -\mathrm{d}u\mathrm{d}v + [2 + \beta_W(u)]\,\mathrm{d}x^2 + [2 - \beta_W(u)]\,\mathrm{d}y^2\,, \tag{2.22}$$

and the solution describes a plane wave with a single (+) polarization state propagating in $z$ direction.

The metric (2.18) of an exact gravitational wave pulse of finite duration $2T$ is now extended to the spacetime regions before the arrival of the pulse and after its passage. The solution is characterized by an arbitrary wave

factor $\beta_W$ that is constrained by $|\beta_W{}'| \ll \frac{1}{T}$ throughout the pulse. Before the arrival of the gravitational wave ($u < -T$) the wave and background factors $\beta_W$ and $L_B$ have values of 0 and 1, respectively, and the metric is given by

$$\mathrm{d}s^2 = -\mathrm{d}u\mathrm{d}v + \mathrm{d}x^2 + \mathrm{d}y^2\,, \tag{2.23}$$

i.e., the spacetime is flat. After the passage of the wave ($u > T$) the wave factor $\beta_W$ is again 0, but the background factor is now a linear function in $u$, namely $L_B = 1 - \frac{u}{u_f}$, where the constant $u_f$ is defined by

$$u_f = \frac{1 + \mathcal{O}\left[\beta_W{}'T\right]^2}{\int_{-T}^{T}(\beta_W{}')^2\mathrm{d}u}\,, \qquad |\beta_W{}'| \ll \frac{1}{T}\,. \tag{2.24}$$

The extended metric after the passage of the wave

$$\mathrm{d}s^2 = -\mathrm{d}u\mathrm{d}v + \left(1 - \frac{u}{u_f}\right)^2\left(\mathrm{d}x^2 + \mathrm{d}y^2\right)\,, \tag{2.25}$$

clearly has a spacetime singularity at $u = u_f > T$. (At $u_f$ we the background factor $L_B = 0$, therefore $g_{xx} = g_{yy} = 0$.) This singularity is only a coordinate singularity and not physical, since the components of the Riemann tensor associated with the metric of the pulse (2.18)

$$R^x_{uxu} = \frac{1}{2}R_{uu} - \beta_W{}'' - 2\frac{L_B{}'}{L_B}\beta_W{}'\,, \qquad R^y_{uyu} = R_{uu} - R^x_{uxu}\,, \tag{2.26}$$

vanish when we consider an extended metric with a vanishing $\beta_W = 0$. The spacetime is completely flat in the regions outside the pulse where $\beta_W$ vanishes, and thus also at the $u = u_f$ after the passage of the wave where the coordinate singularity appears.

We can avoid the coordinate singularity at $u = u_f > T$ by employing a coordinate transformation $(u, v, x, y) \to (\mathcal{U}, V, X, Y)$ in the spacetime region after the passage of the wave; explicitly

$$u = \mathcal{U}\,, \quad x = \frac{X}{1 - \frac{\mathcal{U}}{u_f}}\,, \quad y = \frac{Y}{1 - \frac{\mathcal{U}}{u_f}}\,, \quad v = \frac{X^2 + Y^2}{u_f - \mathcal{U}}\,. \tag{2.27}$$

For the flat spacetime region after the passage of the wave we then recover a Minkowskian metric

$$\mathrm{d}s^2 = -\mathrm{d}\mathcal{U}\mathrm{d}V + \mathrm{d}X^2 + \mathrm{d}Y^2\,, \tag{2.28}$$

in standard Cartesian coordinates, where $U = T - Z$ and $V = T + Z$.

The complete flatness of the spacetime regions preceding and following the passage of the wave is a distinctive feature for this type of exact gravitational wave solution. The stress-energy carried by the gravitational wave does not curve the spacetime outside $-T < u < T$ because the wave region is bounded by completely flat 2-surfaces of constant $u$ and $v$.

Test particles in moving along straight lines in coordinates $(t, x, y, z)$ before the arrival of the gravitational wave remain in geodesic motion throughout the passage of the pulse and afterwards. Two test particles that are separated along the $z$ direction (the direction of propagation of the wave) have a constant proper separation $\Delta s = \Delta z$ throughout the passage of the wave; the exact gravitational wave solution considered here is completely transverse, like a plane wave in the transverse traceless (TT) gauge in linear theory. Two particles separated along a direction transverse to the direction of propagation experience a proper separation

$$\Delta s = L_B(u)\sqrt{e^{2\beta_W(u)}\left(\Delta x\right)^2 + e^{-2\beta_W(u)}\left(\Delta y\right)^2}, \tag{2.29}$$

during the passage of the wave. A gravitational wave radiation field has caustic properties if dust particles propagating on this background are accelerated in such a way that any two particles at rest before the interaction with the radiation field (independent of their initial separation) will collide in a finite time after the impact of the radiation field. All plane gravitational wave of limited duration, i.e., the sandwich solutions considered above, and with a fixed polarization will exhibit caustic properties [14].

For the discussion following in Chapters 5-7 of test particle motion and the propagation of electromagnetic waves in gravitational wave spacetimes we will choose a particular exact gravitational wave [4], with the "background

factor" $L_B$ and the "wave factor" $\beta_W$ given by

$$\begin{aligned} L_B(u) &= \sqrt{\cos\left(b_{(\mathrm{gw})}u\right)\cosh\left(b_{(\mathrm{gw})}u\right)}\,, \\ \beta_W(u) &= \frac{1}{2}\ln\left[\frac{\cos\left(b_{(\mathrm{gw})}u\right)}{\cosh\left(b_{(\mathrm{gw})}u\right)}\right]\,, \end{aligned} \tag{2.30}$$

respectively, belonging to the class of solutions introduced in (2.18). The parameter $b_{(\mathrm{gw})}$ is related to the frequency of the gravitational wave.

Finally, let us briefly consider the symmetry properties of exact plane gravitational waves. In analogy to electromagnetic waves these solutions were found to admit a 5-parameter group of motion, as has been demonstrated by Bondi, Pirani and Robinson in 1959 [12]. There nonflat solutions of the vacuum field equations were defined as being purely gravitational and representing plane waves by demanding that they have the same degree of symmetry as plane electromagnetic waves in a flat spacetime, i.e., that their motion groups have similar structure.

The field $F_{\mu\nu}(u)$ of a plane electromagnetic wave traveling in positive $z$ direction on the background of a flat spacetime $\mathrm{d}s^2 = \eta_{\mu\nu}\mathrm{d}x^\mu\mathrm{d}x^\nu$ in coordinates $(t, x, y, z)$ (where $u = t - z$) is invariant under a 5-parameter subgroup of the group of inhomogeneous Lorentz transformations. The transformation group is comprised of a 3-parameter group of translations in $x$ and $y$ direction (along null 3-surfaces of constant $u$), preserving the electromagnetic field,

$$T_a = \begin{cases} a^0: & \xi^\mu_1 = (1,0,0,1) \\ a^1: & \xi^\mu_2 = (0,1,0,0) \\ a^2: & \xi^\mu_3 = (0,0,1,0) \end{cases} \tag{2.31}$$

and a 2-parameter group of "null rotations", preserving the null 3-surfaces of constant $u$,

$$T_b = \begin{cases} b^1: & \xi^\mu_4 = (x,u,0,x) = x\xi^\mu_1 + u\xi^\mu_2 \\ b^2: & \xi^\mu_5 = (y,0,u,y) = y\xi^\mu_1 + u\xi^\mu_3 \end{cases} \tag{2.32}$$

where $a^0$, $a^k$, $b^k$ (with $k = 1, 2$) are the five independent parameters character-

izing the transformation group, and where $\xi^{\mu}_{A}$ are the infinitesimal generators of the transformations.

In Chapter 5 we will discuss the symmetry properties of gravitational plane waves (namely the constants of motion and the associated Killing vectors) and discuss their application to the propagation of massive and massless test particles in these spacetimes.

## 2.4 Exact electromagnetic plane waves as generators of background curvature

A metric tensor with identical metric coefficients $L_B^2(u)$ in coordinate directions $x$ and $y$

$$\mathrm{d}s^2 = -\mathrm{d}u\mathrm{d}v + L_B^2(u)\left(\mathrm{d}x^2 + \mathrm{d}y^2\right) , \tag{2.33}$$

(in the same null coordinate system as considered before) leads to the vanishing of all components of the associated Ricci tensor $R_{\mu\nu}$ and reduces the vacuum field equations to $L_B''(u) = 0$. This metric is a flat-spacetime metric and thus can't represent a gravitational wave. Now let $A^\flat = A(u)\mathrm{d}x$ be the 1-form of an arbitrary electromagnetic potential which satisfies Maxwell's equations in this metric. The nonzero components of the associated Faraday 2-form $F^\flat = \mathrm{d}A^\flat$ are

$$\begin{aligned} F &= A'(u)\mathrm{d}u \wedge \mathrm{d}x \\ &= A'(u)\mathrm{d}t \wedge \mathrm{d}x - A'(u)\mathrm{d}z \wedge \mathrm{d}x = E_x\mathrm{d}t \wedge \mathrm{d}x + B_y\mathrm{d}z \wedge \mathrm{d}x \,, \end{aligned} \tag{2.34}$$

therefore the electromagnetic four-potential represents an electromagnetic plane wave propagating in $z$ direction, with the electric field vector oscillating in $x$ direction and the magnetic field vector oscillating in $y$ direction. The presence of such an electromagnetic wave in a spacetime region makes it not empty, and we have to consider the energy-momentum tensor of the

electromagnetic wave

$$\begin{aligned} T^{\mu\nu} &= \frac{1}{4\pi}\left(F^{\mu\nu}F^{\nu}_{\alpha} - \frac{1}{4}g^{\mu\nu}F_{\alpha\beta}F^{\alpha\beta}\right), \\ T_{(\mathrm{em})} &= T_{uu} = \frac{1}{4\pi}\frac{[A'(u)]^2}{L_B^2(u)}, \end{aligned} \tag{2.35}$$

which now provides the source term for the nonvacuum field equations

$$L_B'' + \left(4\pi T_{(em)}\right) L_B = 0\,, \tag{2.36}$$

and thus produces a background curvature in a spacetime region through which the electromagnetic wave propagates, in analogy to the exact gravitational wave discussed in Sec. 2.3. In fact, if the "wave factor" $\beta_W(u)$ of an exact gravitational wave and the stress-energy tensor $T_{(\mathrm{em})}$ of an exact electromagnetic wave are related by

$$\beta_W(u) = \sqrt{4\pi}\int^u \sqrt{T_{(\mathrm{em})}}\mathrm{d}u\,, \tag{2.37}$$

both plane-wave solutions will produce the same background curvature $L_B(u)$. Test particles propagating on these backgrounds will experience the same relative motion, regardless whether we consider the curved spacetime of the exact gravitational wave vacuum solution or the curved background produced by the stress-energy of the electromagnetic wave.

In the discussion following in Chapters 6 and 7 of spacetime curvature generated by an electromagnetic pulse we will focus on a particular exact electromagnetic wave [15], with the "background factor" $L_B$ given by

$$L_B(u) = cos(b_{(\mathrm{em})}u)\,, \tag{2.38}$$

belonging to the class of solutions introduced in (2.33). The parameter $b_{(\mathrm{em})}$ is related to the frequency of the electromagnetic wave.

This particular exact electromagnetic wave and the exact gravitational wave (2.30) we consider above produce the same background curvature $L_B(u)$

only if the frequencies of the two wave solutions are related by

$$b_{(\mathrm{em})}u = \arccos\left(\sqrt{\cos(b_{(\mathrm{gw})}u)\cosh(b_{(\mathrm{gw})}u)}\right) . \tag{2.39}$$

In general we expect differences for the geodesic motion of uncharged particles depending on the nature of the radiation field.

# 3. FRICTION FORCES IN GENERAL RELATIVITY

Without external forces a massive test particle propagates along the geodesics of the background geometry, as we will see in Sec. 5.2 for timelike trajectories in the radiation field generated by an exact gravitational wave. Such friction forces cause deviation from geodesic motion and lead to accelerated or decelerated orbits governed by the equations of motion

$$ma(U)^\alpha = m\nabla_U U^\alpha = f_{(\mathrm{rad})}\,. \tag{3.1}$$

One particular example for the effects of friction forces in general relativity is the deceleration of test particle motion in a matter distribution, e.g., described by the stress-energy tensor of a perfect fluid.

In the following we want to consider a deviation from geodesic test particle motion due to a scattering of radiation by the particles. The particles are assumed to interact with the radiation field of an emitting source by absorbing and re-emitting radiation, causing the so-called Poynting-Robertson drag that is modeled by a radiation force built up from the energy-momentum tensor of the radiation field and the scattering cross section. This approach dates back to the pioneering works of Poynting [16] and Robertson [17], who derived the corrections to the motion of planets in the Solar system due to the scattering of the solar radiation in the context of Newtonian gravity and in the weak field approximation, respectively.

## *3.1 The Poynting-Robertson effect in special relativity*

Poynting first described the effect of absorption and re-emission of solar radiation on a dust particle orbiting the Sun (in the theory of the luminiferous aether) in 1903, where the interaction of the particle with the radiation gen-

erates a tangential drag which eventually causes the particle to fall into the Sun due to a loss of angular momentum. The particle motion is retarded by a back-pressure of the solar radiation, which Poynting understood as radiation that accumulates in front of the particle and thins out behind. A pencil of radiation is considered as a stream of momentum along the axis of the pencil. During the absorption of radiation by a moving surface momentum is transfered from the stream of radiation to the surface, resulting in normal pressure and tangential stress on the surface. The surface loses momentum isotropically with the re-emission of radiation, but there is an overall tangential force [16, 17]

$$f_{(\mathrm{rad})} = \frac{Rv}{c^2}\,, \tag{3.2}$$

where $R$ is the rate with which particle absorbs/re-emits energy, $v$ is the particle velocity in the aether and $c$ is the velocity of light.

Poynting's approach was recalculated by Robertson in 1937, in the theory of special relativity and Newtonian gravity. A particle is considered in orbital motion around a star with outward radial radiation. In the particle's rest frame the radiation pressure applies not directly side-on but slightly on the particle's forward side in terms of its orbital motion. The transfer of energy through the absorption and subsequent (isotropic) re-emission of radiation by the particle can be thought of as a force acting on the particle in the rest frame; this force has a component in opposite direction to the tangential component of the particle's orbital motion, acting as a drag force. If the drag force dominates the outward radial force the loss of angular momentum due to the drag will cause orbital decay. There exists a critical luminosity (like the Eddington limit of the hydrostatic equilibrium of a star [18], where the outward radial radiation force balances the inward gravitational force) at which the body is momentarily at rest separating inward spiral from outward spiral

Let us briefly sketch the Poynting-Robertson formalism in the weak field approximation [17]. We consider the motion of a small, spherical body with

unit four-velocity $u^\alpha$ in Minkowski coordinates

$$\mathrm{d}s^2 = \eta_{\mu\nu}\mathrm{d}x^\mu \mathrm{d}x^\nu \,, \tag{3.3}$$

in a beam of plane-parallel radiation from the Sun. The radiation is a beam of energy density that carries momentum in the direction $l^\alpha$, with radiation pressure in the same direction; i.e., a radiation field of photons propagating along null geodesics of the background with a four-momentum $l_\alpha$). We now introduce a reference frame in which the particle is at rest and where all radiation that falls upon the particle is absorbed and then (isotropically) re-emitted at the same rate. (The same rate of absorption and re-emission ensures that the particle mass is a constant of motion.) We now establish equations of motion (3.1) where the proper rate of change $m\hat{u}^\alpha$ of the spatial energy-momentum vector of the particle (in the rest frame) equals the force $\phi$ (in direction of the spatial direction of the null vector $\hat{l}^\alpha$ of the incoming beam) acting on the particle. Since the particle is at rest in this reference frame, we can apply the classical theory of radiation pressure to determine the force, i.e. it is $\phi = A\delta$, where $A$ is the effective cross section and $\delta$ is the 00-component of the original energy tensor of the incoming beam, but in the rest frame. The equations of motion in the rest frame read as [17]

$$\frac{m\mathrm{d}\hat{u}^\alpha}{\mathrm{d}\tau} = \frac{\phi}{c\hat{l}^0}\left(\hat{l}^\alpha - \hat{l}^0\hat{u}^\alpha\right) \,, \qquad \hat{l}^0 = \hat{l}_\alpha\hat{u}^\alpha = w \,, \tag{3.4}$$

where the first term is the four-force due to the incident radiation and the second term represents the re-emitted radiation. In the original inertial frame we the find [17]

$$\frac{m\mathrm{d}u^\alpha}{\mathrm{d}s} = \frac{fw}{c}\left(l^\alpha - wu^\alpha\right) \,, \tag{3.5}$$

where the radiation force is given by $f = \phi w^{-2}$.

Robertson also calculated the perihelion precession for quasi-Newtonian orbits as the leading general relativistic correction to his slow motion calculation.

Beyond the pioneering work outlined above the Poynting-Robertson formalism has been applied to slowly evolving meteor orbits by Wyatt and

Whipple in 1950 [19], and has been extended to radiating bodies of finite size by Guess in 1962 [20] and by Abramowicz, Ellis and Lanza in 1990 [21], who considered purely radial motion in an exterior Schwarzschild background to model jets and solar winds.

## 3.2 The general relativistic Poynting-Robertson effect

The generalization to the framework of general relativity has been developed in [22, 23], where a Poynting-Robertson-like effect on test particles orbiting in the equatorial plane of a Schwarzschild or Kerr spacetime has been considered, and in [24], where a self-consistent radiation flux (i.e., without the requirement that the radiation field itself be a test field) was instead used to investigate a such an interaction in the Vaidya spherically symmetric spacetime [25]. More recently, in [26], the Poynting-Robertson formalism has been employed to study the deceleration of particle motion in a Tolman metric generated by a photon gas source.

We now consider a test body in orbital motion in a spherically symmetric exterior Schwarzschild spacetime or an axially symmetric exterior Kerr spacetime without requiring slow motion and apply the simple Robertson scenario (without taking into account the finite size of the radiating body) in the context of strong gravitational fields and arbitrary motion. The radiation of the central body is now modeled by test photons in an outward radial motion with respect to locally nonrotating observers.

Let us briefly sketch some basic features of the Poynting-Robertson formalism in a general relativistic context, as introduced in great detail in [22]. Test particle motion is considered in the metric of a stationary axisymmetric spacetime

$$\mathrm{d}s^2 = g_{tt}\mathrm{d}t^2 + 2g_{t\phi}\mathrm{d}t\mathrm{d}\phi + g_{\phi\phi}\mathrm{d}\phi^2 + g_{rr}\mathrm{d}r^2 + g_{\theta\theta}\mathrm{d}\theta^2\,, \tag{3.6}$$

where all the metric coefficients depend only on $r$ and $\theta$ of a Boyer-Lindquist-like coordinate system $\{t, r, \theta, \phi\}$ adapted to the spacetime symmetries, i.e., with a pair of commuting Killing vectors $\partial_t$ (timelike) and $\partial_\phi$ (spacelike). A

family of zero angular momentum observer (ZAMO) observers is introduced, with a four-velocity

$$n = (-g^{tt})^{1/2}(\partial_t - \frac{g_{t\phi}}{g_{\phi\phi}}\partial_\phi)\,, \tag{3.7}$$

and with an associated orthonormal frame adapted to the ZAMOs

$$e_{\hat{t}} = n\,, \quad e_{\hat{r}} = \frac{1}{\sqrt{g_{rr}}}\partial_r\,, \quad e_{\hat{\theta}} = \frac{1}{\sqrt{g_{\theta\theta}}}\partial_\theta\,, \quad e_{\hat{\phi}} = \frac{1}{\sqrt{g_{\phi\phi}}}\partial_\phi\,,. \tag{3.8}$$

A pure electromagnetic radiation test field is superposed on the gravitational background characterized by an energy-momentum tensor

$$T^{\alpha\beta} = \Phi^2 k^\alpha k^\beta, \qquad k^\alpha k_\alpha = 0\,, \tag{3.9}$$

where $\Phi = (g_{\theta\theta}g_{\phi\phi})^{-1/4}\Phi_0$ has been determined from the conservation of $T^{\alpha\beta}$, and where $k$ is the four-momentum of a photon tangent to a null geodesic in the equatorial plane. Only photons in outward radial motion with respect to the ZAMOs are considered, namely

$$k = E(n)[n + \hat{\nu}(k,n)], \qquad \hat{\nu}(k,n) = e_{\hat{r}}\,, \tag{3.10}$$

with the relative energy of the photon $E(n) = E(-g^{tt})^{1/2}$, the conserved energy associated with the timelike Killing vector field $E = -k_t$ and the unit vector direction of the relative velocity $\hat{\nu}(k,n)$. The four-velocity of a test particle of mass $m$ moving in the equatorial plane and accelerated by its interaction with the radiation field can be decomposed in the observer frame as

$$\begin{aligned} U &= \gamma(U,n)[n + \nu(U,n)]\,, \\ \nu(U,n) \equiv \nu^{\hat{r}} e_{\hat{r}} + \nu^{\hat{\phi}} e_{\hat{\phi}} &= \nu\sin\alpha e_{\hat{r}} + \nu\cos\alpha e_{\hat{\phi}}\,, \end{aligned} \tag{3.11}$$

where $\gamma(U,n) = (1-||\nu(U,n)||^2)^{-1/2}$ is the Lorentz factor and the abbreviated notation $\nu^{\hat{a}} = \nu(U,n)^{\hat{a}}$ has been used. Here $\nu = ||\nu(U,n)||$ is the magnitude and $\alpha$ is the polar angle of the spatial velocity $\nu(U,n)$ in the $r-\phi$ tangent plane, respectively. Using relations between the coordinate and the frame

components of $U$ and solving for the magnitude and polar angle leads to

$$\begin{aligned}\tan\alpha &= \sqrt{\frac{g_{rr}}{g_{\phi\phi}}}\frac{\mathrm{d}r}{\mathrm{d}t}\left(\frac{\mathrm{d}\phi}{\mathrm{d}t}+\frac{g_{t\phi}}{g_{\phi\phi}}\right)^{-1}, \\ \nu &= -g^{tt})^{1/2}\sqrt{g_{rr}\left(\frac{\mathrm{d}r}{\mathrm{d}t}\right)^2+g_{\phi\phi}\left(\frac{\mathrm{d}\phi}{\mathrm{d}t}+\frac{g_{t\phi}}{g_{\phi\phi}}\right)^2}. \end{aligned} \tag{3.12}$$

The interaction of the particle with the radiation field is subsequently modeled through the introduction of a radiation force observed in the particle's rest frame

$$\mathcal{F}_{(\mathrm{rad})}(U)^\alpha = -\sigma P(U)^\alpha{}_\beta\, T^\beta{}_\mu\, U^\mu \tag{3.13}$$

where $P(U)^\alpha{}_\beta = \delta^\alpha_\beta + U^\alpha U_\beta$ project orthogonally to $U$ and where $\sigma$ is the momentum-transfer cross section. The equation of motion of the particle in the observer frame thus become

$$ma(U) = \mathcal{F}_{(\mathrm{rad})}(U)\,, \tag{3.14}$$

where $m$ is the mass of the particle and $a(U) = \nabla_U U$ is its four-acceleration.

It is convenient to decompose the photon four-momentum $k$ (3.10) (already decomposed with respect to the ZAMOs)further with respect to the particle four-velocity $U$, namely,

$$k = E(U)[U + \hat{\mathcal{V}}(k,U)] \equiv E(n)[n + \hat{\nu}(k,n)]\,. \tag{3.15}$$

By introducing the polar decomposition (3.11) of the spatial particle velocity $U$ the relative energy and the relative direction of propagation of the photons become

$$\begin{aligned} E(U) &= \gamma E(n)[1-\nu\cos(\alpha-\pi/2)] = \gamma E(n)[1-\nu\sin\alpha]\,, \\ \hat{\mathcal{V}}^{\hat{t}} &= \gamma\nu\frac{\sin\alpha-\nu}{1-\nu\sin\alpha}\,, \quad \hat{\mathcal{V}}^{\hat{r}} = \frac{1}{\gamma(1-\nu\sin\alpha)} - \gamma\nu\sin\alpha\,, \\ \hat{\mathcal{V}}^{\hat{\phi}} &= -\gamma\nu\cos\alpha \end{aligned} \tag{3.16}$$

respectively. The frame components of the particle four-acceleration $a(U)$

in the equatorial plane $(a(U)^{\hat{t}},\ a(U)^{\hat{r}},\ a(U)^{\hat{\theta}},\ a(U)^{\hat{\phi}})$ can thus be explicitly expressed in terms of the frame components of the photon four-momentum (3.16), and the equations of motion are obtained as

$$\begin{aligned}
\frac{\mathrm{d}\nu}{\mathrm{d}\tau} &= -\frac{\sin\alpha}{\gamma}[a(n)^{\hat{r}} + 2\nu\cos\alpha\,\theta(n)^{\hat{r}}{}_{\hat{\phi}}] - \frac{Ag^{tt}}{\sqrt{g_{\theta\theta}g_{\phi\phi}}}(1-\nu\sin\alpha)(\sin\alpha-\nu)\,, \\
\frac{\mathrm{d}\alpha}{\mathrm{d}\tau} &= -\frac{\gamma\cos\alpha}{\nu}[a(n)^{\hat{r}} + 2\nu\cos\alpha\,\theta(n)^{\hat{r}}{}_{\hat{\phi}} + \nu^2 k_{(\mathrm{lie})}(n)^{\hat{r}}] \\
&\quad -\frac{Ag^{tt}}{\sqrt{g_{\theta\theta}g_{\phi\phi}}}\,\frac{(1-\nu\sin\alpha)\cos\alpha}{\nu}\,, \\
\frac{\mathrm{d}r}{\mathrm{d}\tau} &= \frac{\gamma\nu\sin\alpha}{\sqrt{g_{rr}}}\,, \qquad A = \tilde{\sigma}\Phi_0^2 E^2\,,
\end{aligned} \tag{3.17}$$

in terms of the magnitude and the polar angle of the spatial particle four-velocity; $k_{(\mathrm{lie})}(n)^{\hat{r}}$ denotes the radial component of the Lie curvature vector associated with the $\phi$ coordinate lines.

The equations of motion admit the special solutions $\alpha = \pm\pi/2$ (radial outward/inward motion with respect to the ZAMOs). There are no circular orbits, i.e., solutions with constant $\alpha = 0$ and motion in $\phi$ direction only, because clearly the drag force in azimuthal direction forbids them. There exists a critical value of the radial coordinate $r_{(\mathrm{crit})}$ for which the particle co-moves with the ZAMOs in a circular orbit, namely, if $\nu$ is chosen to vanish initially the spatial particle velocity in the rest frame will remain zero if

$$-\frac{Ag^{tt}}{\sqrt{g_{\theta\theta}g_{\phi\phi}}} = a(n)^{\hat{r}}\,. \tag{3.18}$$

This condition represents the radial balance between the gravitational attraction and the radiation pressure. It is possible to rewrite this equilibrium condition using the general relativistic generalization of the Eddington luminosity, and subsequently identify the radiation constant $A$ in terms of parameters related to the emitting body and to the Thomson scattering process; for more details see [22] and references therein.

In Chapter 6 we will apply the general relativistic Poynting-Robertson formalism to the propagation of massive neutral test particles in the radia-

tion field described by an exact solution of the Einstein-Maxwell equations representing the curved spacetime associated with a plane electromagnetic wave [27].

# 4. THE OPTICAL MEDIUM ANALOGY OF A CURVED SPACETIME

For test electromagnetic fields propagating on a curved spacetime one can always neglect back reaction effects on the metric due to the electromagnetic field. Solving Maxwell's equations on a given background in general, however, is not an easy task and exact solutions only exist within very special (highly symmetric) contexts. Over the years a number of methods and approximations have been developed in order to tackle the problem of solving Maxwell's equations on curved backgrounds.

In this chapter we want to introduce the so-called optical medium analogy of a given spacetime which was developed decades ago and has been widely used to study both the propagation of electromagnetic waves in a gravitational field and scattering processes by either static or rotating black holes as well as by some cosmological solution, e.g., the Gödel universe [28, 29, 30, 31].

Mashhoon and Grishchuk [32] have considered the propagation of electromagnetic waves in a weak gravitational radiation field superposed to a Minkowskian background, characterized by $g_{\mu\nu} = \eta_{\mu\nu} + h_{\mu\nu}$. The gravitational field was treated as a hypothetical dispersive medium with a dielectric tensor $\epsilon_{ik} = \mu_{ik} = \delta_{ik} - h_{ik}$, and the electromagnetic field $F_{\mu\nu}$ could thus be described by Maxwell's equations in a medium in flat spacetime. The electromagnetic field vector was then decomposed into its undisturbed initial part and the perturbation induced by the dispersion of the electromagnetic wave. An analysis of the perturbation in the Fourier domain demonstrated that the dispersion in the gravitational medium results in a splitting of the Fourier components $(\Omega_{\rm em}, \mathbf{K}_{\rm em})$ of the electromagnetic wave, with $\Omega$ and $\mathbf{K}$ referring to frequency and wave vector, respectively. Each $(\Omega_{\rm em}, \mathbf{K}_{\rm em})$ in the initial Fourier spectrum picks up two scattered components $(\Omega_{\rm em} \pm \Omega_{\rm g}, \mathbf{K}_{\rm em} \pm \mathbf{K}_{\rm g})$

with a relative amplitude of the order of $\epsilon$, where $(\Omega_{\rm g}, \mathbf{K}_{\rm g})$ is a Fourier component of the gravitational field. It was proved that electromagnetic phenomena in the background of a weak gravitational wave radiation field propagate with a frequency which is simply related to that of the background solution.

In Chapter 7 we will discuss the application of the optical medium analogy to a curved background associated with the exact gravitational and electromagnetic plane waves introduced above. In Chapter 8 we will generalize our results by considering a spacetime of colliding strong gravitational waves; we will apply the optical medium analogy to study the optical properties of the collision region and analyze the propagation of electromagnetic waves in this framework.

## 4.1 The optical medium analogy of an arbitrary gravitational field

Consider an arbitrary gravitational field described by the line element $\mathrm{d}s^2 = g_{\alpha\beta}\mathrm{d}x^\alpha \mathrm{d}x^\beta$ written in coordinates $x^\alpha = (t, x, y, z)$. An electromagnetic field in that background can be thought of as propagating in flat spacetime but in the presence of a medium whose properties are determined by conformally invariant quantities constructed from the metric tensor. In fact, the covariant Faraday tensor $F_{\mu\nu}$ and its rescaled contravariant counterpart $\sqrt{-g}F^{\mu\nu}$ can be decomposed as $F_{\mu\nu} \to (\mathbf{E}, \mathbf{B})$ and $\sqrt{-g}F^{\mu\nu} \to (-\mathbf{D}, \mathbf{H})$ to yield the usual Maxwell's equations in a medium [33, 34, 35, 28, 29]

$$\begin{aligned} \nabla \cdot \mathbf{B} &= \ 0\,, & \nabla \times \mathbf{E} &= -\partial_t \mathbf{B}\,, \\ \nabla \cdot \mathbf{D} &= \ 4\pi\rho\,, & \nabla \times \mathbf{H} &= \partial_t \mathbf{D} + 4\pi \mathbf{J}\,, \end{aligned} \tag{4.1}$$

where the current vector $J_\mu \to (\rho, \mathbf{J})$ satisfies the conservation law

$$\partial_t \rho + \nabla \cdot \mathbf{J} = 0\,. \tag{4.2}$$

The above set of equations is completed by the constitutive relations

$$D_a = \epsilon_{ab} E_b - (\mathbf{M} \times \mathbf{H})_a \,, \qquad B_a = \mu_{ab} H_b + (\mathbf{M} \times \mathbf{E})_a \,, \tag{4.3}$$

where

$$\epsilon_{ab} = \mu_{ab} = -\sqrt{-g}\, \frac{g^{ab}}{g_{tt}} \tag{4.4}$$

play the role of electric and magnetic permeability tensors and

$$M_a = -\frac{g_{ta}}{g_{tt}} \tag{4.5}$$

is a vector field associated with rotations of the reference frame. Within this framework, the description of electromagnetic fields in a curved spacetime is equivalently accomplished by solving Maxwell's equations in a flat spacetime but in the presence of a medium, whose properties are fully specified by the associated constitutive relations. The effective material medium is in general anisotropic and has no birefringence, due to the proportionality between polarization tensors. Furthermore, the conformal invariance of Maxwell's equations is reflected, in the present formulation, by the independence of the dielectric tensors $\epsilon_{ab}$ and $\mu_{ab}$ from a conformal factor in the metric components, a property also shared by the "spatial" vector $\mathbf{M}$.

Following [29], if one introduces the complex vectors

$$\mathbf{F} = \mathbf{E} + i\mathbf{H} \,, \qquad \mathbf{S} = \mathbf{D} + i\mathbf{B} \,, \tag{4.6}$$

the constitutive relations read

$$S_a = \epsilon_{ab} F_b + i(\mathbf{M} \times \mathbf{F})_a \,. \tag{4.7}$$

Furthermore, it is possible to write the electromagnetic equations (4.1) in a form which is particularly suitable for the discussion of wave phenomena, i.e.,

$$\frac{1}{i} \nabla \times \mathbf{F} = \partial_t \mathbf{S} + 4\pi \mathbf{J} \,, \qquad \nabla \cdot \mathbf{S} = 4\pi\rho \,. \tag{4.8}$$

Plane waves satisfy the above equations in a small spacetime region, where

the metric tensor can be always assumed to vary in space and time only slightly with respect to the wavelength and the period of the wave, respectively. Therefore, one can apply there the standard tools of ordinary wave optics to study the optical properties of the equivalent medium.

For instance, in the absence of currents, one may look for solutions of the form

$$\mathbf{E} = \mathbf{E}_0 e^{i(n\mathbf{k}\cdot\mathbf{x}-\omega t)}\,, \quad \mathbf{E}_0 = const.\,, \quad |\mathbf{k}| = \omega\,, \tag{4.9}$$

where $n$ is an effective refraction index. Similar expressions hold for $\mathbf{B}$, $\mathbf{H}$ and $\mathbf{D}$. Maxwell's equations (4.1) then imply

$$\mathbf{n}\times\mathbf{E} = \mathbf{B}\,, \qquad \mathbf{n}\times\mathbf{H} = -\mathbf{D} \tag{4.10}$$

and $\mathbf{n}\cdot\mathbf{B} = 0 = \mathbf{n}\cdot\mathbf{D}$, where $\mathbf{n} = (n/\omega)\mathbf{k} = n\mathbf{e}$ and $\mathbf{e} = \mathbf{k}/\omega$ is the spatial unit vector of the photon direction. A substitution of the constitutive relations (4.3) into the equations (4.10) leads to

$$[\epsilon_{ik} + \varepsilon_{ijr}\varepsilon_{suk}(\mathbf{n}-\mathbf{M})_j(\mathbf{n}-\mathbf{M})_u(\epsilon^{-1})_{rs}]E_k = 0\,, \tag{4.11}$$

where $\varepsilon_{ijk}$ denotes the Levi-Civita alternating symbol. One finds a similar equation for $H_k$. The existence of eigensolutions for $\mathbf{E}$ implies the following generalized Fresnel equation [34, 35]

$$n^2\epsilon_{\mathbf{ee}} - 2n\epsilon_{\mathbf{eM}} + \epsilon_{\mathbf{MM}} - \det(\epsilon) = 0\,, \tag{4.12}$$

where $\mathbf{e} = \mathbf{k}/\omega$ is the spatial unit vector of the photon direction and the compact notation $X_{ab}A^aB^b = X_{\mathbf{AB}}$ has been introduced for contraction of a generic matrix $X_{ab}$ with vectors $A_a$ and $B_b$. The above equation (4.12) gives the relation between the effective refraction index of the medium, the components of the polarization tensors and the direction of propagation of the electromagnetic wave. The solution for the refraction index is thus given by

$$n = \frac{1}{\epsilon_{\mathbf{ee}}}\left[\epsilon_{\mathbf{eM}} + \sqrt{\det(\epsilon)\,[\epsilon_{\mathbf{ee}} - (\epsilon^{-1})_{\mathbf{cc}}]}\right]\,, \tag{4.13}$$

where $\mathbf{c} = \mathbf{M}\times\mathbf{e}$ and $\det(\epsilon) = \epsilon_1\epsilon_2\epsilon_3$, in a coordinate system in which electric

and magnetic permeability tensors are diagonal, i.e., $\epsilon_{ab} = \mathrm{diag}[\epsilon_1, \epsilon_2, \epsilon_3] = \mu_{ab}$. In the special case $M_a = 0$, the above expression simplifies to

$$n = \sqrt{\frac{\det(\epsilon)}{\epsilon_{\mathbf{ee}}}}\,. \tag{4.14}$$

In the special case $M_a = 0$, the above expression (4.13) simplifies to

$$n = \sqrt{\frac{\det(\epsilon)}{\epsilon_{\mathbf{ee}}}}\,. \tag{4.15}$$

With the optical properties of the effective medium equivalent equivalent to an arbitrary gravitational field thus determined, standard tools of ordinary wave optics can then be employed to study the deflection of photon paths in the gravitational field background.

# 5. ELECTROMAGNETIC WAVES IN AN EXACT GRAVITATIONAL WAVE SPACETIME

In the following we will consider the propagation of a test electromagnetic field in a spacetime representing an exact gravitational plane wave with single polarization, belonging to the class of solutions introduced in Sec. 2.3. We will discuss in detail the propagation of photons and massive particles on this background, and we will calculate the induced changes on the four-potential field $A^\mu$ of a plane electromagnetic wave. By choosing a suitable photon round-trip in a Michelson interferometer, we will be able to identify the physical effects of the exact gravitational wave on the electromagnetic field, i.e. phase shift, change of the polarization vector, angular deflection and delay. The results will then be applied to study the response of an interferometric gravitational wave detector beyond the linear approximation of the general theory of relativity, extending analysis by Finn [36], Rakhmanov [37] and Braginsky et al [38].

The results of this chapter have been published in *Class. Quantum Grav.* **28**, 235007 (2011) [39].

## *5.1 An exact solution representing a gravitational plane wave with single polarization*

The spacetime metric of an exact gravitational plane wave with a single polarization state (+ state) can be written in the "Rosen form" as follows [3, 4]

$$g = -\frac{1}{2}(\mathrm{d}u \otimes \mathrm{d}v + \mathrm{d}v \otimes \mathrm{d}u) + F(u)^2 \mathrm{d}x \otimes \mathrm{d}x + G(u)^2 \mathrm{d}y \otimes \mathrm{d}y\,, \qquad (5.1)$$

with $\sqrt{-\det \mathrm{g}} = F(u)G(u)/2$ and the inverse

$$g^{-1} = -2(\partial_u \otimes \partial_v + \partial_v \otimes \partial_u) + \frac{1}{F(u)^2}\partial_x \otimes \partial_x + \frac{1}{G(u)^2}\partial_y \otimes \partial_y \,. \tag{5.2}$$

The coordinates $(u, v, x, y)$ are adapted to the spacetime symmetries; i.e., $\partial_v$, $\partial_x$, $\partial_y$ are all Killing vectors. We point out that the two null coordinates $u$ and $v$ are related to a standard temporal coordinate $t$ and a spatial coordinate $z$ (the direction of propagation of the wave) by the transformation

$$u = t - z, \qquad v = t + z \,, \tag{5.3}$$

which implies

$$\partial_u = \frac{1}{2}\left(\partial_t - \partial_z\right) , \qquad \partial_v = \frac{1}{2}\left(\partial_t + \partial_z\right) . \tag{5.4}$$

The inverse of this transformation is then

$$t = (u + v)/2 \,, \qquad z = (v - u)/2 \,, \tag{5.5}$$

and therefore we have

$$\partial_t = \partial_u + \partial_v \,, \qquad \partial_z = \partial_v - \partial_u \,. \tag{5.6}$$

The vacuum Einstein field equations associated with equation (5.1) reduce to the single equation $R_{uu} = 0$, i.e.

$$\frac{F''(u)}{F(u)} + \frac{G''(u)}{G(u)} = 0 \,, \tag{5.7}$$

where a prime denotes differentiation with respect to $u$. The wave is then propagating along the positive $z$ axis with axes of polarization aligned with the coordinate axes $x$ and $y$.

In the following we will consider a sandwich-wave solution, i.e., a curved spacetime region in the interval $u \in [0, a^2/\tau]$ between two Minkowskian regions $u \in (-\infty, 0) \cup (a^2/\tau, \infty)$, where the constant parameters $a$ and $\tau$ have

been introduced, with $\tau$ representing the duration of the interaction of particles or fields with the wave and $1/a$ the overall curvature of the wave region. A possible choice of metric functions is as follows:

$$
\begin{aligned}
F(u) &= \begin{cases} 1 & u \leq 0 \qquad\quad \text{(I)} \\ \cos(u/a) & 0 \leq u \leq a^2/\tau \qquad \text{(II)} \\ \alpha + \beta u & a^2/\tau \leq u \qquad\quad \text{(III)} \end{cases} \\
G(u) &= \begin{cases} 1 & u \leq 0 \qquad\quad \text{(I)} \\ \cosh(u/a) & 0 \leq u \leq a^2/\tau \qquad \text{(II)} \\ \gamma + \delta u, & a^2/\tau \leq u \qquad\quad \text{(III)} \end{cases}
\end{aligned}
\tag{5.8}
$$

where labels I, II and III refer to in zone, wave zone and out zone, respectively. For a more detailed account of exact gravitational plane waves see e.g. [4].

The constants $\alpha$, $\beta$, $\gamma$ and $\delta$ can be found by requiring $C^1$ regularity conditions at the boundary of the sandwich, $u = 0$ and $u = \frac{a^2}{\tau}$, that is

$$
\begin{aligned}
\alpha &= \cos\left(\frac{a}{\tau}\right) + \frac{a}{\tau}\sin\left(\frac{a}{\tau}\right), \qquad \beta = -\frac{1}{a}\sin\left(\frac{a}{\tau}\right), \\
\gamma &= \cosh\left(\frac{a}{\tau}\right) - \frac{a}{\tau}\sinh\left(\frac{a}{\tau}\right), \qquad \delta = \frac{1}{a}\sinh\left(\frac{a}{\tau}\right).
\end{aligned}
\tag{5.9}
$$

We point out that for $u < 0$ with the choice $F(u) = 1 = G(u)$ the spacetime is flat (Minkowski) and the metric reduces to

$$
g = -\frac{1}{2}(\mathrm{d}u \otimes \mathrm{d}v + \mathrm{d}v \otimes \mathrm{d}u) + \mathrm{d}x \otimes \mathrm{d}x + \mathrm{d}y \otimes \mathrm{d}y\,, \qquad \sqrt{-\det \mathrm{g}} = \frac{1}{2}\,. \tag{5.10}
$$

The coordinates $(t, x, y, z)$ associated with $(u, v, x, y)$ by means of (5.3) are then standard Cartesian coordinates. Finally, in order to compare the results of the present analysis with existing literature we recall that the metric functions $F$ and $G$ in the linearized approximation and in the transverse-traceless gauge are usually such that

$$
F(u)^2 = 1 + h_+(u)\,, \qquad G(u)^2 = 1 - h_+(u)\,, \tag{5.11}
$$

where $h_+$ is a first order perturbation to the flat background, see e.g. [37].

## 5.2 Geodesics of photons and massive test particles

Let us consider null and timelike geodesics with respect to the coordinates $(u, v, x, y)$ in all spacetime regions. The geodesic equations and their the four-velocity normalization condition

$$\begin{aligned} \frac{d^2x^\alpha}{d\lambda^2} + \Gamma^\alpha{}_{\mu\nu}\left(x(\lambda)\right) \frac{dx^\mu}{d\lambda}\frac{dx^\nu}{d\lambda} &= 0\,, \\ g_{\mu\nu}\left(x(\lambda)\right) \frac{dx^\mu}{d\lambda}\frac{dx^\nu}{d\lambda} &= \rho \end{aligned} \tag{5.12}$$

(where the $\Gamma^\alpha{}_{\mu\nu}$ denote the Christoffel symbols constructed from $g_{\mu\nu}$, and where the parameter $\lambda$ is a proper time parameter along the geodesics) can be explicitly solved by taking into account the Killing vector fields $\xi$ admitted by the spacetime metric. The independent Killing vectors are associated with constants of motion along the geodesic, namely

$$\xi_\mu\, P^\mu = const.\,, \tag{5.13}$$

with $P^\alpha$ denoting the vector tangent to these world lines. The second-order equations of motion are thus reduced to a first-order system $P^\alpha = \mathrm{d}x^\alpha/\mathrm{d}\lambda$, with

$$P^\alpha \nabla_\alpha P^\beta = \rho\,, \qquad P^\alpha P_\alpha = \rho\,, \tag{5.14}$$

where the parameter $\rho$ discriminates among the classes of geodesics we are considering, i.e. $\rho = -1, 0, 1$ corresponding to timelike, null and spacelike geodesics, respectively.

$P^\mu = dx^\mu/d\lambda$ that can be parametrized with the Killing constants and simply integrated. In the spacetime metric (5.1) representing an exact gravitational wave there exist three spacelike translational Killing vectors $\xi_{(1)} = \partial_x$ and $\xi_{(2)} = \partial_y$ and $\xi_{(3)} = \partial_v$ in all spacetime regions (in zone, wave zone, out zone) since the metric is independent from $x$, $y$ and $v$ in all regions. The associated constants of motion are $p_x$, $p_y$ and $p_v$, respectively.

The solutions for the geodesics, using $u$ as a convenient parameter, can be written as follows (see e.g. [14] or [40])

$$\begin{aligned} u(\lambda) &= -2p_v\lambda + u_c\,, \qquad v(u) = \frac{1}{4p_v^2}\int^u \left(-\rho + \frac{p_x^2}{F(u)^2} + \frac{p_y^2}{G(u)^2}\right) du + v_c\,, \\ x(u) &= -\frac{p_x}{2p_v}\int^u \frac{du}{F(u)^2} + x_c\,, \qquad y(u) = -\frac{p_y}{2p_v}\int^u \frac{du}{G(u)^2} + y_c\,, \end{aligned} \tag{5.15}$$

where the quantities $p_v$, $p_x$ and $p_y$ (covariant components of the momentum) are Killing constants, while $(u_c, v_c, x_c, y_c)$ mark coordinates of a generic point. The associated four-momentum is

$$P = -2p_v\partial_u - \frac{1}{2p_v}\left(-\rho + \frac{p_x^2}{F(u)^2} + \frac{p_y^2}{G(u)^2}\right)\partial_v + \frac{p_x}{F(u)^2}\partial_x + \frac{p_y}{G(u)^2}\partial_y\,, \tag{5.16}$$

or equivalently

$$P^\flat = \frac{1}{4p_v}\left(-\rho + \frac{p_x^2}{F(u)^2} + \frac{p_y^2}{G(u)^2}\right)\mathrm{d}u + p_v\mathrm{d}v + p_x\mathrm{d}x + p_y\mathrm{d}y\,. \tag{5.17}$$

Note that within the linear approximation (small overall curvature of the wave region, $a \to \infty$) we recover the well known results in the wave region [37]

$$P^\flat_{(\mathrm{lin})} = \frac{1}{4p_v}\left[-\rho + p_x^2(1-h_+) + p_y^2(1+h_+)\right]\mathrm{d}u + p_v\mathrm{d}v + p_x\mathrm{d}x + p_y\mathrm{d}y\,. \tag{5.18}$$

With the choice of $F$ and $G$ functions given in (5.8) we can also identify

$$h_+(u) \approx -\frac{u^2}{a^2} + O\left(\frac{u^3}{a^3}\right)\,. \tag{5.19}$$

By specifying the metric in the various regions of spacetime we find $C^1$ solutions of the geodesic equations before, during and after the passage of the wave:

- **Region I.** The geodesics are straight lines from $(u_s, v_s, x_s, y_s)$ to $(0, v_0, x_0, y_0)$:

$$\begin{aligned} u(\lambda) &= -2p_v\lambda + u_s\,, \qquad v(u) = \frac{1}{4p_v^2}(-\rho + p_x^2 + p_y^2)u + \tilde{v}_s\,, \\ x(u) &= -\frac{p_x}{2p_v}u + \tilde{x}_s\,, \qquad y(u) = -\frac{p_y}{2p_v}u + \tilde{y}_s\,, \end{aligned} \tag{5.20}$$

with

$$\begin{aligned} \tilde{x}_s &= \frac{p_x}{2p_v}u_s + x_s\,, \qquad \tilde{y}_s = \frac{p_y}{2p_v}u_s + y_s\,, \\ \tilde{v}_s &= v_s - \frac{1}{4p_v^2}(-\rho + p_x^2 + p_y^2)u_s\,. \end{aligned} \tag{5.21}$$

The associated momentum is

$$P_{_I} = -2p_v\partial_u - \frac{1}{2p_v}(-\rho + p_x^2 + p_y^2)\partial_v + p_x\partial_x + p_y\partial_y\,. \tag{5.22}$$

- **Region II.** The geodesics connect the spacetime points from $(0, v_0, x_0, y_0)$ to $(\frac{a^2}{\tau}, v_1, x_1, y_1)$:

$$\begin{aligned} x(u) &= -\frac{p_x}{2p_v}a\tan\left(\frac{u}{a}\right) + x_0\,, \qquad y(u) = -\frac{p_y}{2p_v}a\tanh\left(\frac{u}{a}\right) + y_0\,, \\ v(u) &= \frac{1}{4p_v^2}\left[-\rho u + p_x^2 a\tan\left(\frac{u}{a}\right) + p_y^2 a\tanh\left(\frac{u}{a}\right)\right] + v_0 \\ u(\lambda) &= -2p_v\lambda + u_s\,. \end{aligned} \tag{5.23}$$

The associated momentum is

$$\begin{aligned} P_{_{II}} &= -2p_v\partial_u - \frac{1}{2p_v}\left(-\rho + \frac{p_x^2}{\cos^2\left(\frac{u}{a}\right)} + \frac{p_y^2}{\cosh^2\left(\frac{u}{a}\right)}\right)\partial_v \\ &\quad + \frac{p_x}{\cos^2\left(\frac{u}{a}\right)}\partial_x + \frac{p_y}{\cosh^2\left(\frac{u}{a}\right)}\partial_y\,. \end{aligned} \tag{5.24}$$

In the linearized regime the above relations have the following limit:

$$\begin{aligned} u(\lambda) &= -2p_v\lambda + u_s\,, \\ v(u) &= \frac{u}{4p_v^2}\left[-\rho + (p_x^2+p_y^2) + \frac{(p_x^2-p_y^2)}{3a^2}u^2\right] + v_0 \\ &= v_s - \frac{\lambda}{2p_v}(-\rho + p_x^2 + p_y^2) - \frac{\lambda}{2p_v}(p_x^2-p_y^2)f_+(\lambda) \\ x(u) &= -\frac{p_x}{2p_v}\left(1+\frac{u^2}{3a^2}\right)u + x_0 \\ y(u) &= -\frac{p_y}{2p_v}\left(1-\frac{u^2}{3a^2}\right)u + y_0\,, \end{aligned} \tag{5.25}$$

where, following [37],

$$\begin{aligned} f_+(\lambda) &= \frac{1}{\lambda}\int_0^\lambda h_+(u(\lambda))\mathrm{d}\lambda \approx -\frac{1}{a^2\lambda}\int_0^\lambda u^2(\lambda)\mathrm{d}\lambda \\ &= \frac{1}{6p_v a^2\lambda}[(u_s - 2p_v\lambda)^3 - u_s^3] \end{aligned} \tag{5.26}$$

denotes the average amplitude of the gravitational wave and hence

$$\begin{aligned} P_{II} &= -2p_v\partial_u - \frac{1}{2p_v}\left[-\rho + p_x^2 + p_y^2 + \frac{u^2}{a^2}(p_x^2-p_y^2)\right]\partial_v \\ &\quad + p_x\left(1+\frac{u^2}{a^2}\right)\partial_x + p_y\left(1-\frac{u^2}{a^2}\right)\partial_y \\ &= p_{_I} + \frac{u^2}{a^2}\left[(p_x^2-p_y^2)\partial_v + p_x\partial_x - p_y\partial_y\right]\,. \end{aligned} \tag{5.27}$$

- **Region III.** The geodesics connect the spacetime points $(\frac{a^2}{\tau}, v_1, x_1, y_1)$ and $(u_e, v_e, x_e, y_e)$, where $P_e$ denotes an arbitrary point in the out zone:

$$\begin{aligned} v(u) &= -\frac{1}{4p_v^2}\left(\rho u + \frac{p_x^2}{\beta\,(\alpha+\beta u)} + \frac{p_y^2}{\delta\,(\gamma+\delta u)}\right) + \tilde{v}_1 \\ x(u) &= \frac{p_x}{2p_v}\frac{1}{\beta\,(\alpha+\beta u)} + \tilde{x}_1\,, \qquad y(u) = \frac{p_y}{2p_v}\frac{1}{\delta\,(\gamma+\delta u)} + \tilde{y}_1\,, \\ u(\lambda) &= -2p_v\lambda + u_s\,, \end{aligned} \tag{5.28}$$

with

$$\begin{aligned}\tilde{x}_1 &= x_1 + \frac{p_x}{2p_v}\frac{a}{\sin\left(\frac{a}{\tau}\right)\cos\left(\frac{a}{\tau}\right)}\,, \qquad \tilde{y}_1 = y_1 - \frac{p_y}{2p_v}\frac{a}{\sinh\left(\frac{a}{\tau}\right)\cosh\left(\frac{a}{\tau}\right)}\,,\\ \tilde{v}_1 &= v_1 + \frac{a}{4p_v^2}\left(\rho\frac{a}{\tau} - \frac{p_x^2}{\sin\left(\frac{a}{\tau}\right)\cos\left(\frac{a}{\tau}\right)} + \frac{p_y^2}{\sinh\left(\frac{a}{\tau}\right)\cosh\left(\frac{a}{\tau}\right)}\right)\,. \quad (5.29)\end{aligned}$$

The associated momentum is

$$\begin{aligned}P_{III} &= -2p_v\partial_u - \frac{1}{2p_v}\left(-\rho + \frac{p_x^2}{(\alpha+\beta u)^2} + \frac{p_y^2}{(\gamma+\delta u)^2}\right)\partial_v\\ &\quad + \frac{p_x}{(\alpha+\beta u)^2}\partial_x + \frac{p_y}{(\gamma+\delta u)^2}\partial_y\,. \quad (5.30)\end{aligned}$$

### 5.2.1 Matching conditions

By imposing a matching condition at the boundaries I-II and II-III, we can relate the solutions in all three regions to the initial spacetime points $(u_s, v_s, x_s, y_s)$.

- **Matching of the boundary I-II.** We find

$$\begin{aligned}\lambda_0 &= \frac{u_s}{2p_v}\,, \qquad v_0 = v_s - \frac{1}{4p_v^2}(-\rho + p_x^2 + p_y^2)u_s\,,\\ x_0 &= \frac{p_x}{2p_v}u_s + x_s\,, \qquad y_0 = \frac{p_y}{2p_v}u_s + y_s\,. \quad (5.31)\end{aligned}$$

- **Matching of the boundary II-III.** We find

$$\begin{aligned}x_1 &= -\frac{p_x}{2p_v}a\tan\left(\frac{a}{\tau}\right) + x_0 = x_s + \frac{p_x}{2p_v}\left[u_s - a\tan\left(\frac{a}{\tau}\right)\right]\,,\\ y_1 &= -\frac{p_y}{2p_v}a\tanh\left(\frac{a}{\tau}\right) + y_0 = y_s + \frac{p_y}{2p_v}\left[u_s - a\tanh\left(\frac{a}{\tau}\right)\right]\,,\\ v_1 &= \frac{a}{4p_v^2}\left[-\rho\frac{a}{\tau} + p_x^2\tan\left(\frac{a}{\tau}\right) + p_y^2\tanh\left(\frac{a}{\tau}\right)\right] + v_0\\ &= \frac{1}{4p_v^2}\Bigg[\rho\left(u_s - \frac{a^2}{\tau}\right) + p_x^2\left(a\tan\left(\frac{a}{\tau}\right) - u_s\right)\\ &\quad + p_y^2\left(a\tanh\left(\frac{a}{\tau}\right) - u_s\right)\Bigg] + v_s\,, \quad \lambda_1 = \frac{u_s - \frac{a^2}{\tau}}{2p_v}\,. \quad (5.32)\end{aligned}$$

The associated momenta at the boundaries are

$$P_{I-II} = -2p_v\partial_u - \frac{1}{2p_v}\left(-\rho + p_x^2 + p_y^2\right)\partial_v + p_x\partial_x + p_y\partial_y\,, \tag{5.33}$$

and

$$\begin{aligned} P_{II-III} &= -2p_v\partial_u - \frac{1}{2p_v}\left(-\rho + \frac{p_x^2}{\cos^2\left(\frac{a}{\tau}\right)} + \frac{p_y^2}{\cosh^2\left(\frac{a}{\tau}\right)}\right)\partial_v \\ &\quad + \frac{p_x}{\cos^2\left(\frac{a}{\tau}\right)}\partial_x + \frac{p_y}{\cosh^2\left(\frac{a}{\tau}\right)}\partial_y\,. \end{aligned} \tag{5.34}$$

### 5.2.2 Coordinate transformation in region III

In the flat region III it is convenient to restore Cartesian coordinates. This is practically accomplished by the double mapping $(u, v, x, y) \to (\mathbf{U}, V, X, Y) \to (T, Z, X, Y)$, as specified above, namely
$(u, v, x, y) \to (\mathcal{U}, V, X, Y)$:

$$\begin{aligned} U &= u\,, \quad X = F(u)x\,, \quad Y = G(u)y\,, \\ V &= v + F(u)F'(u)x^2 + G(u)G'(u)y^2\,, \end{aligned} \tag{5.35}$$

and
$(u, v, x, y) \to (\mathcal{U}, V, X, Y)$:

$$T = \frac{\mathcal{U}+V}{2}\,, \quad Z = \frac{V-\mathcal{U}}{2}\,, \quad X = X\,, \quad Y = Y\,. \tag{5.36}$$

Thus in region III we obtain

$$\begin{aligned} X(\mathcal{U}) &= \frac{p_x}{2p_v\beta} + \tilde{x}_1\left(\alpha + \beta\mathcal{U}\right)\,, \qquad Y(\mathcal{U}) = \frac{p_y}{2p_v\delta} + \tilde{y}_1\left(\gamma + \delta\mathcal{U}\right)\,, \\ V(\mathcal{U}) &= -\rho\frac{\mathcal{U}}{4p_v^2} + \tilde{x}_1^2\beta\left(\alpha + \beta\mathcal{U}\right) + \tilde{y}_1^2\delta\left(\gamma + \delta\mathcal{U}\right) \\ &\quad + \frac{p_x}{p_v}\tilde{x}_1 + \frac{p_y}{p_v}\tilde{y}_1 + \tilde{v}_1\,, \qquad U(\lambda) = -2p_v\lambda + u_s\,, \end{aligned} \tag{5.37}$$

which can be presented in the same way as the geodesics in region I, i.e.,

$$\begin{aligned} X(\mathcal{U}) &= -\frac{Q_x}{2Q_v}\mathcal{U} + \tilde{X}_s\,, \qquad Y(\mathcal{U}) = -\frac{Q_y}{2Q_v}\mathcal{U} + \tilde{Y}_s\,, \\ V(\mathcal{U}) &= \frac{1}{4Q_v^2}\left(-\rho + Q_x^2 + Q_y^2\right)\mathcal{U} + \tilde{V}_s\,, \\ \mathcal{U}(\lambda) &= -2Q_v\lambda + \mathcal{U}_s \end{aligned} \tag{5.38}$$

with

$$\begin{aligned} \mathcal{U}_s &= u_s\,, \quad Q_v = p_v\,, \quad Q_x = -2p_v\beta\tilde{x}_1\,, \quad Q_y = -2p_v\delta\tilde{y}_1\,, \\ \tilde{X}_s &= \frac{p_x}{2p_v\beta} + \alpha\tilde{x}_1\,, \quad \tilde{Y}_s = \frac{p_y}{2p_v\delta} + \gamma\tilde{y}_1\,, \\ \tilde{V}_s &= \tilde{v}_1 + \tilde{x}_1\left(\frac{p_x}{p_v} + \alpha\beta\tilde{x}_1\right) + \tilde{y}_1\left(\frac{p_y}{p_v} + \gamma\delta\tilde{y}_1\right)\,. \end{aligned} \tag{5.39}$$

The associated transformed momentum in region III is then

$$\begin{aligned} P_{III} &= -2p_v\Big\{\partial_{\mathcal{U}} + \left[-\frac{\rho}{4p_v^2} + (\beta\tilde{x}_1)^2 + (\delta\tilde{y}_1)^2\right]\partial_V \\ &\qquad + (\beta\tilde{x}_1)\,\partial_X + (\delta\tilde{y}_1)\,\partial_Y\Big\}\,, \end{aligned} \tag{5.40}$$

or equivalently, by using the quantities $Q_v$, $Q_x$, $Q_y$ defined above

$$P_{III} = -2Q_v\partial_{\mathcal{U}} - \frac{1}{2Q_v}\left(-\rho + Q_x^2 + Q_y^2\right)\partial_V + Q_x\partial_X + Q_y\partial_Y\,. \tag{5.41}$$

By passing to the standard Cartesian temporal and spatial coordinates $T, X, Y, Z$ we rewrite the momentum as

$$\begin{aligned} P_{III} &= -Q_v\left[\frac{1}{4Q_v^2}\left(-\rho + Q_x^2 + Q_y^2\right) + 1\right]\partial_T \\ &\qquad -Q_v\left[\frac{1}{4Q_v^2}\left(-\rho + Q_x^2 + Q_y^2\right) - 1\right]\partial_Z + Q_x\partial_X + Q_y\partial_Y\,. \end{aligned} \tag{5.42}$$

With the choice of the parameter $\rho$ we may now specify if we are considering

the null geodesics associated with an electromagnetic wave ($\rho = 0$) or the timelike geodesics representing a massive particle ($\rho = -1$), e.g. the mirrors of a Michelson interferometer.

## 5.3 Scattering of electromagnetic waves by the gravitational wave

We now want to consider the propagation of a test electromagnetic field on the background of an exact gravitational plane wave with single (+) polarization, in order to extend the recent analysis of Finn in [36], in which the gravitational wave has been considered in the linear approximation. Maxwell's equation in the Lorenz gauge

$$\Box A_\alpha \equiv g^{\mu\nu}\nabla_\mu\nabla_\nu A_\alpha = 0\,, \quad \nabla_\mu A^\mu = 0\,. \tag{5.43}$$

can be easily solved for the vector potential $A$, in this case leading to

$$A^\flat = \frac{A_0}{\sqrt{FG}}\, e^{i\phi}\, e^\flat\,. \tag{5.44}$$

This solution represents a field, which is not a wave in general, propagating in a direction associated with positive $v, x, y$ coordinates. Since it is a wave in region I, we will refer to $\phi$ as the phase and $e_\mu$ as the polarization vector of the field also in the other regions.

In general, the phase $\phi$ is given by

$$\phi = \left(\int^u p_u \mathrm{d}u\right) + p_v v + p_x x + p_y y\,, \quad p_u = p_u(u) = \frac{1}{4p_v}\left(\frac{p_x^2}{F^2} + \frac{p_y^2}{G^2}\right)\,, \tag{5.45}$$

and the polarization vector by

$$e^\flat = e_A^\flat \cos(\vartheta) + e_B^\flat \sin(\vartheta)\,, \tag{5.46}$$

which is orthogonal to $p$ and a linear combination of two independent vectors

$e_A$ and $e_B$:

$$e^\flat_A = \frac{p_x}{2p_v F}\mathrm{d}u + F\mathrm{d}x\,, \qquad e^\flat_B = \frac{p_y}{2p_v G}\mathrm{d}u + G\mathrm{d}y\,, \tag{5.47}$$

both also orthogonal to $p$.

The phase $\phi$ is constant along the integral curves of $p$, namely

$$\nabla_p \phi = p^\alpha \partial_\alpha \phi = p^\alpha p_\alpha = 0\,. \tag{5.48}$$

The polarization vector is parallely transported along the integral curves of $p$:

$$\nabla_p e^\flat = 0\,, \tag{5.49}$$

and its contravariant expression is represented by

$$e = -\frac{1}{p_v}\left(\frac{p_x}{F}\cos(\vartheta) + \frac{p_y}{G}\sin(\vartheta)\right)\partial_v + \frac{\cos(\vartheta)}{F}\partial_x + \frac{\sin(\vartheta)}{G}\partial_y\,. \tag{5.50}$$

It should be stressed that the solution found above has associated invariants

$$I_1 = \frac{1}{2}F^{\alpha\beta}F_{\alpha\beta}\,, \qquad I_2 = \frac{1}{2}{}^*F^{\alpha\beta}F_{\alpha\beta} \tag{5.51}$$

given by

$$\begin{aligned} I_1 &= -\frac{4iA_0^2\cos(2\vartheta)(\dot{F}G - \dot{G}F)p_v e^{2i\phi}}{(FG)^2}\,, \\ I_2 &= \frac{4iA_0^2\sin(2\vartheta)(\dot{F}G - \dot{G}F)p_v e^{2i\phi}}{(FG)^2}\,; \end{aligned} \tag{5.52}$$

therefore, in general, this field is nonsingular, even if in the flat spacetime before the passage of the gravitational wave (i.e., in the region I, where $F = 1 = G$) it represents an electromagnetic wave ($I_1 = 0 = I_2$). After the passage of the wave, in the transformed coordinates, we have

$$\lim_{u\to\infty} I_1 = 0 = \lim_{u\to\infty} I_2\,, \tag{5.53}$$

that is, again a wave-like behavior.

For our analysis of the response of the interferometer we have not considered the electromagnetic field inside the wave region since we are only interested in the emerging field. Discussion about the properties of the electromagnetic field in the presence of a linearized gravitational wave can be found for instance in [38] where the wave zone is also treated in analogy with an optically active medium.

### 5.3.1 Electromagnetic field before the passage of the wave: region I

The spacetime before the passage of the wave, corresponding to $F_I = 1 = G_I$, is flat. The metric is

$$\mathrm{d}s^2 = -\mathrm{d}u\mathrm{d}v + \mathrm{d}x^2 + \mathrm{d}y^2, \tag{5.54}$$

and it can be reduced to its standard form by using the transformation in (5.3).

The solution for the vector potential $A$ in this region is

$$A_I^\flat = A_0\, e^{i\phi_I}\, e_I^\flat\,, \tag{5.55}$$

where the phase $\phi_I$ is given by

$$\begin{aligned} \phi_I &= \frac{1}{4p_v}\left(p_x^2 + p_y^2\right) u + p_v v + p_x x + p_y y + C_I \\ &= p_\alpha x^\alpha + C_I\,, \qquad p_\alpha = \text{const.}\,, \end{aligned} \tag{5.56}$$

with $p^\flat = p_\alpha \mathrm{d}x^\alpha$ the null vector seen above and a constant

$$C_I = -\frac{1}{4p_v}(p_x^2 + p_y^2)u_s\,. \tag{5.57}$$

The polarization vector reads

$$e_I = -\frac{1}{p_v}\left[p_x\cos(\vartheta) + p_y\sin(\vartheta)\right]\partial_v + \cos(\vartheta)\partial_x + \sin(\vartheta)\partial_y\,. \tag{5.58}$$

### 5.3.2 Electromagnetic field after the passage of the wave: region III

After the passage of the wave, i.e., when $u > \frac{a^2}{\tau}$, the metric functions are $F_{III} = \alpha + \beta u$ and $G_{III} = \gamma + \delta u$, but the spacetime is still flat. Maxwell's equation is solved by

$$A^\flat_{III} = \frac{A_0}{\sqrt{F_{III}G_{III}}}\, e^{i\phi_{III}}\, e^\flat_{III} = \frac{A_0}{\sqrt{(\alpha+\beta u)(\gamma+\delta u)}}\, e^{i\phi_{III}}\, e^\flat_{III}\,. \tag{5.59}$$

This solution of the Maxwell's equations has a 'phase'

$$\begin{aligned}\phi_{III} &= -\frac{p_x^2}{4p_v\beta(\alpha+\beta u)} - \frac{p_y^2}{4p_v\delta(\gamma+\delta u)} \\ &\quad + p_v v + p_x x + p_y y + C_{III}\,,\end{aligned} \tag{5.60}$$

or equivalently, with the coordinate transformation introduced in (5.35)

$$\begin{aligned}\phi_{III} &= C_{III} + p_v V - \frac{p_v\beta}{\alpha+\beta u}\left(\frac{p_x}{2p_v\beta} - X\right)^2 \\ &\quad - \frac{p_v\delta}{\gamma+\delta u}\left(\frac{p_y}{2p_v\delta} - Y\right)^2\end{aligned} \tag{5.61}$$

with a constant

$$C_{III} = \frac{a}{4p_v}\left(-\frac{p_x^2}{\sin\left(\frac{a}{\tau}\right)\cos\left(\frac{a}{\tau}\right)} + \frac{p_y^2}{\sinh\left(\frac{a}{\tau}\right)\cosh\left(\frac{a}{\tau}\right)}\right)\,. \tag{5.62}$$

The 'phase'in region III, from equation (5.60), is generically a function of the coordinates $u, v, x, y$ (or equivalently, from equation (5.61), of the coordinates $U, V, X, Y$). It is dominated by its value along the null geodesics, namely

$$\begin{aligned}\phi_{III(\mathrm{d})} &= \frac{Q_x^2+Q_y^2}{4Q_v}U + Q_v V + Q_x X + Q_y Y + \tilde{C}_{III} \\ &= Q_\alpha X^\alpha + \tilde{C}_{III}\,,\end{aligned} \tag{5.63}$$

with

$$\tilde{C}_{III} = C_{III} + Q_v \left( \tilde{V}_s - \tilde{v}_1 \right) . \tag{5.64}$$

In fact, let us consider the 'phase'given by (5.61) along a generic curve $X^\alpha = X^\alpha(\lambda)$ as a function of the parameter $\lambda$ along that curve, and require its variation to be vanishing

$$\frac{d}{d\lambda}\phi_{III} = 0 \, , \tag{5.65}$$

in order to determine the dominant part. We find that this extremal condition is satisfied exactly by the null geodesics given by (5.42).

In addition, we can say that even if our general solution for the electromagnetic field after the passage of the gravitational wave is not exactly a plane wave, it is dominated by a plane wave with the wave vector aligned with that of a null geodesic of the background, with the phase given by (5.63).

The 'polarization'vector is given by

$$\begin{aligned} e_{III} &= -\frac{1}{p_v}\left( \frac{p_x}{\alpha+\beta u}\cos(\vartheta) + \frac{p_y}{\gamma+\delta u}\sin(\vartheta) \right)\partial_v \\ &\quad + \frac{\cos(\vartheta)}{\alpha+\beta u}\partial_x + \frac{\sin(\vartheta)}{\gamma+\delta u}\partial_y \, , \end{aligned} \tag{5.66}$$

or, transformed, by

$$\begin{aligned} e_{III} &= \left[ 2\beta\frac{\cos(\vartheta)}{\alpha+\beta\mathcal{U}}\left( X - \frac{p_x}{2p_v\beta} \right) + 2\delta\frac{\sin(\vartheta)}{\gamma+\delta\mathcal{U}}\left( Y - \frac{p_y}{2p_v\delta} \right) \right]\partial_V \\ &\quad + \cos(\vartheta)\partial_X + \sin(\vartheta)\partial_Y \, . \end{aligned} \tag{5.67}$$

Similar to what happens for the 'phase'the 'polarization'vector is also dominated by the corresponding value along the null geodesics as in equation (5.42), in the sense that the $e^X_{III}$ and $e^Y_{III}$ components do not depend on the curve, while the $e^V_{III}$ component reaches its extremal value on the null geodesics, namely

$$e_{III\,(\mathrm{d})} = -\frac{1}{Q_v}\left[ Q_x\cos(\vartheta) + Q_y\sin(\vartheta) \right]\partial_V + \cos(\vartheta)\partial_X + \sin(\vartheta)\partial_Y \, , \tag{5.68}$$

with $\tilde{V}_s$ and $Q_\alpha = \text{const.}$ given by (5.39), where the $Q_\alpha$ are the components

of the dominant wave vector as emerging after the scattering by the gravitational wave. Summarizing, the dominant part of the electromagnetic field can be written as

$$A_{III\,(\mathrm{d})} = A_0 e^{i\phi_{III\,(\mathrm{d})}} e_{III\,(\mathrm{d})} \tag{5.69}$$

and represents the electromagnetic wave emerging after the interaction.

### 5.3.3 Variation in the wave and polarization vector, phase shift

We will now consider the variation in the properties of the electromagnetic wave, by comparing the dominant parts of the solutions before and after the passage of the gravitational wave.

Concerning the covariant components of the wave vector we find $Q_\alpha = p_\alpha + \Delta p_\alpha$ with

$$\begin{aligned}
\Delta p_u &= \left[p_v \frac{x_0^2}{a^2} - \frac{p_x^2}{4p_v}\right] \sin^2\left(\frac{a}{\tau}\right) + \left[p_v \frac{y_0^2}{a^2} + \frac{p_y^2}{4p_v}\right] \sinh^2\left(\frac{a}{\tau}\right) \\
&\quad + p_x \sin\left(\frac{a}{\tau}\right) \cos\left(\frac{a}{\tau}\right) \frac{x_0}{a} - p_y \sinh\left(\frac{a}{\tau}\right) \cosh\left(\frac{a}{\tau}\right) \frac{y_0}{a}\,, \\
\Delta p_x &= 2p_v \sin\left(\frac{a}{\tau}\right) \frac{x_0}{a} - p_x \left[1 - \cos\left(\frac{a}{\tau}\right)\right]\,, \\
\Delta p_y &= -2p_v \sinh\left(\frac{a}{\tau}\right) \frac{y_0}{a} - p_y \left[1 - \cosh\left(\frac{a}{\tau}\right)\right]\,, \qquad \Delta p_v = 0\,,
\end{aligned} \tag{5.70}$$

where equation (5.30) has been used. For the contravariant components of the wave vector we find $Q^\alpha = p^\alpha + \Delta p^\alpha$ with

$$\Delta p^u = 0\,, \quad \Delta p^x = \Delta p_x\,, \quad \Delta p^y = \Delta p_y\,, \quad \Delta p^v = -2\Delta p_u\,. \tag{5.71}$$

The contravariant polarization vector has a variation only in the $v$ component, namely

$$\begin{aligned}
\Delta e_v &= \left(\left[1 - \cos\left(\frac{a}{\tau}\right)\right] \frac{p_x}{p_v} - 2\sin\left(\frac{a}{\tau}\right) \frac{x_0}{a}\right) \cos(\vartheta) \\
&\quad + \left(\left[1 - \cosh\left(\frac{a}{\tau}\right)\right] \frac{p_y}{p_v} + 2\sinh\left(\frac{a}{\tau}\right) \frac{y_0}{a}\right) \sin(\vartheta)\,.
\end{aligned} \tag{5.72}$$

After the passage of the gravitational wave and in terms of the dominant

mode analysis discussed above, the phase of the electromagnetic wave is shifted by

$$\begin{aligned}\Delta\phi &= \phi_{III} - \phi_I = Q_x\tilde{X}_s + Q_y\tilde{Y}_s + Q_v\tilde{V}_s - p_x\tilde{x}_s - p_y\tilde{y}_s - p_v\tilde{v}_s + \tilde{C}_{III} - C_I \\ &= -\frac{a}{4p_v}\left[p_x^2\tan\left(\frac{a}{\tau}\right) + p_y^2\tanh\left(\frac{a}{\tau}\right)\right] + p_v(v_s - v_0)\,. \qquad (5.73)\end{aligned}$$

Note that the transformed coordinates $(\mathcal{U}, V, X, Y)$ are Cartesian, so that the new metric functions are such that $F_{III} = G_{III} = 1$. As a consequence, the amplitude of the dominant part of the electromagnetic field is unaffected by the passage of the gravitational wave.

The existence of an exact solution for the phase shift between the in zone and out zone, where special relativity holds and there is no residual gauge freedom of general relativity, makes us more confident about the physical interpretation of the response of a gravitational interferometer. In this respect, we should also mention that, in the limit of a weak gravitational wave ($a \gg 1$), we recover the results of Rakhmanov in [37]. In this limit mention should also be given to the pioneering work of Mashhoon and Grishchuk [32].

## 5.4 Response of a Michelson interferometer

Let us now consider the motion of photons along $x$ or $y$ axes which represent the direction of the arm of a Michelson interferometer with the beam splitter in the origin [41]. The photons start at the beam-splitter (denoted by $*$) and are reflected once by an end mirror at a distance $L$ from the origin, denoted by small $s$ (we regard the mirrors as fixed and therefore don't consider the timelike geodesics associated with them). At the start of proper time, $\lambda = 0$, the photon is assumed at the generic point $P_{s,x}$ or $P_{s,y}$ on the mirror (where $x_s = L$ and $y_s = 0$ or $x_s = 0$ and $y_s = L$), where the momentum is $p_x$ or $p_y$ in negative $x$ or $y$ direction (towards the origin). In the points $P_{s,x}$ and $P_{s,y}$ we have imposed $v_s = u_s$, thereby ensuring $z_s = 0$. The momenta $p_x$ and $p_y$ are constrained by demanding $z_* = 0$ in the origin, namely

$$p_x = 2p_v\,, \quad p_y = 2p_v\,, \quad p_v < 0\,. \qquad (5.74)$$

The choice of a negative momentum $p_v$ ensures that $u$ increases with $\lambda$.

In this case the parametric equations for the unperturbed photon are

$$\begin{aligned} u &= -2p_v\lambda + u_s\,, \\ x &= \kappa_x\left[(u-u_s)-L\right]\,, \quad y = \kappa_y\left[(u-u_s)-L\right]\,, \quad z = 0\,, \end{aligned} \tag{5.75}$$

where the choice of $\kappa_x$ and $\kappa_y$ distinguishes the motion of photons. A factor $\kappa_x = 1$ signifies the motion of a photon in positive $x$ direction (towards the end-mirror), and $\kappa_x = -1$ the motion in negative $x$ direction (towards the beam splitter). Positive and negative $y$ direction are distinguished along the same lines.

For photons after the interaction we use the parametric equations (5.38) and (5.39) with $p_x$, $x_s$, $p_y$ and $y_s$ defined as above, and we obtain

$$\begin{aligned} \mathcal{U} &= -2p_v\lambda + u_s\,, \\ X &= \kappa_x\left[\frac{Q_x}{2p_v}\mathcal{U} - \tilde{X}_s\right]\,, \quad Y = \kappa_y\left[\frac{Q_y}{2p_v}\mathcal{U} - \tilde{Y}_s\right] \\ Z &= \frac{1}{2}\left[\left(\kappa_x^2\frac{Q_x^2}{4p_v^2} + \kappa_y^2\frac{Q_y^2}{4p_v^2} - 1\right)\mathcal{U} + \tilde{V}_s\right]\,, \end{aligned} \tag{5.76}$$

where

$$\begin{aligned} \tilde{V}_s &= \tilde{v}_1 + \kappa_x^2\tilde{x}_1\left(2+\alpha\beta\tilde{x}_1\right) + \kappa_y^2\tilde{y}_1\left(2+\gamma\delta\tilde{y}_1\right)\,, \\ \tilde{v}_1 &= u_s - \kappa_x^2\left[u_s + a\cot\left(\frac{a}{\tau}\right)\right] - \kappa_y^2\left[u_s - a\coth\left(\frac{a}{\tau}\right)\right]\,. \end{aligned} \tag{5.77}$$

The directions of motion (towards the mirror or the origin, along the $x$ or the $y$ axis) are again specified by the choice of factors $\kappa_x$ and $\kappa_y$.

The motion of the photons emerging from the gravitational wave is dependent on the coordinate time $u_s$ at the start of proper time, the initial momentum $p_v$ of the photon, the interferometer arm length $L$, the curvature

$\frac{1}{a}$ and duration $\tau$ of the gravitational wave; explicitly

$$\begin{aligned}
\tilde{x}_1 &= L + u_s + a\cot\left(\frac{a}{\tau}\right), \quad \tilde{y}_1 = L + u_s - a\coth\left(\frac{a}{\tau}\right), \\
Q_x &= 2p_v\left[\frac{L+u_s}{a}\sin\left(\frac{a}{\tau}\right) + \cos\left(\frac{a}{\tau}\right)\right], \\
Q_y &= -2p_v\left[\frac{L+u_s}{a}\sinh\left(\frac{a}{\tau}\right) - \cosh\left(\frac{a}{\tau}\right)\right], \\
\tilde{X}_s &= \left[L + u_s + \frac{a^2}{\tau}\right]\cos\left(\frac{a}{\tau}\right) + \left[\frac{a}{\tau}(L+u_s) - a\right]\sin\left(\frac{a}{\tau}\right), \\
\tilde{Y}_s &= \left[L + u_s + \frac{a^2}{\tau}\right]\cosh\left(\frac{a}{\tau}\right) - \left[\frac{a}{\tau}(L+u_s) + a\right]\sinh\left(\frac{a}{\tau}\right), \quad (5.78)
\end{aligned}$$

We consider two photons (or photon beams), making the round trip through the interferometer along the $x$ and $y$ axes respectively, and arriving again at the beam splitter afterwards (see Fig. 5.1):

A photon starts from the origin at $u^* = u_s + L$, and we can foresee three possible scenarios

- **Scenario I.** The photons travel from the origin to the mirror unperturbed and are reflected by the mirror (in $P'_{s,x}$ or $P'_{s,y}$) at $u'_s = u_s + 2L$. On the return trip they encounter the gravitational wave, and return to the origin at $\tilde{\mathcal{U}}^{*'}_x$ or $\tilde{\mathcal{U}}^{*'}_y$, respectively.

- **Scenario II.** The photons encounter the gravitational wave on the way to the mirror, where they are reflected at $\tilde{\mathcal{U}}'_{s,x}$ or $\tilde{\mathcal{U}}'_{s,y}$ (depending on the interferometer arm we consider). They return to the origin in the post-wave region and arrive there again at $\tilde{\mathcal{U}}^{*'}_x$ or $\tilde{\mathcal{U}}^{*'}_y$, respectively.

- **Scenario III.** The photons pass the interferometer round trip without encountering the gravitational wave. They are reflected by the mirror (in $P'_{s,x}$ or $P'_{s,y}$) at $u'_s = u_s + 2L$, and arrive in the origin again at $u^{*'} = u_s + 3L$.

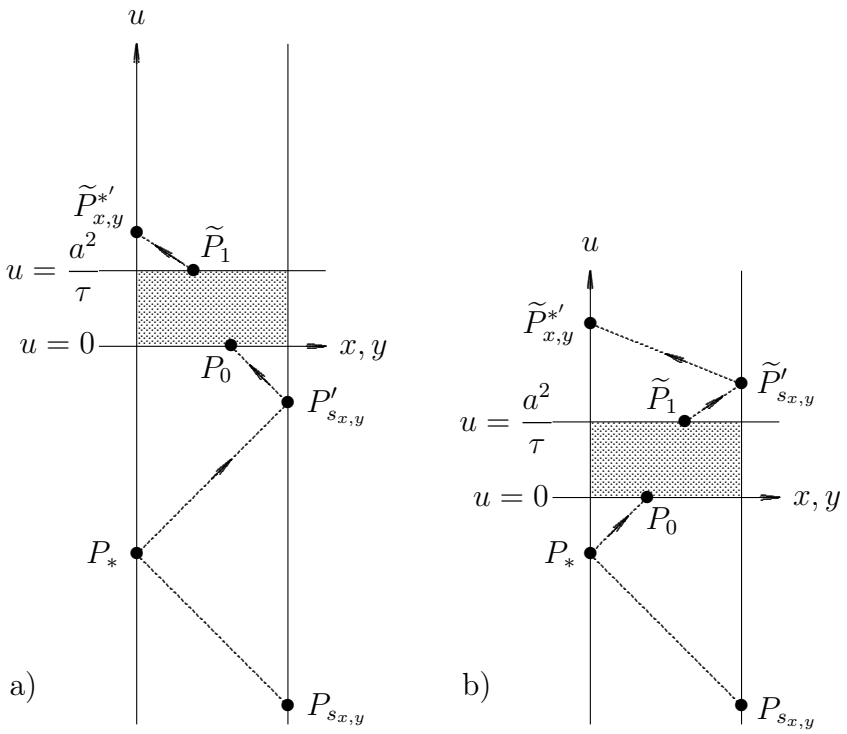


*Fig. 5.1:* The two possible scenarios for the interaction of a photon with a gravitational wave during an interferometer round trip: a) scenario I, and b) scenario II. (The slopes of the geodesics have been exaggerated for graphic depiction.)

The two photons emerging from the gravitational wave experience a deflection in the $Z$ direction of

$$\begin{aligned} \tilde{Z}^{*'}_x &= \frac{1}{2}\left[\left(\frac{Q_x}{p_v}+1\right)L + u_s - \tilde{\mathcal{U}}^{*'}_x\right], \\ \tilde{Z}^{*'}_y &= \frac{1}{2}\left[\left(\frac{Q_y}{p_v}+1\right)L + u_s - \tilde{\mathcal{U}}^{*'}_y\right], \end{aligned} \tag{5.79}$$

respectively, and arrive at the origin at a coordinate time

$$\begin{aligned} \tilde{\mathcal{U}}^{*'}_x &= \frac{a^2}{\tau} + a\frac{2L + (L+u_s)\cos\left(\frac{a}{\tau}\right) - a\sin\left(\frac{a}{\tau}\right)}{(L+u_s)\sin\left(\frac{a}{\tau}\right) + a\cos\left(\frac{a}{\tau}\right)}, \\ \tilde{\mathcal{U}}^{*'}_y &= \frac{a^2}{\tau} - a\frac{2L + (L+u_s)\cosh\left(\frac{a}{\tau}\right) - a\sinh\left(\frac{a}{\tau}\right)}{(L+u_s)\sinh\left(\frac{a}{\tau}\right) - a\cosh\left(\frac{a}{\tau}\right)}. \end{aligned} \tag{5.80}$$

We can regard the path of a single photon traveling through the interferometer as the center of a photon beam. The deflection decreases the intensity of the interference pattern of the two photon beams, but the magnitude of the deflection compared to the cross section of the photon beam is very small, whereas the change in the interference pattern of two photon beams due to their shifted phase is a much greater effect.

It should also be noted that the expressions for the deflection and delay of photons arriving at the origin after the passage of the wave are the same for scenarios I and II. They are distinguished by the relation between $u_s$ and $L$. In scenario I, the photons have to leave the origin at $L < |u^*| < 2L$ to meet the wave on the return trip towards the origin, while in scenario II the photons leave from the origin at $0 < |u^*| < L$ in order to encounter the wave on the way to the mirror.

When the two photon beams arrive at the beam splitter again after the round trip, they have a relative phase shift

$$\Delta\phi = \Delta\phi_x - \Delta\phi_y = p_v a \left[\tanh\left(\frac{a}{\tau}\right) - \tan\left(\frac{a}{\tau}\right)\right] \tag{5.81}$$

between the ingoing electromagnetic wave and the dominant part of the outgoing field, which is the significant response of a Michelson interferometer to the presence of an exact gravitational wave. The relative change in polarization is

$$\begin{aligned} \Delta e_v &= 2\left[1 - \cos\left(\frac{a}{\tau}\right) - \frac{u_s + L}{a}\sin\left(\frac{a}{\tau}\right)\right]\cos(\vartheta) \\ &\quad -2\left[1 - \cosh\left(\frac{a}{\tau}\right) + \frac{u_s + L}{a}\sinh\left(\frac{a}{\tau}\right)\right]\sin(\vartheta)\ . \end{aligned} \tag{5.82}$$

The scenario considered (I or II) is distinguished by the choice of $u_s$ in terms of $L$ as above, yielding different expressions for the relative change in polarization. The relative phase shift depends only on the dimension of the gravitational wave, not on the construction of the interferometer.

No matter how small the physical effects of an exact gravitational wave on an electromagnetic field (represented by the phase shift, the change of the

polarization vector, and the angular deflection and delay of photon beams making the round trip in the interferometer) might be, they could still potentially be measured by way of different detection methods.

# 6. THE SCATTERING OF MASSIVE PARTICLES BY RADIATION FIELDS

Let a massive test particle be scattered by a radiation field filling a spacetime region and imagine that the source of radiation is unknown. For the purpose of the present investigation we have considered three different kinds of radiation: a photon test field in a flat spacetime background, an exact solution of the Einstein field equations for a strong plane gravitational wave (with single polarization state for simplicity), an exact solution of the Einstein-Maxwell equations representing the curved spacetime associated with a plane electromagnetic wave.

The scattering of massive and massless neutral scalar particles by plane gravitational waves has been investigated both in the classical and quantum regime by Garriga and Verdaguer [42]. They also defined the classical cross section for scattering of geodesic particles in the case in which the wave region is sandwiched between two flat spacetime regions. In Chapter 5 we have discussed null and timelike geodesics in a spacetime representing an exact gravitational plane wave with single polarization; the propagation of a test electromagnetic field on this background was also investigated there. It has been shown that the physical effects due to the exact gravitational wave on the electromagnetic field, i.e., phase shift, change of the polarization vector, angular deflection and delay of photon beams in a Michelson interferometer, could be measured by various detection methods [39].

An electromagnetic wave propagating over a spacetime region makes it not empty and not flat. Therefore, the spacetime curvature associated with an electromagnetic pulse, namely the associated gravitational field, induces observable effects on test particle motion. Unlike the case of a plane gravitational wave the resulting motion will no longer be geodesic, but massive

particles will be accelerated by the radiation field filling the associated spacetime region. The features of test particle motion in the gravitational field associated with an electromagnetic plane wave have been recently investigated in [27], where the particles were assumed to interact with the radiation field by absorbing and re-emitting radiation, causing a drag force responsible for deviation from geodesic motion. This radiation scattering process is a Poynting-Robertson-like effect in the full framework of general relativity, as introduced in Chapter 3. The interaction with the radiation field has been modeled there by a force term entering the equations of motion given by the four-momentum density of radiation observed in the particle's rest frame with a multiplicative constant factor expressing the strength of the interaction itself.

In this chapter we will discuss the scattering of massive particles propagating in the field of an exact gravitational plane wave and of an electromagnetic wave in a general relativistic context. In both cases the interaction has a finite duration, and the initial state of the particle is assumed to be the same. The spacetime region containing the radiation field is sandwiched between two Minkowskian zones, so that the "in" and "out" regions are unambiguously determined. The particles will interact differently with the gravitational wave background and the electromagnetic radiation field, and subsequently will emerge in the outer flat region with different four-momenta. The different nature of the host environment will also be evident by comparing the corresponding classical scattering cross sections.

The discussion detailed in this chapter has been published in *Phys. Rev. D* **86**, 064016 (2012) [43].

## *6.1 Scattering of particles by a radiation field in a flat spacetime*

Let us consider a Minkowski spacetime with metric written in either Cartesian or related null coordinates as

$$\mathrm{d}s^2 = -\mathrm{d}t^2 + \mathrm{d}x^2 + \mathrm{d}y^2 + \mathrm{d}z^2 = -2\mathrm{d}u\,\mathrm{d}v + \mathrm{d}x^2 + \mathrm{d}y^2\,, \qquad (6.1)$$

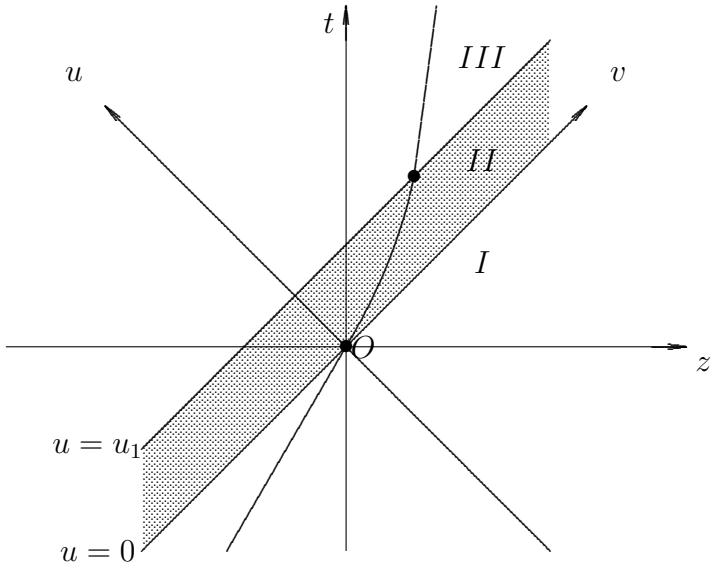


*Fig. 6.1:* The null coordinate relationships in the $t - z$ plane (orthogonal to the plane wave fronts aligned with the $x - y$ planes) for a sandwich spacetime divided into three zones by the null hypersurfaces $u = 0$ and $u = u_1 > 0$. Shown also is a suggestive world line of a particle (entering zone II at the origin of coordinates) which is deflected by the radiation field in zone II from its geodesic motion in zones I and III.

where $u = (t - z)/\sqrt{2}\,,\ v = (t + z)/\sqrt{2}\,$. The latter form privileges the three Killing vectors $\partial_v, \partial_x, \partial_y$ which will remain when a wave zone is introduced later where the metric will depend on $u$. Fig. 6.1 illustrates the relationships between the coordinates for the case of an interaction strip corresponding to a $u$ coordinate interval $[0, u_1]$.

It is also useful to introduce a family of "static" fiducial observers which are at rest with respect to the spatial coordinates $(x, y, z)$ and characterized by the 4-velocity vector $m = \partial_t$ with the associated adapted orthonormal spatial triad $e_{\hat{x}} = \partial_x$, $e_{\hat{y}} = \partial_y$, $e_{\hat{z}} = \partial_z$.

A test particle with rest mass $\mu$ and four-velocity $U^\alpha = \mathrm{d}x^\alpha/\mathrm{d}\tau$ (so $U \cdot U = -1$) has four-momentum $P = \mu U$, but we will use the specific four-momentum, namely the four-velocity itself: $\tilde{P} = P/\mu = U$; we drop the tilde

notation below and the modifier "specific." The observer decomposition of $U$ is then (let $a, b, c = 1, 2, 3$)

$$U = U^\alpha \partial_\alpha = \gamma(m + \nu^{\hat{a}} e_{\hat{a}}) \,, \;\; \gamma = (1 - \delta_{\hat{a}\hat{b}} \nu^{\hat{a}} \nu^{\hat{b}})^{-1/2} \,. \tag{6.2}$$

For geodesic motion, the constant four-velocity $U = U_{(0)}$ can be parametrized in terms of the conserved specific momenta $p_v$, $p_x$ and $p_y$ (introducing as well $p_\perp^2 = p_x^2 + p_y^2$) associated with the three Killing vectors mentioned above as

$$\begin{aligned} U_{(0)} &= -p_v \left( \partial_u + \frac{1 + p_\perp^2}{2p_v^2} \partial_v \right) + p_x \partial_x + p_y \partial_y \\ &= -\frac{1}{\sqrt{2}} p_v \left( 1 + \frac{1 + p_\perp^2}{2p_v^2} \right) \partial_t + p_x \partial_x + p_y \partial_y \\ &\quad -\frac{p_v}{\sqrt{2}} \left( -1 + \frac{1 + p_\perp^2}{2p_v^2} \right) \partial_z \,, \end{aligned} \tag{6.3}$$

where $p_v < 0$ for $U$ to be future-pointing. Then the velocity decomposition is

$$\begin{aligned} \gamma_{(0)} &= -\frac{p_v}{\sqrt{2}} \left( 1 + \frac{1 + p_\perp^2}{2p_v^2} \right) \,, \\ \nu_{(0)}^{\hat{x}} &= \frac{p_x}{\gamma_{(0)}} \,, \quad \nu_{(0)}^{\hat{y}} = \frac{p_y}{\gamma_{(0)}} \,, \quad \nu_{(0)}^{\hat{z}} = -\frac{p_v}{\sqrt{2}\gamma_{(0)}} \left( -1 + \frac{1 + p_\perp^2}{2p_v^2} \right) \,, \end{aligned} \tag{6.4}$$

which can be easily inverted to yield

$$p_v = -\frac{\gamma_{(0)}}{\sqrt{2}} (1 - \nu_{(0)}^{\hat{z}}) \,, \qquad p_x = \gamma_{(0)} \nu_{(0)}^{\hat{x}} \,, \qquad p_y = \gamma_{(0)} \nu_{(0)}^{\hat{y}} \,. \tag{6.5}$$

Choosing the zero of proper time at the $u = 0$ hyperplane, the corresponding parametric equations of the particle's straight line trajectory are then

$$\begin{aligned} u &= -p_v \tau \,, \qquad v = \frac{1 + p_\perp^2}{2p_v^2} u + v_0 \,, \\ x &= -\frac{p_x}{p_v} u + x_0 \,, \qquad y = -\frac{p_y}{p_v} u + y_0 \,, \end{aligned} \tag{6.6}$$

so that $x_0 = y_0 = z_0 = 0$ puts the initial position at the origin of coordinates and

$$\begin{aligned} t &= \frac{1}{\sqrt{2}}\left[\left(\frac{1+p_\perp^2}{2p_v^2}+1\right)u + v_0\right], \\ z &= \frac{1}{\sqrt{2}}\left[\left(\frac{1+p_\perp^2}{2p_v^2}-1\right)u + v_0\right]. \end{aligned} \tag{6.7}$$

Correspondingly, a photon following a null geodesic path has four-momentum

$$K = -K_v\partial_u - K_u\partial_v + K_x\partial_x + K_y\partial_y\,, \tag{6.8}$$

where the null condition is $2K_uK_v = K_\perp^2 \equiv K_x^2 + K_y^2$. For the special case of photons traveling along the positive $z$ direction, one has $K_x = K_y = K_v = 0$ and $K = -K_u\partial_v$, useful for comparison with the nonflat case below.

The observer decomposition is

$$K = \omega_K(m + \hat{\nu}_K)\,, \qquad \hat{\nu}_K = \hat{\nu}_K^a\partial_a\,, \qquad \hat{\nu}_K\cdot\hat{\nu}_K = 1\,, \tag{6.9}$$

where $\omega_K = K^t = -K_t = -(K_u + K_v)/\sqrt{2}$ is the relative energy and the unit vector $\hat{\nu}_K^a = K^a/K^t$ gives the relative direction of propagation with respect to the static observers.

Suppose now that a test radiation field representing a coherent beam of a given frequency fills a certain spacetime region confined to the region between two null hypersurfaces $u = 0$ and $u = u_1$ as in Fig. 6.1. The associated energy-momentum tensor is assumed to be of the form

$$T = \phi_0 K\otimes K\,, \tag{6.10}$$

where $K$ is the geodesic null vector given by (6.8) and $\phi_0$ is a constant representing the associated energy flux. The geodesic property of $K$ makes $T$ divergence-free, i.e., $\nabla_\alpha T^{\alpha\beta} = 0$.

A neutral massive particle moving through the spacetime region occupied by such a radiation field will be scattered in a way which depends on the interaction. The simplest way to model this interaction is through the

introduction of a "radiation force," which is constructed from the energy-momentum tensor introduced in (6.10) and is orthogonal to the particle's four-velocity $U$ (just as the 4-acceleration vector), so that

$$f_{(\mathrm{rad})}(U)_\alpha = -\sigma P(U)_{\alpha\beta} T^\beta{}_\mu U^\mu \,, \tag{6.11}$$

where $P(U) = g + U \otimes U$ is the orthogonal projector to $U$ and $\sigma$ models the absorption and re-emission of radiation by the test particle. This force is just proportional to the momentum of the field as observed in the rest frame of the particle. The equations of motion of the particle thus become

$$\mu a(U)^\alpha = f_{(\mathrm{rad})}(U)^\alpha \,, \qquad a(U)^\alpha = \nabla_U U^\alpha \,, \tag{6.12}$$

or explicitly

$$\frac{\mathrm{d}U^\alpha}{\mathrm{d}\tau} = -A[K^\alpha + U^\alpha (U \cdot K)](U \cdot K) \,, \qquad A = \sigma\phi_0/\mu \equiv \tilde{\sigma}\phi_0 \,. \tag{6.13}$$

In the case of a particle orbiting a massive source in the presence of a superimposed radiation field, an interaction of this kind leads to a drag force causing deviation from geodesic motion. This is the so called Poynting-Robertson effect (see Refs. [16, 17, 22, 23] and references therein).

The equations of motion (6.13) then become

$$\frac{\mathrm{d}\nu^{\hat{a}}}{\mathrm{d}\tau} = -A\omega_K^2 (\nu^{\hat{a}} - \nu_K^{\hat{a}})(1 - \nu_{K\hat{b}}\nu^{\hat{b}}) \,, \tag{6.14}$$

whose solution is straightforward assuming $\tau = 0$ at the initial null hyperplane $u = 0$ where $\nu^{\hat{a}} = \nu^{\hat{a}}_{(0)}$,

$$\nu^{\hat{a}} = \nu_K^{\hat{a}} + \frac{\nu^{\hat{a}}_{(0)} - \nu_K^{\hat{a}}}{\left[1 + \tau A\omega_K^2 (1 - \nu_{K\hat{c}}\nu^{\hat{c}}_{(0)})\right]} \,, \tag{6.15}$$

which can be simplified by introducing the parameter $1/\tau_* = A\omega_K^2(1 -$

$\nu_{K\hat{c}}\nu^{\hat{c}}_{(0)}$) to yield

$$\nu^{\hat{a}} = \nu^{\hat{a}}_K + \frac{\nu^{\hat{a}}_{(0)} - \nu^{\hat{a}}_K}{1+\tau/\tau_*}\,, \qquad \gamma = \gamma_{(0)}\frac{1+\tau/\tau_*}{\sqrt{1+2\gamma^2_{(0)}(1-\nu_{K\hat{c}}\nu^{\hat{c}}_{(0)})\tau/\tau_*}}\,. \quad (6.16)$$

The parametric equations for the test particle's trajectory during the interaction with the radiation field are then obtained by integrating the equations $\mathrm{d}x^\alpha/\mathrm{d}\tau = U^\alpha$, i.e.,

$$\frac{\mathrm{d}t}{\mathrm{d}\tau} = \gamma\,, \quad \frac{\mathrm{d}x^{\hat{a}}}{\mathrm{d}\tau} = \gamma\nu^{\hat{a}}\,. \quad (6.17)$$

By introducing the notation

$$\mathcal{I}(a,b,c,d;\xi) \equiv \int_0^\xi \frac{a+b\xi'}{\sqrt{c+d\xi'}}\,\mathrm{d}\xi' = \frac{2}{3d^2}(3ad-2bc+db\xi')\,\sqrt{c+d\xi'}\Big|_0^\xi\,, \quad (6.18)$$

the corresponding solution can be explicitly written in the form

$$\begin{aligned} t - t_0 &= \gamma_{(0)}\,\mathcal{I}\left(1, 1/\tau_*, 1, 2\gamma^2_{(0)}(1-\nu_{K\hat{c}}\nu^{\hat{c}}_{(0)})/\tau_*; \tau\right)\,, \\ x^a - x^a_0 &= \gamma_{(0)}\,\mathcal{I}\left(\nu^{\hat{a}}_{(0)}, \nu^{\hat{a}}_K/\tau_*, 1, 2\gamma^2_{(0)}(1-\nu_{K\hat{c}}\nu^{\hat{c}}_{(0)})/\tau_*; \tau\right)\,, \end{aligned} \quad (6.19)$$

where the quantities $\gamma_{(0)}$, $\nu^{\hat{a}}_{(0)}$ and $x^\alpha_0$ refer to the (constant) frame components of the particle four-velocity at the start of the interaction and the initial position there.

In the simplest case of a radiation field composed of photons all propagating along the $z$ direction, i.e., with $\hat{\nu}^a_K = \delta^a_z$ and $K = \sqrt{2}\omega_K\partial_v$ the radiation force is

$$\begin{aligned} \frac{1}{\mu}f_{(\mathrm{rad})}(U) &= -A\,\omega_K^2\gamma(1-\nu^{\hat{z}})\Big\{[\gamma^2(1-\nu^{\hat{z}})-1]m \\ &\quad +\gamma^2(1-\nu^{\hat{z}})(\nu^{\hat{x}}e_{\hat{x}} + \nu^{\hat{y}}e_{\hat{y}}) - [\gamma^2\nu^{\hat{z}}(\nu^{\hat{z}}-1)+1]e_{\hat{z}}\Big\}\,, \end{aligned} \quad (6.20)$$

and the general solution (6.16) becomes

$$\begin{aligned} \gamma &= \frac{\gamma_{(0)}}{\Sigma}[1 + A\omega_K^2(1-\nu_{(0)}^{\hat{z}})\tau]\,, \\ \left[\nu^{\hat{x}}, \nu^{\hat{y}}, 1-\nu^{\hat{z}}\right] &= \frac{\gamma_{(0)}}{\gamma\Sigma}\left[\nu_{(0)}^{\hat{x}}, \nu_{(0)}^{\hat{y}}, 1-\nu_{(0)}^{\hat{z}}\right]\,, \end{aligned} \tag{6.21}$$

where $\Sigma = \sqrt{1 + 2A\omega_K^2\gamma_{(0)}^2(1-\nu_{(0)}^{\hat{z}})^2\tau}$. The parametric equations (6.19) of the accelerated orbit then simplify to

$$\begin{aligned} t - t_0 &= \frac{1}{3\gamma_{(0)}(1-\nu_{(0)}^{\hat{z}})}\left[\Sigma\tau - \frac{\Sigma-1}{A\omega_K^2\gamma_{(0)}^2(1-\nu_{(0)}^{\hat{z}})^2}(1-3\gamma_{(0)}^2(1-\nu_{(0)}^{\hat{z}}))\right]\,, \\ x - x_0 &= \nu_{(0)}^{\hat{x}}\frac{\Sigma-1}{A\omega_K^2\gamma_{(0)}(1-\nu_{(0)}^{\hat{z}})^2}\,, \quad y - y_0 = \nu_{(0)}^{\hat{y}}\frac{\Sigma-1}{A\omega_K^2\gamma_{(0)}(1-\nu_{(0)}^{\hat{z}})^2}\,, \\ z - z_0 &= \frac{1}{3\gamma_{(0)}(1-\nu_{(0)}^{\hat{z}})}\left[\Sigma\tau - \frac{\Sigma-1}{A\omega_K^2\gamma_{(0)}^2(1-\nu_{(0)}^{\hat{z}})^2}\right. \\ &\quad \left.\times(1-3\gamma_{(0)}^2(1-\nu_{(0)}^{\hat{z}})\nu_{(0)}^{\hat{z}})\right]\,. \end{aligned} \tag{6.22}$$

The corresponding solutions for $u$ and $v$ are given by

$$\begin{aligned} u &= \frac{\Sigma-1}{\sqrt{2}A\omega_K^2\gamma_{(0)}(1-\nu_{(0)}^{\hat{z}})}\,, \\ v - v_0 &= \frac{\sqrt{2}}{3\gamma_{(0)}(1-\nu_{(0)}^{\hat{z}})}\left[\Sigma\tau - \frac{\Sigma-1}{A\omega_K^2\gamma_{(0)}^2(1-\nu_{(0)}^{\hat{z}})^2}\right. \\ &\quad \left.\times\left(1 - \frac{3}{2}\gamma_{(0)}^2(1-{\nu_{(0)}^{\hat{z}}}^2)\right)\right]\,. \end{aligned} \tag{6.23}$$

The parametric equations for the orbit using $u$ as parameter and re-expressing the initial 3-velocity quantities in terms of the initial momenta

are then given by

$$\begin{aligned} u &= \frac{1}{2p_v A\omega_K^2}\left(1-\sqrt{1+4p_v^2 A\omega_K^2\tau}\right), \\ v-v_0 &= \frac{u}{2p_v^2}(1+p_\perp^2)-\frac{A\omega_K^2 u^2}{p_v}\left(1-\frac{2}{3}p_v A\omega_K^2 u\right), \\ x-x_0 &= -\frac{p_x}{p_v}u\,, \qquad y-y_0=-\frac{p_y}{p_v}u\,, \end{aligned} \tag{6.24}$$

where

$$\tau_1 = -\frac{u_1}{p_v}(1-p_v A\omega_K^2 u) \tag{6.25}$$

relates the proper time interval of the interaction to the interval $u_1$. The associated four-velocity is

$$U = e^{-\zeta_{(\mathrm{tf})}(u)}\left[-p_v\partial_u - \frac{1}{2p_v}\left(e^{2\zeta_{(\mathrm{tf})}(u)}+p_\perp^2\right)\partial_v + p_x\partial_x + p_y\partial_y\right], \tag{6.26}$$

where we have introduced the notation ("tf" for test field)

$$e^{\zeta_{(\mathrm{tf})}(u)} = 1-2p_v A\omega_K^2 u\,. \tag{6.27}$$

This quantity, evaluated at $u=u_1$ ($\tau=\tau_1$) where the interaction with the wave ends, should be compared with the initial four-velocity $U_{(0)}$, at $u=0$ ($\tau=0$), given in (6.3). In this case, since the spacetime is flat everywhere, we can image $U_{(0)}$ (trivially) parallely transported along the particle trajectory up to the same spacetime point where $U$ is located, at the end of the interaction. The comparison then results in a boost relating these two vectors, namely

$$U = \gamma(U,U_{(0)})\Big[U_{(0)} + ||\nu(U,U_{(0)})||\hat{\nu}(U,U_{(0)})\Big], \tag{6.28}$$

with the spacelike unit direction-vector of the relative velocity (notation: $U$ with respect to $U_{(0)}$) given by

$$\hat{\nu}(U,U_{(0)}) = -\frac{P(U_{(0)})\partial_v}{p_v} = -\frac{1}{p_v}\partial_v - U_{(0)} = -\frac{1}{\sqrt{2}\omega_K p_v}K - U_{(0)}\,, \tag{6.29}$$

where $P(U_{(0)})$ projects orthogonally to $U_{(0)}$ and $K = \omega_K(\partial_t + \partial_z) = \sqrt{2}\omega_K \partial_v$ is the photon field. The relative speed is instead

$$||\nu(U, U_{(0)})|| = \tanh(\zeta_{(\mathrm{tf})}(u_1)) \,, \tag{6.30}$$

demonstrating that $\zeta_{(\mathrm{tf})}(u)$ can be interpreted as the rapidity boost parameter for the four-velocity relative to the initial four-velocity. Note that this shows that $U$ lies in the plane of $U_{(0)}$ and $K$. In other words the final specific momentum $U$ is just the result of a boost of the initial specific momentum $U_{(0)}$ along the direction of the relative velocity of the wave vector of the radiation field with respect to it.

This simple analysis can be easily generalized to a sandwich spacetime in which the plane wave zone is a portion of an electrovac plane-wave spacetime in between two flat spacetime regions as above, either representing the exact gravitational field due to an electromagnetic plane wave or to a gravitational plane wave. The resulting change in four-momentum or four-velocity of the test particle from $u = 0$ to $u = u_1$ can then be compared with the flat spacetime case with either no interaction or an interaction with a test electromagnetic field as just evaluated. While the scattering by a gravitational plane wave is well known, the electrovac case is not, nor has any comparison been made with the Poynting-Robertson-like interaction, as we will do below.

## 6.2 Scattering of particles by a gravitational plane wave

Consider the interaction of a test particle with a gravitational radiation field described by the spacetime metric of an exact gravitational plane wave with a single polarization state (+ state) [44] traveling in the positive $z$ direction orthogonal to the symmetry planes (with the same relationship between the coordinates as above)

$$\begin{aligned} \mathrm{d}s^2 &= -\mathrm{d}t^2 + F(u)^2\mathrm{d}x^2 + G(u)^2\mathrm{d}y^2 + \mathrm{d}z^2 \\ &= -2\mathrm{d}u\mathrm{d}v + F(u)^2\mathrm{d}x^2 + G(u)^2\mathrm{d}y^2 \,, \end{aligned} \tag{6.31}$$

with

$$F(u) = \cos(b_{(\mathrm{gw})}u)\,, \qquad G(u) = \cosh(b_{(\mathrm{gw})}u)\,, \tag{6.32}$$

where $\omega_{(\mathrm{gw})} = b_{(\mathrm{gw})}/\sqrt{2}$ is the frequency of the gravitational wave under consideration, and $s = b_{(\mathrm{gw})}u = \omega_{(\mathrm{gw})}(t-z)$ is a convenient combination used below. [1] We continue to use the same static frame as in the flat case.

The gravitational wave is sandwiched between two Minkowskian regions $u \in (-\infty, 0) \cup (u_1, \infty)$, and the metric would have a coordinate horizon at $b_{(\mathrm{gw})}u = \frac{\pi}{2}$ where the metric is degenerate but this is avoided by restricting the coordinate $u$ to the interval $[0, u_1]$ with $b_{(\mathrm{gw})}u_1 < \frac{\pi}{2}$. The matching conditions impose restrictions on the metric functions $F$ and $G$ before and after the passage of the wave where the spacetime is Minkowskian. As discussed in detail by Rindler in [4], a possible choice to extend the metric for all values of $u$ is the following

$$\begin{array}{ccc} & F & G \\ \text{(I)} & 1 & 1 \\ \text{(II)} & \cos(b_{(\mathrm{gw})}u) & \cosh(b_{(\mathrm{gw})}u) \\ \text{(III)} & (\alpha + \beta u) & (\gamma + \delta u) \end{array} \tag{6.33}$$

where labels I, II and III refer to the in zone ($u \leq 0$), the wave zone ($0 < u < u_1$) and the out zone ($u \geq u_1$), respectively. Values of the constants $\alpha$, $\beta$, $\gamma$ and $\delta$ can be completely determined by requiring $C^1$ regularity conditions at the boundaries $u = 0$ and $u = u_1$ of the sandwich, that is

$$\begin{aligned} &F(0) = 1 = G(0)\,, && F'(0) = 0 = G'(0)\,, \\ &F(u_1) = \alpha + \beta u_1\,, && G(u_1) = \gamma + \delta u_1\,, \\ &F'(u_1) = \beta\,, && G'(u_1) = \delta\,, \end{aligned} \tag{6.34}$$

[1] The discussion of the particle motion in inertial coordinates detailed below recalls some of the results already discussed in Sec. 5.2, but in a gravitational wave spacetime with more general metric functions and in a slightly different null coordinate system.

which in this case imply

$$\begin{aligned}
\alpha &= \cos(b_{(\mathrm{gw})}u_1) + b_{(\mathrm{gw})}u_1 \sin(b_{(\mathrm{gw})}u_1)\,, \qquad \beta = -b_{(\mathrm{gw})} \sin(b_{(\mathrm{gw})}u_1)\,, \\
\gamma &= \cosh(b_{(\mathrm{gw})}u_1) - b_{(\mathrm{gw})}u_1 \sinh(b_{(\mathrm{gw})}u_1)\,, \\
\delta &= b_{(\mathrm{gw})} \sinh(b_{(\mathrm{gw})}u_1)\,. \qquad (6.35)
\end{aligned}$$

Let us consider the wave region (II), with functions $F$ and $G$ given by (6.32). As in the flat spacetime case, a test particle with mass $\mu$ entering the wave region follows a geodesic path with four-velocity $U$ and associated four-momentum $P = \mu U$ given by (see, e.g., Ref. [12])

$$U = -p_v \partial_u - \frac{1}{2p_v}\left(1 + \frac{p_x^2}{F(u)^2} + \frac{p_y^2}{G(u)^2}\right)\partial_v + \frac{p_x}{F(u)^2}\partial_x + \frac{p_y}{G(u)^2}\partial_y\,, \quad (6.36)$$

where the conserved specific momenta $p_v$, $p_x$ and $p_y$ still allow the complete integration of the geodesic equations. Using the explicit form of the metric functions $F$ and $G$ valid in the wave zone and imposing the matching at the boundary I–II where the geodesics join at the spacetime point with coordinates $(0, v_0, x_0, y_0)$ then gives

$$\begin{aligned}
u &= -p_v \tau\,, \quad v = \frac{1}{2p_v^2}\left(u + \frac{p_x^2}{b_{(\mathrm{gw})}} \tan(b_{(\mathrm{gw})}u) + \frac{p_y^2}{b_{(\mathrm{gw})}} \tanh(b_{(\mathrm{gw})}u)\right) + v_0\,, \\
x &= -\frac{p_x}{b_{(\mathrm{gw})}p_v} \tan(b_{(\mathrm{gw})}u) + x_0\,, \quad y = -\frac{p_y}{b_{(\mathrm{gw})}p_v} \tanh(b_{(\mathrm{gw})}u) + y_0\,. \quad (6.37)
\end{aligned}$$

Clearly, these geodesic world lines should be matched with the straight lines of the in zone at $u = 0$.

The geodesic four-velocity in the inertial coordinates and with the metric functions conveniently re-expressed in terms of $s = \omega_{(\mathrm{gw})}(t - z)$ is

$$\begin{aligned}
U &= -\frac{p_v}{\sqrt{2}}\left[1 + \frac{1}{2p_v^2}\left(1 + \frac{p_x^2}{\cos^2 s} + \frac{p_y^2}{\cosh^2 s}\right)\right]\partial_t + \frac{p_x}{\cos^2 s}\partial_x + \frac{p_y}{\cosh^2 s}\partial_y \\
&\quad -\frac{p_v}{\sqrt{2}}\left[-1 + \frac{1}{2p_v^2}\left(1 + \frac{p_x^2}{\cos^2 s} + \frac{p_y^2}{\cosh^2 s}\right)\right]\partial_z\,. \qquad (6.38)
\end{aligned}$$

Coordinate and frame components of the four-velocity are now related by

$$U^t = \gamma\,, \quad \frac{U^x}{U^t} = \frac{\nu^{\hat{x}}}{\cos s}\,, \quad \frac{U^y}{U^t} = \frac{\nu^{\hat{y}}}{\cosh s}\,, \quad \frac{U^z}{U^t} = \nu^{\hat{z}}\,. \tag{6.39}$$

Using the relations (6.5) at $s = 0$ to express the Killing constants $(p_v, p_x, p_y)$ in terms of the initial values $\nu^{\hat{a}}_{(0)} \equiv \nu^{\hat{a}}(0)$ at the start of the interaction, one finds with some manipulation

$$\begin{aligned} \gamma &= \frac{\gamma_{(0)}}{2(1-\nu^{\hat{z}}_{(0)})}\frac{V(s)}{\cos^2 s\cosh^2 s}\,, \\ \left[\nu^{\hat{x}}, \nu^{\hat{y}}, 1-\nu^{\hat{z}}\right] &= 2(1-\nu^{\hat{z}}_{(0)})\frac{\cos s\cosh s}{V(s)} \\ &\quad \times \left[\nu^{\hat{x}}_{(0)}\cosh s, \nu^{\hat{y}}_{(0)}\cos s, (1-\nu^{\hat{z}}_{(0)})\cos s\cosh s\right]\,, \end{aligned} \tag{6.40}$$

where

$$V(s) = \left[2(1-\nu^{\hat{z}}_{(0)})\cos^2 s + {\nu^{\hat{x}}_{(0)}}^2\sin^2 s\right]\cosh^2 s - {\nu^{\hat{y}}_{(0)}}^2\cos^2 s\sinh^2 s\,. \tag{6.41}$$

Finally, the parametric equations for the particle's geodesic orbit are

$$\begin{aligned} t - t_0 &= \frac{1}{\omega_{(\mathrm{gw})}(1-\nu^{\hat{z}}_{(0)})}\left[\left(1 - \frac{{\nu^{\hat{x}}_{(0)}}^2 + {\nu^{\hat{y}}_{(0)}}^2}{2(1-\nu^{\hat{z}}_{(0)})}\right)s\right. \\ &\quad \left. + \frac{{\nu^{\hat{x}}_{(0)}}^2\tan s + {\nu^{\hat{y}}_{(0)}}^2\tanh s}{2(1-\nu^{\hat{z}}_{(0)})}\right]\,, \qquad x - x_0 = \frac{\nu^{\hat{x}}_{(0)}\tan s}{\omega_{(\mathrm{gw})}(1-\nu^{\hat{z}}_{(0)})}\,, \\ z - z_0 &= \frac{1}{\omega_{(\mathrm{gw})}(1-\nu^{\hat{z}}_{(0)})}\left[\left(\nu^{\hat{z}}_{(0)} - \frac{{\nu^{\hat{x}}_{(0)}}^2 + {\nu^{\hat{y}}_{(0)}}^2}{2(1-\nu^{\hat{z}}_{(0)})}\right)s\right. \\ &\quad \left. + \frac{{\nu^{\hat{x}}_{(0)}}^2\tan s + {\nu^{\hat{y}}_{(0)}}^2\tanh s}{2(1-\nu^{\hat{z}}_{(0)})}\right]\,, \qquad y - y_0 = \frac{\nu^{\hat{y}}_{(0)}\tanh s}{\omega_{(\mathrm{gw})}(1-\nu^{\hat{z}}_{(0)})}\,, \\ s &= \omega_{(\mathrm{gw})}\gamma_{(0)}(1-\nu^{\hat{z}}_{(0)})\tau\,, \end{aligned} \tag{6.42}$$

where $(t_0, x_0, y_0, z_0)$ denote the coordinates of the spacetime point where the interaction between the test particle and the gravitational wave starts.

## 6.3 Scattering of particles by an electromagnetic plane wave

Now instead let the test particle interact with a photon radiation field in the gravitational field generated by an electromagnetic plane wave propagating along the positive $z$ axis exactly as in the flat spacetime case in Sec. 6.1. The corresponding conformally flat line element found by Griffiths [15] is given by (6.31) with functions

$$F = \cos(b_{(\mathrm{em})}u) = G\,, \tag{6.43}$$

differing from the corresponding gravitational wave case only by a trigonometric rather than hyperbolic cosine appearing in $G$, so that the above analysis with the additional interaction with the radiation field is easily repeated as done in Ref. [27], allowing a comparison between these two cases as well as with the flat one. However, the present case corresponds to a nonvacuum spacetime which is a solution of the Einstein equations with energy-momentum tensor

$$T = \phi_0 K \otimes K\,, \quad K = b_{(\mathrm{em})}\partial_v = \sqrt{2}\omega_{(\mathrm{em})}\partial_v\,, \tag{6.44}$$

where $\phi_0 = 1/4\pi$ and $\omega_{(\mathrm{em})}$ is the frequency of the wave. This corresponds to the flat case of Sec. 6.1 with $K_u < 0$ and $K_x = K_y = K_v = 0$ and $\omega_{(\mathrm{em})} = \omega_K$, which makes the energy-momentum tensors agree. For convenience we introduce the parameter $s = b_{(\mathrm{em})}u = \omega_{(\mathrm{em})}(t - z)$.

As in the previous section, the metric would have a coordinate horizon at $b_{(\mathrm{em})}u = \pi/2$ but this is avoided by restricting the coordinate $u$ to the interval $[0, u_1]$ with $u_1 < \pi/(2b_{(\mathrm{em})})$. Similarly let the electromagnetic wave spacetime be sandwiched between two Minkowskian regions $u \in (-\infty, 0) \cup (u_1, \infty)$, again as in Fig. 6.1. The matching conditions (6.34) at the two null hypersurface boundaries now imply

$$\begin{aligned} \alpha &= \cos(b_{(\mathrm{em})}u_1) + b_{(\mathrm{em})}u_1 \sin(b_{(\mathrm{em})}u_1) = \gamma\,, \\ \beta &= -b_{(\mathrm{em})} \sin(b_{(\mathrm{em})}u_1) = \delta\,. \end{aligned} \tag{6.45}$$

Again consider the behavior of neutral test particles in such a spacetime with the additional interaction with the radiation field deflecting them from geodesic motion. However, now the radiation field is not a test field superimposed on a given gravitational background, so that the treatment is self-consistent.

The observer decomposition of the radiation force of equations (6.11) and (6.12) is formally the same as in equation (6.20), with $\omega_K$ replaced by $\omega_{(\mathrm{em})}$ and the parameter $A$ defined as in equation (6.13). The flat spacetime equations of motion (6.14) with $\nu^{\hat{a}}_K = \delta^{\hat{a}}_{\hat{z}}$ acquire an extra term proportional to $\omega_{(\mathrm{em})}$ which now explicitly depends on the coordinate $u$ through $s$,

$$\begin{aligned}
\frac{\mathrm{d}\nu^{\hat{x}}}{\mathrm{d}\tau} &= -A\,\omega^2_{(\mathrm{em})}(1-\nu^{\hat{z}})\nu^{\hat{x}} - \omega_{(\mathrm{em})}\gamma\nu^{\hat{x}}\tan s\,(\nu^{\hat{x}2}+\nu^{\hat{y}2}+\nu^{\hat{z}}-1)\,,\\
\frac{\mathrm{d}\nu^{\hat{y}}}{\mathrm{d}\tau} &= -A\,\omega^2_{(\mathrm{em})}(1-\nu^{\hat{z}})\nu^{\hat{y}} - \omega_{(\mathrm{em})}\gamma\nu^{\hat{y}}\tan s\,(\nu^{\hat{x}2}+\nu^{\hat{y}2}+\nu^{\hat{z}}-1)\,,\\
\frac{\mathrm{d}\nu^{\hat{z}}}{\mathrm{d}\tau} &= A\,\omega^2_{(\mathrm{em})}(1-\nu^{\hat{z}})^2 + \omega_{(\mathrm{em})}\gamma\tan s\,(\nu^{\hat{y}2}+\nu^{\hat{x}2})(1-\nu^{\hat{z}})\,. \qquad (6.46)
\end{aligned}$$

These must be completed with the evolution equations for $t$, $x$, $y$ and $z$ (6.39), i.e.,

$$\frac{\mathrm{d}t}{\mathrm{d}\tau} = \gamma\,, \qquad \frac{\mathrm{d}x}{\mathrm{d}\tau} = \frac{\gamma\nu^{\hat{x}}}{\cos s}\,, \qquad \frac{\mathrm{d}y}{\mathrm{d}\tau} = \frac{\gamma\nu^{\hat{y}}}{\cos s}\,, \qquad \frac{\mathrm{d}z}{\mathrm{d}\tau} = \gamma\nu^{\hat{z}}\,, \qquad (6.47)$$

which can be integrated exactly, first re-expressing the derivatives in terms of $s$ through $\mathrm{d}s/\mathrm{d}\tau = \omega_{(\mathrm{em})}\gamma(1-\nu^{\hat{z}})$. This simplifies the velocity equations to

$$\begin{aligned}
\frac{\mathrm{d}\nu^{\hat{x}}}{\mathrm{d}s} &= -\frac{A}{\gamma}\omega_{(\mathrm{em})}\nu^{\hat{x}} - \frac{\nu^{\hat{x}}}{1-\nu^{\hat{z}}}(\nu^{\hat{x}2}+\nu^{\hat{y}2}+\nu^{\hat{z}}-1)\tan s\,,\\
\frac{\mathrm{d}\nu^{\hat{y}}}{\mathrm{d}s} &= -\frac{A}{\gamma}\omega_{(\mathrm{em})}\nu^{\hat{y}} - \frac{\nu^{\hat{y}}}{1-\nu^{\hat{z}}}(\nu^{\hat{x}2}+\nu^{\hat{y}2}+\nu^{\hat{z}}-1)\tan s\,,\\
\frac{\mathrm{d}\nu^{\hat{z}}}{\mathrm{d}s} &= \frac{A}{\gamma}\omega_{(\mathrm{em})}(1-\nu^{\hat{z}}) + (\nu^{\hat{y}2}+\nu^{\hat{x}2})\tan s\,. \qquad (6.48)
\end{aligned}$$

The corresponding solutions are then easily obtained:

$$\begin{aligned}
\gamma &= \frac{\gamma_{(0)}}{\cos^2 s}\frac{1+(1-\nu^{\hat{z}}_{(0)})(W(s)\cos^2 s - W(0))}{1+A\gamma_{(0)}(1-\nu^{\hat{z}}_{(0)})\omega_{(\mathrm{em})}s}\,, \\
\left[\nu^{\hat{x}}, \nu^{\hat{y}}, 1-\nu^{\hat{z}}\right] &= \frac{\cos s}{1+(1-\nu^{\hat{z}}_{(0)})(W(s)\cos^2 s - W(0))} \\
&\quad \times \left[\nu^{\hat{x}}_{(0)}, \nu^{\hat{y}}_{(0)}, (1-\nu^{\hat{z}}_{(0)})\cos s\right]\,, \qquad (6.49)
\end{aligned}$$

where $\nu^{\hat{a}}_{(0)} \equiv \nu^{\hat{a}}(0)$ and

$$W(s) = \frac{1}{2} + \frac{1}{2}\frac{(1+A\gamma_{(0)}(1-\nu^{\hat{z}}_{(0)})\omega_{(\mathrm{em})}s)^2}{\gamma^2_{(0)}(1-\nu^{\hat{z}}_{(0)})^2}\,. \qquad (6.50)$$

When $A = 0$ (geodesic case) the solution is still given by equation (6.49) with $W(s) = W(0)$. As in the previous section the integration of the equations of motion has been carried out by assuming that the interaction starts at a proper time $\tau = 0$ associated with $s = 0$, and that before the interaction the test particle moves along geodesic lines described by (6.6) and (6.7). Again the values $\nu^{\hat{a}}_{(0)}$ refer to the particle's initial spatial velocity at the start of the interaction, whose relation with the Killing constants $(p_v, p_x, p_y)$ is still given by (6.5).

Using (6.49), the equation for $s$ then becomes

$$\frac{\mathrm{d}s}{\mathrm{d}\tau} = \frac{\gamma_{(0)}(1-\nu^{\hat{z}}_{(0)})\omega_{(\mathrm{em})}}{1+A\gamma_{(0)}(1-\nu^{\hat{z}}_{(0)})\omega_{(\mathrm{em})}s}\,, \qquad (6.51)$$

whose solution is

$$s = \frac{\sqrt{1+2A\omega^2_{(\mathrm{em})}\gamma^2_{(0)}(1-\nu^{\hat{z}}_{(0)})^2\tau} - 1}{A\omega_{(\mathrm{em})}\gamma_{(0)}(1-\nu^{\hat{z}}_{(0)})}\,. \qquad (6.52)$$

Equations (6.47) can then be integrated to obtain the solution for the accelerated orbit (see Ref. [27] for details) leading finally to the parametric equations for the orbit in terms of the coordinates $(u, v, y, z)$ with $u$ as the

parameter

$$
\begin{aligned}
u &= \frac{s}{b_{(\mathrm{em})}} = \frac{1}{Ap_v b_{(\mathrm{em})}^2}\left(1-\sqrt{1+2Ap_v^2 b_{(\mathrm{em})}^2\tau}\right)\,,\\
v-v_0 &= \frac{1}{2p_v^2}\left(u+\frac{p_\perp^2}{b_{(\mathrm{em})}}\tan(b_{(\mathrm{em})}u)\right)-\frac{Ab_{(\mathrm{em})}^2u^2}{2p_v}\left(1-\frac{A}{3}p_v b_{(\mathrm{em})}^2 u\right)\,,\\
x-x_0 &= -\frac{p_x}{b_{(\mathrm{em})}p_v}\tan(b_{(\mathrm{em})}u)\,,\\
y-y_0 &= -\frac{p_y}{b_{(\mathrm{em})}p_v}\tan(b_{(\mathrm{em})}u)\,,
\end{aligned}
\tag{6.53}
$$

with associated four-velocity

$$
\begin{aligned}
U &= e^{-\zeta_{(\mathrm{em})}(u)}\Bigg\{-p_v\partial_u-\frac{1}{2p_v}\left[e^{2\zeta_{(\mathrm{em})}(u)}+\frac{p_\perp^2}{\cos^2(b_{(\mathrm{em})}u)}\right]\partial_v\\
&\quad+\frac{p_x}{\cos^2(b_{(\mathrm{em})}u)}\partial_x+\frac{p_y}{\cos^2(b_{(\mathrm{em})}u)}\partial_y\Bigg\}\,,
\end{aligned}
\tag{6.54}
$$

where we have introduced the notation

$$
e^{\zeta_{(\mathrm{em})}(u)} = 1-Ap_v b_{(\mathrm{em})}^2 u\,. \tag{6.55}
$$

## 6.4 Test particle motion after the interaction with a radiation field

Let us now consider a test particle emerging from its interaction in region II with a yet unspecified radiation field (including the flat case with a test radiation field) entering the flat spacetime region III (see equation (6.33)) at the point $P_1$ with coordinates $(u_1, v_1, x_1, y_1)$ associated with a proper time value $\tau_1$. Although the spacetime in region III is flat, the metric functions $F(u)$ and $G(u)$ for both the case of electromagnetic and gravitational wave do not have the value 1 associated with flat coordinates. In fact, they can be represented by

$$
F(u) = \alpha+\beta u\,, \qquad G(u) = \gamma+\delta u\,. \tag{6.56}
$$

Clearly, this representation also holds in the flat case with $\alpha = 1 = \gamma$ and $\beta = 0 = \delta$. Standard Cartesian coordinates must be obtained by two successive coordinate transformations, namely $(u, v, x, y) \to (\mathcal{U}, V, X, Y)$

$$\begin{aligned} \mathcal{U} &= u\,, \qquad X = F(u)\,x\,, \qquad Y = G(u)\,y\,, \\ V &= v + \frac{1}{2}F(u)F'(u)\,x^2 + \frac{1}{2}G(u)G'(u)\,y^2\,, \end{aligned} \tag{6.57}$$

for which $\partial_V = \partial_v$ and then $(\mathcal{U}, V, X, Y) \to (T, X, Y, Z)$

$$T = \frac{\mathcal{U} + V}{\sqrt{2}}\,, \qquad Z = \frac{V - \mathcal{U}}{\sqrt{2}}\,, \qquad X = X\,, \qquad Y = Y\,. \tag{6.58}$$

Let us denote the specific four-momentum in region III and in $(\mathcal{U}, V, X, Y)$ coordinates by

$$U = -Q_V\left(\partial_{\mathcal{U}} + \frac{1 + Q_\perp^2}{2Q_V^2}\partial_V\right) + Q_X\partial_X + Q_Y\partial_Y\,, \tag{6.59}$$

where $Q_V, Q_X, Q_Y$ are constant. The emerging particle four-velocity and the parametric equations for its trajectory are then explicitly obtained (in both coordinate systems) by imposing matching conditions at the boundary II–III where $\tau = \tau_1$, and will be discussed below in the three different cases.

Finally consider a collection of particles labeled by their initial coordinates $x_0$ and $y_0$ along the transverse directions $x$ and $y$ to the wave propagation. Particles scattered by the wave pulse will have different outgoing momentum four-vectors, depending on their initial data. The matching at the boundary II–III of the wave-zone and out-zone four-momenta provide a map between the transverse components of the four-momentum in any spacelike plane associated with the static observer's rest space in the final Minkowski region and the initial location of those particles in a similar plane in the initial Minkowski region. Therefore, one can define a classical differential scattering cross section associated with this transverse scattering map in terms of the outgoing momentum components as follows [42]

$$\mathrm{d}\sigma_{\text{class}} = \mathrm{d}x_0\mathrm{d}y_0 = |J|\mathrm{d}Q_X\mathrm{d}Q_Y\,, \tag{6.60}$$

where $J$ denotes the Jacobian of the transformation between $(Q_X, Q_Y)$ and $(x_0, y_0)$.

### 6.4.1 Flat spacetime with test radiation field

In the simplest case of a test radiation field superimposed on a flat spacetime we find (see equation (6.26))

$$Q_V = p_v e^{-\zeta_{(\mathrm{tf})}(u_1)}\,, \qquad Q_X = p_x e^{-\zeta_{(\mathrm{tf})}(u_1)}\,, \qquad Q_Y = p_y e^{-\zeta_{(\mathrm{tf})}(u_1)}\,. \tag{6.61}$$

Thus the transverse differential scattering cross section vanishes in this case. The effect of the test field on the particle's four-velocity has been examined in Sec. 6.1, considering the initial and final 4-velocity vectors, as given by (6.3) and (6.26), in flat spacetime. In the case of a test radiation field the vectors are related by a boost,

$$\begin{aligned} U - U_{(0)} \equiv \Delta U_{(\mathrm{tf})} \;=\; & \left(e^{-\zeta_{(\mathrm{tf})}(u_1)} - 1\right)\Big[ - p_v \partial_u \\ & - \frac{1}{2p_v}\left(-e^{\zeta_{(\mathrm{tf})}(u_1)} + p_\perp^2\right)\partial_v + p_x\partial_x + p_y\partial_y\Big]\,. \end{aligned} \tag{6.62}$$

The effect of the wave on the particle's 4-velocity can be also summarized by a boost if one considers both the initial and the final 4-velocity vectors in the same flat spacetime. We can write

$$U = \gamma(U, U_{(0)})[U_{(0)} + \nu(U, U_{(0)})] \tag{6.63}$$

with

$$\gamma(U, U_{(0)}) = 1 - U_{(0)} \cdot \Delta U_{(\mathrm{tf})}\,, \qquad \nu(U, U_{(0)}) = \frac{P(U_{(0)})\Delta U_{(\mathrm{tf})}}{1 - U_{(0)} \cdot \Delta U_{(\mathrm{tf})}}\,, \tag{6.64}$$

where $P(U_{(0)})$ projects orthogonally to $U_{(0)}$ and the scalar product here refers to the flat spacetime metric.

### 6.4.2 Gravitational wave radiation field

In order to obtain the values of the constant components of the emerging four-momentum we first apply the coordinate transformation (6.57) to the four-velocity (6.59). Next we require the latter to match at the boundary II–III where $\tau = \tau_1 = -u_1/p_v$, i.e., at the spacetime point $P_1$ with coordinates $(u_1, v_1, x_1, y_1)$, with the wave-zone four-velocity (6.36) with functions $F$ and $G$ given by (6.32). By identifying the components there we finally get the result

$$\begin{aligned} Q_V &= p_v\,, \quad Q_X = p_v \sin(b_{(\mathrm{gw})}u_1) b_{(\mathrm{gw})} x_0 + p_x \cos(b_{(\mathrm{gw})}u_1)\,, \\ Q_Y &= -p_v \sinh(b_{(\mathrm{gw})}u_1) b_{(\mathrm{gw})} y_0 + p_y \cosh(b_{(\mathrm{gw})}u_1)\,, \end{aligned} \tag{6.65}$$

where the following relations have been used

$$\begin{aligned} v_1 &= \frac{1}{2p_v^2}\left[u_1 + \frac{p_x^2}{b_{(\mathrm{gw})}} \tan\left(b_{(\mathrm{gw})}u_1\right) + \frac{p_y^2}{b_{(\mathrm{gw})}} \tanh\left(b_{(\mathrm{gw})}u_1\right)\right] + v_0\,, \\ x_1 &= -\frac{p_x}{b_{(\mathrm{gw})}p_v} \tan\left(b_{(\mathrm{gw})}u_1\right) + x_0\,, \\ y_1 &= -\frac{p_y}{b_{(\mathrm{gw})}p_v} \tanh\left(b_{(\mathrm{gw})}u_1\right) + y_0\,, \end{aligned} \tag{6.66}$$

to re-express the coordinates at the boundary $P_1$ in terms of those of $P_0$ associated with $\tau = 0$, where the interaction between the test particle and the gravitational wave starts. Note that also the flat spacetime coordinate frames $\{\partial_{\mathcal{U}}, \partial_V, \partial_X, \partial_Y\}$ and $\{\partial_u, \partial_v, \partial_x, \partial_y\}$ have been identified to make the comparison, and that the momentum $p_v$ is conserved here.

The differential (transverse) scattering cross section (6.60) is then given by

$$\mathrm{d}\sigma^{(\mathrm{gw})}_{\mathrm{class}} = \frac{\mathrm{d}Q_X \mathrm{d}Q_Y}{p_v^2 b_{(\mathrm{gw})}^2 \sin(b_{(\mathrm{gw})}u_1) \sinh(b_{(\mathrm{gw})}u_1)}\,. \tag{6.67}$$

The effect of the wave on the particle's 4-velocity can be also summarized by a boost if one considers both the initial and the final 4-velocity vectors in the same flat spacetime. In this sense, by using equation (6.59) and its analogous for $U_{(0)}$ before the passage of the wave (i.e., with $Q_V, Q_X, Q_Y$ replaced by

$p_v, p_x, p_y$), we can write

$$U - U_{(0)} \equiv \Delta U_{(\mathrm{gw})} = -\frac{1}{2p_v}(Q_\perp^2 - p_\perp^2)\partial_v + (Q_X - p_x)\partial_x + (Q_Y - p_y)\partial_y \,, \quad (6.68)$$

as in (6.62), so that the relative decomposition $U = \gamma(U, U_{(0)})(U_{(0)} + \nu(U, U_{(0)})$ is accomplished with

$$\gamma(U, U_{(0)}) = 1 - U_{(0)} \cdot \Delta U_{(\mathrm{gw})} \,, \qquad \nu(U, U_{(0)}) = \frac{P(U_{(0)})\Delta U_{(\mathrm{gw})}}{1 - U_{(0)} \cdot \Delta U_{(\mathrm{gw})}} \,, \quad (6.69)$$

as in (6.64), where $P(U_{(0)})$ projects orthogonally to $U_{(0)}$ and the scalar product here refers to the flat spacetime metric. The direct evaluation of the relative velocity $\nu(U, U_{(0)})$ follows straightforwardly from equation (6.65). Note that equation (6.69) is the curved spacetime counterpart of equation (6.29) of the flat case examined previously. For instance, assuming $x_0 = 0 = y_0$, from (6.65) we have

$$Q_X = p_x \cos(b_{(\mathrm{gw})} u_1) \,, \quad Q_Y = p_y \cosh(b_{(\mathrm{gw})} u_1) \,, \quad (6.70)$$

and hence $\Delta U_{(\mathrm{gw})}$ becomes

$$\begin{aligned} \Delta U_{(\mathrm{gw})} \;=\; & -\frac{1}{2p_v}[-p_x^2 \sin^2(b_{(\mathrm{gw})} u_1) + p_y^2 \sinh^2(b_{(\mathrm{gw})} u_1)]\partial_v \\ & + p_x[\cos(b_{(\mathrm{gw})} u_1) - 1]\partial_x + p_y[\cosh(b_{(\mathrm{gw})} u_1) - 1]\partial_y \,. \end{aligned} \quad (6.71)$$

### 6.4.3 *Electromagnetic wave radiation field*

In the case of the spacetime of an electromagnetic wave, the matching conditions at $P_1$ with coordinates $(u_1, v_1, x_1, y_1)$ give the following value of the proper time

$$\tau_1 = -\frac{u_1}{p_v}\left(1 - \frac{1}{2}A p_v b_{(\mathrm{em})}^2 u_1\right) \,. \quad (6.72)$$

The relation between "in" and "out" momenta in this case is

$$\begin{aligned} Q_V &= p_v e^{-\zeta_{(\mathrm{em})}(u_1)}\,, \\ Q_X &= [p_v \sin(b_{(\mathrm{em})}u_1) b_{(\mathrm{em})} x_0 + p_x \cos(b_{(\mathrm{em})}u_1)] e^{-\zeta_{(\mathrm{em})}(u_1)}\,, \\ Q_Y &= [p_v \sin(b_{(\mathrm{em})}u_1) b_{(\mathrm{em})} y_0 + p_y \cos(b_{(\mathrm{em})}u_1)] e^{-\zeta_{(\mathrm{em})}(u_1)}\,, \end{aligned} \tag{6.73}$$

where the following relations have been used

$$\begin{aligned} v_1 &= \frac{1}{2p_v^2}\left[u_1 + \frac{p_\perp^2}{b_{(\mathrm{em})}} \tan\left(b_{(\mathrm{em})}u_1\right)\right] \\ &\quad -\frac{\frac{1}{2}Ab_{(\mathrm{em})}^2 u_1^2}{p_v}\left(1 - \frac{1}{3}Ap_v b_{(\mathrm{em})}^2 u_1\right) + v_0\,, \\ x_1 &= -\frac{p_x}{b_{(\mathrm{em})}p_v}\tan\left(b_{(\mathrm{em})}u_1\right) + x_0\,, \\ y_1 &= -\frac{p_y}{b_{(\mathrm{em})}p_v}\tan\left(b_{(\mathrm{em})}u_1\right) + y_0\,. \end{aligned} \tag{6.74}$$

The differential scattering cross section (6.60) is then given by

$$\mathrm{d}\sigma_{\mathrm{class}}^{(\mathrm{em})} = \frac{e^{2\zeta_{(\mathrm{em})}(u_1)}\mathrm{d}Q_X \mathrm{d}Q_Y}{p_v^2 b_{(\mathrm{em})}^2 \sin^2(b_{(\mathrm{em})}u_1)}\,. \tag{6.75}$$

The effect of the wave on the particle's 4-velocity can be similarly summarized by a boost if one considers both the initial and the final 4-velocity vectors in the same flat spacetime, identifying $\{\partial_{\mathcal{U}}, \partial_V, \partial_X, \partial_Y\}$ with $\{\partial_u, \partial_v, \partial_x, \partial_y\}$ in order to make the comparison. Expressing $U$ in region III in the same form as equation (6.59) (but now taking into account (6.73)) and comparing it with the original $U_{(0)}$ before the passage of the electromagnetic wave, we can now write the final difference as $U - U_{(0)} \equiv \Delta U_{(\mathrm{em})}$ with

$$\begin{aligned} \Delta U_{(\mathrm{em})} &= -(Q_V - p_v)\partial_u + \frac{1}{2Q_V p_v}[(1+p_\perp^2)Q_V - (1+Q_\perp^2)p_v]\partial_v \\ &\quad +(Q_X - p_x)\partial_x + (Q_Y - p_y)\partial_y\,. \end{aligned} \tag{6.76}$$

Similarly, the relative decomposition $U = \gamma(U, U_{(0)})(U_{(0)} + \nu(U, U_{(0)}))$ is accomplished with the equivalent of equation (6.69). Here, the direct evaluation

of the relative velocity $\nu(U, U_{(0)})$ follows straightforwardly from (6.73). For instance, for $x_0 = 0 = y_0$ the difference $\Delta U_{(\mathrm{em})}$ becomes

$$\begin{aligned}\Delta U_{(\mathrm{em})} &= -p_v\left(e^{-\zeta_{(\mathrm{em})}(u_1)}-1\right)\partial_u - \frac{1}{2p_v}\Big[\left(e^{\zeta_{(\mathrm{em})}(u_1)}-1\right)\\ &\quad +p_\perp^2\left(\cos^2(b_{(\mathrm{em})}u)e^{-\zeta_{(\mathrm{em})}(u_1)}-1\right)\Big]\partial_v\\ &\quad +\left(e^{-\zeta_{(\mathrm{em})}(u_1)}\cos(b_{(\mathrm{em})}u_1)-1\right)(p_x\partial_x+p_y\partial_y)\,. \qquad (6.77)\end{aligned}$$

## 6.5 The effect of the interaction: a comparative analysis

In the preceding sections we have discussed the scattering of massive neutral test particles be radiation fields of different kinds: a photon test field in a flat spacetime background, or a radiation field generated by a strong plane gravitational wave, or an exact electromagnetic wave in a general relativistic context. We have considered the comparative scenario in which the interaction between radiation fields and particles has a finite duration, i.e., the spacetime region containing the radiation field is sandwiched between two Minkowskian zones, so that the initial state of the particle is assumed to be the same for the three different radiation fields under consideration. The effect of the interaction in all cases is a change in the linear momentum of the particle from its initial state before the scattering and the final state transferred to the particle by the radiation itself. The properties of the different radiation fields determine the final state of the particle and its linear momentum there. In the case in which the radiation field is represented by either a photon test field in a flat spacetime or the self-consistent field of the exact electromagnetic wave, the interaction has been modeled by including a force term *à la* Poynting-Robertson into the equations of motion given by the four-momentum density of radiation observed in the particle's rest frame with a multiplicative constant factor expressing the strength of the interaction itself. The resulting motion is therefore not geodesic in both cases. On the contrary, in the case in which the radiation field is represented by the gravitational field of a single plane gravitational wave, particles propagate along geodesics.

We have computed the boost (related to the simpler specific four-momentum difference $\Delta U$) relating the initial and final 4-momentum of the particle, $U_{(0)}$ and $U$, both understood in the context of the flat spacetime zones which sandwich the interaction region in between. For the various cases and with the notation considered above, we have found for the projection of $\Delta U$ on the transverse $x-y$ plane

$$\begin{aligned}
\Delta U^{\perp}_{(\mathrm{tf})} &= \left(e^{-\zeta_{(\mathrm{tf})}(u_1)}-1\right)\left(p_x\partial_x+p_y\partial_y\right)\,,\\
\Delta U^{\perp}_{(\mathrm{gw})} &= p_x[\cos(b_{(\mathrm{gw})}u_1)-1]\partial_x+p_y[\cosh(b_{(\mathrm{gw})}u_1)-1]\partial_y\,,\\
\Delta U^{\perp}_{(\mathrm{em})} &= \left(e^{-\zeta_{(\mathrm{em})}(u_1)}\cos(b_{(\mathrm{em})}u_1)-1\right)\left(p_x\partial_x+p_y\partial_y\right),
\end{aligned} \tag{6.78}$$

whereas for the projection on the transverse $u-v$ plane

$$\begin{aligned}
\Delta U^{\parallel}_{(\mathrm{tf})} &= -\frac{1}{2p_v}\left[\left(e^{\zeta_{(\mathrm{tf})}(u_1)}-1\right)+p_\perp^2\left(e^{-\zeta_{(\mathrm{tf})}(u_1)}-1\right)\right]\partial_v\\
&\quad -p_v\left(e^{-\zeta_{(\mathrm{tf})}(u_1)}-1\right)\partial_u\\
\Delta U^{\parallel}_{(\mathrm{gw})} &= -\frac{1}{2p_v}[-p_x^2\sin^2(b_{(\mathrm{gw})}u_1)+p_y^2\sinh^2(b_{(\mathrm{gw})}u_1)]\partial_v\\
\Delta U^{\parallel}_{(\mathrm{em})} &= -\frac{1}{2p_v}\left[\left(e^{\zeta_{(\mathrm{em})}(u_1)}-1\right)+p_\perp^2\left(\cos^2(b_{(\mathrm{em})}u)e^{-\zeta_{(\mathrm{em})}(u_1)}-1\right)\right]\partial_v\\
&\quad -p_v\left(e^{-\zeta_{(\mathrm{em})}(u_1)}-1\right)\partial_u\,.
\end{aligned} \tag{6.79}$$

In the limit of small electromagnetic field compared to the duration of the wave $|b_{(\mathrm{em})}|u_1=\sqrt{2}|\omega_{(\mathrm{em})}|u_1\ll 1$ in the final case of the exact electrovac solution field, one obtains the same result as in the first case of a test field with the same frequency $\omega_K=\omega_{(\mathrm{em})}$ and therefore the same radiation field energy-momentum tensor. In the gravitational case the transverse change in the momentum involves a rotation due to the deformation of the plane wave directions by the wave, while in the electromagnetic cases only an overall scaling is involved. For the longitudinal changes, the gravitational case lacks a component along $\partial_u$ because the motion is geodesic and $\partial_v$ is a Killing vector field, while in the other cases the force responsible for the change in momentum itself has a covariant component along $\partial_v$.

This comparative analysis shows how the nature of the interaction of

massive particles with radiation fields of different kinds strongly influences the scattering process, in principle leading to detectable observational consequences.

# 7. LIGHT SCATTERING BY RADIATION FIELDS: THE OPTICAL MEDIUM ANALOGY

In this chapter we will investigate the scattering of light by a radiation field given by either an exact gravitational plane wave or an exact electromagnetic wave, described by the spacetime metrics introduced in the previous chapter to study the scattering of massive test particle. Once again we assume the interaction region to be sandwiched between two flat spacetime regions. We first develop the equivalent medium analogy of the associated background fields as in Chapter 4, by exploring the optical properties of the corresponding effective material media. Using standard tools of ordinary wave optics we then study the deflection of photon paths due to the interaction with the radiation field, allowing for a comparison between the optical properties of the equivalent media associated with the different background fields.

The results discussed in this chapter have been published in *Europhys. Lett.* **102**, 20006 (2013) [45].

## *7.1 The optical medium analogy of a gravitational wave background*

We recall the background of a radiation field (either generated by a gravitational plane wave or an electromagnetic wave) propagating along the $z$ axis of an adapted coordinate system $(t, x, y, z)$, with the background spacetime described by the line element [44]

$$\begin{aligned} \mathrm{d}s^2 &= -\mathrm{d}t^2 + \mathrm{d}z^2 + F(t-z)^2\mathrm{d}x^2 + G^2(t-z)\mathrm{d}y^2 \\ &= -2\mathrm{d}u\mathrm{d}v + F(u)^2\mathrm{d}x^2 + G^2(u)\mathrm{d}y^2\,. \end{aligned} \tag{7.1}$$

where the null coordinates $u = (t - z)/\sqrt{2}$ and $v = (t + z)/\sqrt{2}$ are related to the Cartesian ones in a standard way; radiation fields of this type have been previously introduced in Chapter 6.

In this section we once again consider the (vacuum) case of a gravitational plane wave with a single polarization state (+ state), corresponding to metric functions

$$F(u) = \cos b_{(\mathrm{gw})} u \,, \qquad G(u) = \cosh b_{(\mathrm{gw})} u \,, \tag{7.2}$$

as introduced in equation (6.32) in Sec. 6.2; the gravitational wave is sandwiched between two Minkowskian regions, and by imposing matching conditions at the boundaries the metric is extended to all values of $u$, namely [4]

$$\begin{aligned} F(u) &= \begin{cases} 1 & u \leq 0 \quad \text{(I)} \\ \cos b_{(\mathrm{gw})} u & 0 \leq u \leq u_1 \quad \text{(II)} \\ \alpha + \beta u & u \geq u_1 \quad \text{(III)} \end{cases} \\ G(u) &= \begin{cases} 1 & u \leq 0 \quad \text{(I)} \\ \cosh b_{(\mathrm{gw})} u & 0 \leq u \leq u_1 \quad \text{(II)} \\ \gamma + \delta u, & u \geq u_1 \quad \text{(III)} \end{cases} \end{aligned} \tag{7.3}$$

where labels I, II and III refer to in zone ($u \leq 0$), wave zone ($0 < u < u_1$) and out zone ($u \geq u_1$), respectively, and with the constants $\alpha$, $\beta$, $\gamma$ and $\delta$ defined as in equation (6.35) in Sec. 6.2.

Working out the electromagnetic analogy for the gravitational wave background, we find for the electric and magnetic permeability tensors (4.4) of the corresponding equivalent medium in the wave zone the following expressions

$$\epsilon_{ab} = \mu_{ab} = \mathrm{diag}[\epsilon_1, \epsilon_2, \epsilon_3] = \mathrm{diag}\left[\frac{G}{F}, \frac{F}{G}, FG\right] \,, \tag{7.4}$$

while the rotation vector $M_a = 0$ vanishes identically, so that the medium is

linear and nongyrotropic. In the weak field limit $b_{(\mathrm{gw})}u \ll 1$ we have

$$\begin{aligned}
\epsilon_1 &= \frac{\cosh b_{(\mathrm{gw})}u}{\cos b_{(\mathrm{gw})}u} \sim 1 + b^2_{(\mathrm{gw})}u^2\,, \\
\epsilon_2 &= \frac{1}{\epsilon_1} \sim 1 - b^2_{(\mathrm{gw})}u^2\,, \\
\epsilon_3 &= \cosh b_{(\mathrm{gw})}u \cos b_{(\mathrm{gw})}u \sim 1\,,
\end{aligned} \tag{7.5}$$

up to the second order. The general definition (4.14) of the refraction index then gives

$$n = \frac{FG}{\sqrt{G^2e_1^2 + F^2e_2^2 + F^2G^2e_3^2}}\,. \tag{7.6}$$

The anisotropic properties of the medium are evident considering photons traveling in the three coordinate directions. For instance, for photons along the $x$ axis is $e = \partial_x$ so that $n = n_x = F$, whereas for photons along the $y$ axis is $n = n_y = G$ and for photons along the $z$ axis is $n = n_z = 1$. In fact, starting from the vanishing of the line element $\mathrm{d}s^2 = 0$ for photons, we have

$$\begin{aligned}
\mathrm{d}t^2 &= F(u)^2\mathrm{d}x^2 + G(u)^2\mathrm{d}y^2 + \mathrm{d}z^2 \\
&= \epsilon_2\epsilon_3\mathrm{d}x^2 + \epsilon_1\epsilon_3\mathrm{d}y^2 + \mathrm{d}z^2\,,
\end{aligned} \tag{7.7}$$

so that the travel coordinate time of light can be expressed in terms of an associated optical path

$$\mathrm{d}t = \sqrt{n_x^2\mathrm{d}x^2 + n_y^2\mathrm{d}y^2 + n_z^2\mathrm{d}z^2}\,, \tag{7.8}$$

whereas the identification

$$n_x = \sqrt{\epsilon_2\epsilon_3}\,, \qquad n_y = \sqrt{\epsilon_1\epsilon_3}\,, \qquad n_z = 1\,, \tag{7.9}$$

characterizes the anisotropic properties of the medium. Explicitly, in the wave region, we find

$$n_x = F(u) < 1\,, \qquad n_y = G(u) > 1\,, \tag{7.10}$$

and hence it follows that the $x$ and $y$ axes are naturally defined as the superluminal and subluminal direction of light propagation, respectively. It is worth noticing that such a definition holds only for coordinate components of the velocity of light in the chosen coordinate system.

In the in zone we have simply

$$\epsilon_1 = \epsilon_2 = \epsilon_3 = 1\,, \tag{7.11}$$

so that $n = n_x = n_y = n_z = 1$, whereas in the out zone it is

$$\epsilon_1 = \frac{\gamma + \delta u}{\alpha + \beta u} = \frac{1}{\epsilon_2}\,, \quad \epsilon_3 = (\gamma + \delta u)(\alpha + \beta u)\,. \tag{7.12}$$

As has been discussed before, it is always possible to perform a coordinate transformation $(t, x, y, z) \to (T, X, Y, Z)$ in the out zone that will convert the line element to the standard Minkowskian form; see equations (6.57) in Sec. 6.4 for details. In the new Cartesian coordinates, the electric permeability tensor is again diagonal and has unitary components. Thus the refraction index $n$ in both in and out zone can be set equal to 1, provided the frame $\{\partial_U, \partial_V, \partial_X, \partial_Y\}$ is identified with $\{\partial_u, \partial_v, \partial_x, \partial_y\}$ in order to make the right comparison.

In the limit of geometric optics electromagnetic waves propagate along the null geodesics of the background spacetime [46]. Therefore, one can study how an incoming light beam propagating along a straight line in the in zone is deflected when passing through the scattering region before emerging in the out zone, where it moves again along a straight line but with different direction.

The geodesic motion of photons through the radiation field associated with an exact gravitational wave has been studied previously in Chapter 5, for a similar sandwich scenario but in a slightly different null coordinate system. Let us briefly discuss the propagation of photons on the background described by (7.1) and (7.3).

In the in zone, the constant photon four-momentum $P_I$ can be parametrized in terms of the conserved specific momenta $p_v$, $p_x$ and $p_y$ associated with the

three Killing vectors $\partial_v, \partial_x, \partial_y$ as

$$\begin{aligned} P_I &= -p_v\left(\partial_u + \frac{p_\perp^2}{2p_v^2}\partial_v\right) + p_\perp \\ &= -\frac{1}{\sqrt{2}}p_v\left(1+\frac{p_\perp^2}{2p_v^2}\right)\partial_t + p_\perp \\ &\quad -\frac{p_v}{\sqrt{2}}\left(-1+\frac{p_\perp^2}{2p_v^2}\right)\partial_z\,, \end{aligned} \tag{7.13}$$

where $p_\perp = p_x\partial_x + p_y\partial_y$ (with $p_\perp^2 = p_x^2 + p_y^2$ using the flat spacetime notation for convenience) and $p_v < 0$ for $P_I$ to be future-pointing.

In the wave zone we have instead

$$\begin{aligned} P_{II} &= -p_v\partial_u - \frac{1}{2p_v}\left(\frac{p_x^2}{F(u)^2}+\frac{p_y^2}{G(u)^2}\right)\partial_v \\ &\quad + \frac{p_x}{F(u)^2}\partial_x + \frac{p_y}{G(u)^2}\partial_y\,, \\ &= -\frac{p_v}{\sqrt{2}}\left[1+\frac{1}{2p_v^2}\left(\frac{p_x^2}{F(u)^2}+\frac{p_y^2}{G(u)^2}\right)\right]\partial_t \\ &\quad -\frac{p_v}{\sqrt{2}}\left[-1+\frac{1}{2p_v^2}\left(\frac{p_x^2}{F(u)^2}+\frac{p_y^2}{G(u)^2}\right)\right]\partial_z \\ &\quad + \frac{p_x}{F(u)^2}\partial_x + \frac{p_y}{G(u)^2}\partial_y\,. \end{aligned} \tag{7.14}$$

Finally, in the out zone the constant photon four-momentum in $(U, V, X, Y)$ coordinates is given by

$$P_{III} = -Q_V\left(\partial_U + \frac{Q_\perp^2}{2Q_V^2}\partial_V\right) + Q_\perp\,, \tag{7.15}$$

where $Q_\perp = Q_X\partial_X + Q_Y\partial_Y$ (with $Q_\perp^2 = Q_x^2 + Q_y^2$), and the constants $Q_V, Q_X, Q_Y$ are determined by imposing the matching conditions at the boundary II–III where $u = u_1$. Thus one finds

$$\begin{aligned} Q_V &= p_v\,, \\ Q_X &= p_v\sin(b_{(\mathrm{gw})}u_1)b_{(\mathrm{gw})}x_0 + p_x\cos(b_{(\mathrm{gw})}u_1)\,, \\ Q_Y &= -p_v\sinh(b_{(\mathrm{gw})}u_1)b_{(\mathrm{gw})}y_0 + p_y\cosh(b_{(\mathrm{gw})}u_1)\,, \end{aligned} \tag{7.16}$$

where $x_0$ and $y_0$ denote the initial values of the coordinates $x$ and $y$ along the directions transverse to the wave propagation. The constant specific momenta (7.16) of photons scattered by the gravitational wave are the same found for the scattering of massive particles in equation (6.65) in Sec. 6.4, if their ingoing motion is characterized by the same initial $p_v$, $p_x$, $p_y$. Nevertheless, the outgoing four-momentum vector and the particle trajectory after the interaction with the radiation field depend on the nature of the particle under consideration (massless or massive); see equations (5.38) and (5.40) in Sec. 5.2.

Recalling that at the boundary $u = u_1$ (i.e., the most relevant surface to study light scattering in terms of refraction phenomena) we have

$$\begin{aligned} F(u_1) &= \cos(b_{(\mathrm{gw})}u_1) = n_x|_{u_1} \\ G(u_1) &= \cosh(b_{(\mathrm{gw})}u_1) = n_y|_{u_1}\,, \end{aligned} \tag{7.17}$$

and

$$\begin{aligned} F'(u_1) = -b_{(\mathrm{gw})}\sin(b_{(\mathrm{gw})}u_1) &= n'_x|_{u_1}\,, \\ G'(u_1) = b_{(\mathrm{gw})}\sinh(b_{(\mathrm{gw})}u_1) &= n'_y|_{u_1}\,, \end{aligned} \tag{7.18}$$

(a prime denoting differentiation with respect to $u$), the transverse momentum in the out zone can be written as

$$Q_\perp = Ap_\perp - p_v A' X_0\,, \tag{7.19}$$

where

$$A = \begin{pmatrix} n_x & 0 \\ 0 & n_y \end{pmatrix}\,, \qquad A' = \begin{pmatrix} n'_x & 0 \\ 0 & n'_y \end{pmatrix} \tag{7.20}$$

and $X_0 = (x_0, y_0)$. The symbol $|_{u_1}$ has been omitted for simplicity.

If the photon impacts the wave region (in the transverse plane) at the origin of the coordinates, i.e., $x_0 = 0 = y_0$, equation (7.19) implies

$$Q_x = n_x p_x\,, \qquad Q_y = n_y p_y\,, \tag{7.21}$$

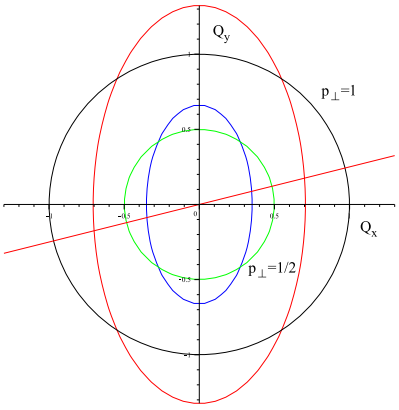


*Fig. 7.1:* [Gravitational wave case] In the space of transverse momenta, the different refraction indices $n_x$ and $n_y$ on the $x$ and $y$ axes imply that an initial circular distribution of momenta for incident photons becomes an ellipse after the refraction process. The plot shows two cases: $p_\perp = 1$ (external circle and ellipse) and $p_\perp = 1/2$ (internal circle and ellipse). The (generic) line intersecting the circle and the ellipse (in both cases) identifies corresponding pairs $(Q_x, Q_y)$ and $(p_x, p_y)$ related by (7.19) with a choice of $X_0 = 0$ and using $b_{(\mathrm{gw})}u_1 = \pi/4$.

expressing along each axis the Snell law of refraction of ordinary optics. Since $n_x \neq n_y$, the relation (7.19) for $X_0 = 0$ can be represented by an ellipse in the space of momenta, as shown in Fig. 7.1.

One can also evaluate the angle between the directions of $p_\perp$ and $Q_\perp$, i.e., the scattering angle $\alpha_{\mathrm{s}}$, defined by

$$\cos\alpha_{\mathrm{s}} = \frac{p_\perp \cdot Q_\perp}{|p_\perp||Q_\perp|} = \frac{n_x p_x^2 + n_y p_y^2}{\sqrt{p_x^2 + p_y^2}\sqrt{n_x^2 p_x^2 + n_y^2 p_y^2}}\,. \tag{7.22}$$

If $p_x = 0$ (or $p_y = 0$), one simply finds $\alpha_{\mathrm{s}} = 0$. Introducing the polar representation of transverse momenta $p_x = p_\perp \cos\psi$, $p_y = p_\perp \sin\psi$, the previous expression becomes

$$\cos\alpha_{\mathrm{s}} = \frac{n_x \cos^2\psi + n_y \sin^2\psi}{\sqrt{n_x^2 \cos^2\psi + n_y^2 \sin^2\psi}}\,, \tag{7.23}$$

which is invariant for $\psi \to \pi - \psi$. Its behavior as a function of $\psi$ is shown

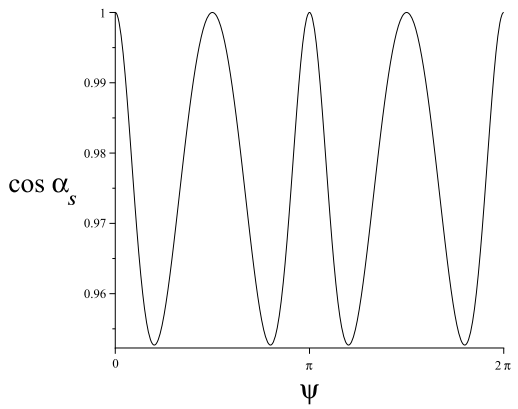


*Fig. 7.2:* [Gravitational wave case] The angle $\alpha_{\rm s}$ given by (7.22) and written as a function of the angle $\psi$ of the polar representation of transverse momenta in the case $b_{(\rm gw)}u_1 = \pi/4$.

in Fig. 7.2. It turns out that the scattering angle $\alpha_{\rm s}$ remains close to zero in the whole range of allowed transverse momenta.

Vice versa, if the incident photon is purely longitudinal, i.e., $p_x = 0 = p_y$, equation (7.19) reduces to $Q_\perp = -p_v A' X_0$. In this case the photon travels along the same direction as the gravitational wave, a fact that makes the whole problem trivial.

## 7.2 The optical medium analogy of an electromagnetic wave background

Once again we want to consider the similar situation in which an electromagnetic plane wave propagates along the positive $z$ axis and is sandwiched between two flat spacetime regions, as shown in Fig. (6.1). As previously introduced in Chapter 6, the corresponding conformally flat line element is given by (7.1) with functions [15]

$$F = \cos(b_{(\rm em)}u) = G\,, \tag{7.24}$$

differing from the corresponding gravitational wave case only by a trigonometric rather than hyperbolic cosine appearing in $G$, so that the above analysis for the case of a gravitational wave is easily repeated. we recall that the present case corresponds to a nonvacuum spacetime which is a solution of the Einstein equations with energy-momentum tensor

$$T = \phi_0 K \otimes K\,, \quad K = b_{(\mathrm{em})}\partial_v\,, \tag{7.25}$$

where $\phi_0 = 1/4\pi$ and the background quantity $b_{(\mathrm{em})}$ is related to the frequency of the wave by $b_{(\mathrm{em})} = \sqrt{2}\omega_{(\mathrm{em})}$.

As in the previous section, the coordinate horizon of the metric at $b_{(\mathrm{em})}u = \pi/2$ is avoided by restricting the coordinate $u$ to the interval $[0, u_1]$ with $u_1 < \pi/(2b_{(\mathrm{em})})$, and we extend the metric (7.24) to all values of $u$. The matching conditions at the two null hypersurface boundaries then imply constants $\alpha = \gamma$, $\beta = \delta$ in the metric functions of the out zone metric, explicitly defined in equation (6.45) in Sec. 6.3.

The previous analysis of the electromagnetic analogy of a gravitational wave spacetime can be repeated straightforwardly for the electromagnetic wave spacetime, now implying in the wave region

$$n_x = n_y = \cos b_{(\mathrm{em})}u \equiv n\,, \tag{7.26}$$

so that $n < 1$. The relation between in- and out-momenta is now given by

$$\begin{aligned} Q_V &= p_v\,, && (7.27)\\ Q_X &= p_v \sin(b_{(\mathrm{em})}u_1)b_{(\mathrm{em})}x_0 + p_x\cos(b_{(\mathrm{em})}u_1)\,, \\ Q_Y &= p_v \sin(b_{(\mathrm{em})}u_1)b_{(\mathrm{em})}y_0 + p_y\cos(b_{(\mathrm{em})}u_1)\,. && (7.28) \end{aligned}$$

The constant specific momenta (7.27) of photons scattered by the radiation field of the electromagnetic wave are different from the ones found for the scattering of massive particles in the same background, even if the ingoing motion of photons and massive particles is characterized by the same initial $p_v$, $p_x$, $p_y$. The deviation from geodesic motion due to the absorption and

re-emission of radiation by the massive test particles appears as an overall scaling factor acting on the four-momentum vector of particles emerging from the interaction; see Eqs. (6.73) in Sec. 6.4. Photons propagate along straight line trajectories before during and after the interaction with the radiation field generated by the electromagnetic wave.

Recalling that at the boundary

$$\begin{aligned} F(u_1) &= \cos(b_{(\mathrm{em})}u_1) = n|_{u_1}\,, \\ F'(u_1) &= -b_{(\mathrm{em})}\sin(b_{(\mathrm{em})}u_1) = n'|_{u_1}\,, \end{aligned} \tag{7.29}$$

the emerging transverse momentum can be written in the same form as in equation (7.19) with $A = nI$ and $A' = n'I$, $I$ being the identity matrix, so that

$$Q_\perp = np_\perp - p_v n' X_0\,. \tag{7.30}$$

For $X_0 = 0$ this relation implies

$$Q_x = np_x\,, \qquad Q_y = np_y\,, \tag{7.31}$$

which can be represented by a circle in the momentum space, as shown in Fig. 7.3. If $X_0 = 0$ (for simplicity) the scattering angle is always $\alpha_{\mathrm{s}} = 0$, showing the difference between scattering by a gravitational and an electromagnetic wave.

## 7.3 The optical properties of the equivalent media

In the preceding sections we have studied the scattering of a light beam by a radiation field of associated optical properties of the equivalent optically active medium, considering the case of an exact gravitational plane wave and that of an exact electromagnetic wave in a general relativistic context.

The most relevant physics involves the plane transverse to the direction of propagation of the wave: here the equivalent medium of the gravitational wave is inhomogeneous and anisotropic, whereas that of an electromagnetic wave is inhomogeneous but isotropic. In both cases the medium is active in

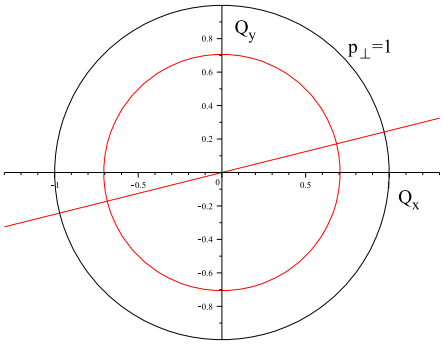


*Fig. 7.3:* [Electromagnetic wave case] In the space of transverse momenta, the coincident refraction indices $n_x = n_y$ on the $x$ and $y$ axes imply that an initial circular distribution of momenta for incident photons remains circular after the refraction process. The plot shows the case $p_\perp = 1$ ($Q_\perp = 1/\sqrt{2}$). The (generic) line intersecting the two circles identifies corresponding pairs $(Q_x, Q_y)$ and $(p_x, p_y)$ related by (7.30) in the case $X_0 = 0$ and using $b_{(\mathrm{em})}u_1 = \pi/4$.

the sense that the refraction index depends on time. Nevertheless, one can treat the scattering process as a series of multiple refractions through media with nearly constant refraction indices all the way up to the boundary of the interaction region, so that we are allowed to adopt the standard tools of ordinary optics.

Moreover, there exist directions in which the effective refraction index of the medium is less than 1 (so that the coordinate components of the velocity of light become greater than 1). This realizes an interesting and novel point of view for looking at the photon scattering by electromagnetic as well as gravitational waves in the exact theory of general relativity, which may also have a counterpart in experiments. For instance, by means of nonlinear optical materials or “metamaterials" available nowadays [47, 48], one can arrange for an analogue material of the above mentioned radiation field spacetimes and compare the geometrization of physical interactions with experimental data. In an experimental scenario, however, we are aware that a number of difficulties arises. For example, in order to mimic the transient

event of a passing gravitational wave one would need to consider a moving optical medium. This can be remedied by constructing a medium that is susceptible to nonlinear effects, such as an optical activation induced by an ultrashort, intense laser pulse. Then the optical medium itself remains at rest but its effective properties change as a propagating front when the medium is activated by the laser pulse. This method has been used previously to create fiber-optical analogs of a black hole's event horizon in laboratory [48].

# 8. LIGHT PROPAGATION IN A COLLIDING GRAVITATIONAL WAVE SPACETIME

We now want to apply the optical medium analogy to study light propagation in the background of an exact solution of Einstein's field equations representing colliding strong gravitational waves. To the best of our knowledge, in the literature so far only the optical medium analogy of single weak [32] and strong [45] gravitational wave pulses has been studied.

In the previous chapter we have worked out the optical medium analogy of a gravitational radiation field sandwiched between two flat regions; we want to generalize our investigation to the case of two exact (i.e., "strong") colliding gravitational waves, exploring in particular the collision region associated with the nonlinear interaction of the waves. It is well known from exact solutions of Einstein's equations that the collision process of two gravitational waves can be associated with two possible scenarios: either the formation of a Killing-Cauchy horizon or that of a spacetime singularity. There are a variety of possible solutions which exhibit one of the two above mentioned features [1, 49]; in the following we will consider the one found by Ferrari and Ibañez [50, 51, 52] in the 1980s. It has the twofold advantage of being mathematically simple and allowing us to switch easily between the horizon-forming and singularity-developing solution by changing the signs of certain metric functions (which are in turn summarizable with a sign indicator).

In this chapter we will discuss in detail the properties of the equivalent optical medium of such a colliding gravitational wave spacetime. We expect that the nonlinear wave interaction leads to a significant modification of the single wave picture discussed in Chapter 7, especially in connection with the presence of singular structures which usually form during the collision process. Given the complexity of the nonlinear interaction of the two

gravitational waves in the framework of general relativity, leading to the formation of either horizons or singularities, the optical medium analogy allows us to simply capture some interesting effects of light propagation on this background.

The following discussion of the refraction index analysis of light propagation in a colliding gravitational wave spacetime has been submitted for publication in *Gen. Relat. Grav.*.

## 8.1 Colliding gravitational wave spacetimes

Exact solutions of the Einstein equations representing colliding gravitational plane waves have been discussed extensively in the literature [1]. The spacetime geometry associated with two colliding gravitational plane waves is characterized by the presence of either a spacetime singularity [49] or a Killing-Cauchy horizon as a result of the nonlinear wave interaction [50, 51, 52]. In general, such spacetimes contain four regions: a flat spacetime region (Petrov type-O), representing the initial situation before the passage of the two oppositely directed plane waves, two Petrov type-N regions, corresponding to the single waves before the interaction, and an interaction region, generally of Petrov type-I. Two commuting spacelike Killing vectors are always present, associated with the plane symmetry assumed for the two colliding waves. (Like an axisymmetric spacetime, the interaction region of two colliding plane waves admits two commuting Killing fields.) The spacetime describing the collision region is most generally characterized by the line element [53]

$$\begin{aligned} \mathrm{d}s^2 &= -e^{M}(\mathrm{d}t^2 - \mathrm{d}z^2) + e^{-U}\left[-2\sinh W\,\mathrm{d}x\,\mathrm{d}y\right. \\ &\quad \left. + \cosh W\left(e^{V}\mathrm{d}x^2 + e^{-V}\mathrm{d}y^2\right)\right], \end{aligned} \tag{8.1}$$

where all metric functions depend on $t$ and $z$.

The electric and magnetic permeability tensors (4.4) of the corresponding

equivalent medium are then given by

$$\epsilon_{ab} = \mu_{ab} = \begin{pmatrix} e^{-V}\cosh W & \sinh W & 0 \\ \sinh W & e^{V}\cosh W & 0 \\ 0 & 0 & e^{-(M+U)} \end{pmatrix}, \tag{8.2}$$

whereas the rotation vector $M_a = 0$ vanishes identically in this case.

For a collinear polarization of the plane waves, the metric function $W$ can be gauged to be zero, so that the metric as well as the resulting electric and magnetic permeability tensors given above are diagonal. One possible solution exhibiting these properties is the Ferrari-Ibañez metric considered below; it shares the most peculiar features of more general solutions of the same kind.

### 8.1.1 The degenerate Ferrari-Ibañez metric

Ferrari and Ibañez [50, 51, 52] found a type-D solution of the Einstein equations that can be interpreted as describing the collision of two linearly polarized gravitational plane waves propagating along a common direction (the $z$ axis) in opposite senses and developing either a nonsingular Killing-Cauchy horizon or a spacetime singularity upon collision. The corresponding line element in the interaction region (hereafter referred to as Region I) can be written as

$$\mathrm{d}s_I^2 = -F_+^2(t)(\mathrm{d}t^2 - \mathrm{d}z^2) + \frac{F_-(t)}{F_+(t)}\mathrm{d}x^2 + \cos^2 z F_+^2(t)\mathrm{d}y^2\,, \tag{8.3}$$

where $t$ and $z$ are dimensionless timelike and spacelike coordinates, respectively, and where all the coordinates have been properly rescaled and are dimensionless. The metric functions are given by

$$F_\pm(t) = 1 \pm \sigma \sin t\,, \qquad \sigma = \pm 1\,, \tag{8.4}$$

with $\sigma = 1$ corresponding to a horizon-forming solution at time $t = \pi/2$, whereas $\sigma = -1$ denotes a singularity-developing one. The interaction region where this form of the metric is valid is depicted in the $t-z$ plane by a triangle

whose vertex represents the initial event of collision and can be identified with the origin of the coordinate system; the horizon/singularity is mapped onto the base of the shaded triangle in Fig. 8.1. Therefore, Region I corresponds to the region $-t \leq z \leq t$, $0 \leq t \leq \pi/2$. The instant of collision is $t = 0$, while $t = \pi/2$ is the instant when the horizon/singularity is created.

If $t < 0$ the two waves are traveling one against the other in the $z$ direction. They are single plane waves propagating in flat spacetime. In order to extend the metric from the interaction region to the remaining parts of the spacetime representing the single wave zones and the flat spacetime zone before the arrival of waves, one must first introduce the two dimensionless null coordinates

$$u = \frac{t-z}{2}\,, \quad v = \frac{t+z}{2} \qquad \Longleftrightarrow \qquad t = u+v\,, \quad z = v-u\,, \tag{8.5}$$

in terms of which the metric (8.3) takes the form

$$\begin{aligned} \mathrm{d}s_I^2 &= -4F_+^2(u+v)\mathrm{d}u\mathrm{d}v \\ &\quad + \frac{F_-(u+v)}{F_+(u+v)}\mathrm{d}x^2 + \cos^2(u-v)F_+^2(u+v)\mathrm{d}y^2\,. \end{aligned} \tag{8.6}$$

The interaction region corresponds to the triangular region in the $u-v$ plane bounded by the lines $u = 0$, $v = 0$ and $u + v = \pi/2$. Following Khan-Penrose [49], the extension of the metric is then obtained simply by performing the substitution rules $u \to u\,\Theta(u)$ and $v \to v\,\Theta(v)$ in (8.6), using the Heaviside step function $\Theta$. The four spacetime regions

$$\begin{array}{llll} u \geq 0\,, \quad v \geq 0\,, \quad u+v < \pi/2 & \text{Region I} & \text{(interaction)} \\ 0 \leq u < \pi/2\,, \quad v < 0 & \text{Region II} & (u\text{−wave}) \\ u < 0\,, \quad 0 \leq v < \pi/2 & \text{Region III} & (v\text{−wave}) \\ u < 0\,, \quad v < 0 & \text{Region IV} & \text{(flat)} \end{array} \tag{8.7}$$

are shown in Fig. 8.1. The resulting extended metric is

$$\begin{aligned} \mathrm{d}s_{II}^2 &= -4F_+^2(u)\mathrm{d}u\mathrm{d}v + \frac{F_-(u)}{F_+(u)}\mathrm{d}x^2 + \cos^2 u F_+^2(u)\mathrm{d}y^2\,, \\ \mathrm{d}s_{III}^2 &= -4F_+^2(v)\mathrm{d}u\mathrm{d}v + \frac{F_-(v)}{F_+(v)}\mathrm{d}x^2 + \cos^2 v F_+^2(v)^2\mathrm{d}y^2\,, \\ \mathrm{d}s_{IV}^2 &= -4\mathrm{d}u\mathrm{d}v + \mathrm{d}x^2 + \mathrm{d}y^2\,. \end{aligned} \tag{8.8}$$

In this way the extended metric in general is $C^0$ (but not $C^1$) along the null boundaries $u = 0$ and $v = 0$, so that the Riemann tensor acquires distributional parts. At the boundaries the Weyl tensor has $\delta$-functions, otherwise it is regular [54] (the Ricci tensor is vanishing everywhere). One wave will be a function of $u$ only (in Region II), the other a function of $v$ only (in Region III). In the $t - z$ plane Region II corresponds to the region $t - \pi \leq z \leq t$, and Region III to the region $-t \leq z \leq \pi - t$. It is worth noting that certain calculations are more easily done in one or the other of these two sets of coordinates, so we will switch back and forth between them as needed.

With a coordinate transformation [54]

$$t = x\,, \quad r = F_+\,, \quad \theta = \frac{\pi}{2} - (u - v)\,, \quad \phi = 1 + y\,, \tag{8.9}$$

it becomes obvious that the collision region I is locally isometric to a Schwarzschild black hole bounded by an event horizon; namely, metric (8.3) transforms to

$$\mathrm{d}s^2 = -\left(1 - \frac{2}{r}\right)\mathrm{d}t^2 + \left(1 - \frac{2}{r}\right)^{-1}\mathrm{d}r^2 + r^2\left(\mathrm{d}\theta^2 + \sin^2\theta\mathrm{d}\phi^2\right)\,, \tag{8.10}$$

which is the interior metric of a Schwarzschild black hole with mass $M = 1$. For both cases $\sigma = \pm 1$ the interaction between the two colliding waves starts at the surfaces $u = v = 0$, which correspond to the radius $r = 1$ in the gravitational field of a Schwarzschild black hole. If we consider $\sigma = 1$ (the horizon-forming scenario) there is no singularity of the metric on the surface $u + v = \pi/2$. Instead, this surface corresponds to the black hole horizon $r = 2$. In the case of $\sigma = -1$ (the singularity-developing scenario) $F_+$ does

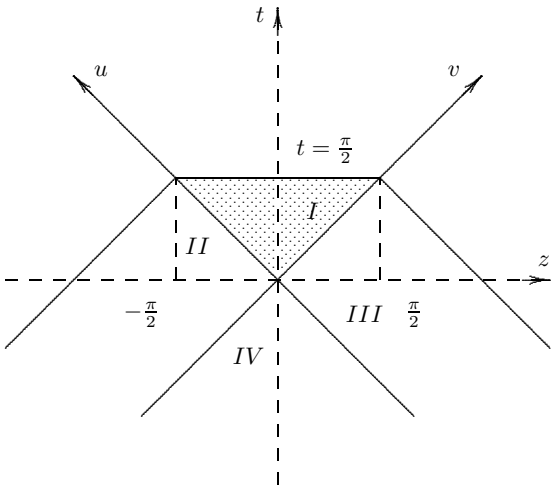


*Fig. 8.1:* The null coordinates $(u, v)$ and the different regions they induce.

tend to zero with $u + v \to \pi/2$, and the the surface $u + v = \pi/2$ corresponds to the Schwarzschild singularity $r = 0$. In this case the there is no horizon that shields the singularity [51].

In other words: the Killing-Cauchy horizon at $u + v = \pi/2$ of a colliding-wave solution with $\sigma = 1$ is merely a coordinate singularity (isometric to the event horizon of a Schwarzschild black hole), whereas the singularity at $u + v = \pi/2$ of a colliding-wave solution with $\sigma = -1$ is a physical singularity (isometric to the Schwarzschild singularity).

## 8.2 Refraction index analysis of the effective optical medium

Let us apply the optical medium analogy developed in Chapter 4 to the Ferrari-Ibañez metric (8.3). The associated effective electric and magnetic permeability tensors (4.4) are given by

$$\epsilon_{ab} \;=\; \mu_{ab} = \mathrm{diag}\left[\epsilon_1, \epsilon_2, \epsilon_3\right] \,, \tag{8.11}$$

with

$$\epsilon_1 = \frac{1}{\epsilon_2} = \frac{\cos^2 z}{\epsilon_3} = \cos z \sqrt{\frac{F_+^3(t)}{F_-(t)}} \,. \tag{8.12}$$

The general definition of the refraction index (4.15) then yields

$$n = \sqrt{\frac{\epsilon_3}{\epsilon_1 e_1^2 + \epsilon_2 e_2^2 + \epsilon_3 e_3^2}}\,, \tag{8.13}$$

where $e_a$ are the components of the spatial unit vector $\mathbf{e}$ of the photon direction; see (4.12).

The above relation (8.13) can be further specified for the cases of photons propagating along the $x$ axis ($\mathbf{e} = (1,0,0)$, $n_x = \sqrt{\epsilon_2\epsilon_3}$), the $y$ axis ($\mathbf{e} = (0,1,0)$, $n_y = \sqrt{\epsilon_1\epsilon_3}$) and the $z$ axis ($\mathbf{e} = (0,0,1)$, $n_z = 1$) only, highlighting the anisotropic properties of the equivalent medium. In terms of the metric functions, region I we find

$$n_x = \sqrt{\frac{F_-(t)}{F_+^3(t)}}\,, \quad n_y = \cos z\,, \quad n_z = 1\,, \tag{8.14}$$

and

$$\epsilon_1 = \frac{n_y}{n_x} = \frac{1}{\epsilon_2}\,, \qquad \epsilon_3 = n_x n_y\,, \tag{8.15}$$

so that the equivalent medium associated with the background metric is homogeneous and optically active along the $x$axis, while along the $y$ axis it is inhomogeneous.

In the collision region, for fixed values of $t$ and $z$ it is $n_x < 1$ if $\sigma = 1$ and $n_x > 1$ if $\sigma = -1$, whereas $n_y < 1$ for both choices of $\sigma$. Hence it follows that for a singularity-developing metric ($\sigma = -1$) the $x$ and $y$ axes are naturally defined as the subluminal and superluminal directions of light propagation, respectively. In particular, the refraction index $n_x$ diverges while approaching the singularity, so that the associated effective medium becomes increasingly opaque in this limit. In the case where the solution has a horizon ($\sigma = 1$), both axes are instead associated with superluminal light propagation, and the refraction index $n_x$ for photons propagating along the $x$ axis goes to zero as the horizon is approached. The possibility of a photon's coordinate speed becoming greater than the speed of light in vacuum is a very interesting effect which may also have a counterpart in experiments. Current technologies allow for the construction nonlinear optical materials (or "metamaterials")

[55] with refraction indices that are, in general, time-dependent and may be very low (less than 1) or even negative. Therefore, in principle, one can arrange for an analogue material of the colliding gravitational wave spacetime under consideration (endowed with the optical properties discussed above) and compare the geometrization of physical interactions with experimental data.

As shown in equation (8.8), the single wave regions II and III are described by the same line element as in equation (8.6), but with metric components depending only on either $u$ or $v$, respectively. Therefore, we find

$$n_x = \sqrt{\frac{F_-(u)}{F_+^3(u)}}\,, \quad n_y = \cos u\,, \quad n_z = 1\,, \tag{8.16}$$

and

$$n_x = \sqrt{\frac{F_-(v)}{F_+^3(v)}}\,, \quad n_y = \cos v\,, \quad n_z = 1\,, \tag{8.17}$$

respectively, with $u$ and $v$ related to $t$ and $z$ by (8.5). The equivalent media in the two single wave regions are thus inhomogeneous and optically active along both $x$ and $y$ axis [45].

Finally, in the flat spacetime region IV we have simply $\epsilon_1 = \epsilon_2 = \epsilon_3 = 1$, so that $n = n_x = n_y = n_z = 1$.

It is also interesting to study the behavior of the effective refraction index (8.13) as a function of $z$ for a given direction on the wave front, i.e., $e_3 = 0$, and selected values of $t$ before and after the collision. At a fixed time $t < 0$, the two waves are confined in the two regions $t - \pi \leq z \leq t$ (progressive wave) and $-t \leq z \leq \pi - t$ (regressive wave), respectively. The spacetime is flat for $-t \leq z \leq t$. At a fixed time $t > 0$, for $t - \pi \leq z \leq -t$ there is the still incoming first wave, whereas for $t \leq z \leq \pi - t$ there is the still incoming second wave. For $-t \leq z \leq t$ the two waves interact. As the time $t$ tends to $\pi/2$, the region of interaction expands and reaches its maximum for $t = \pi/2$ when the singularity is created between $-\pi/2 \leq z \leq \pi/2$. The above situation is summarized and illustrated in Figs. 8.2 and 8.3. The photon direction on the wave front has been chosen as $e_1 = 1/\sqrt{2} = e_2$, so

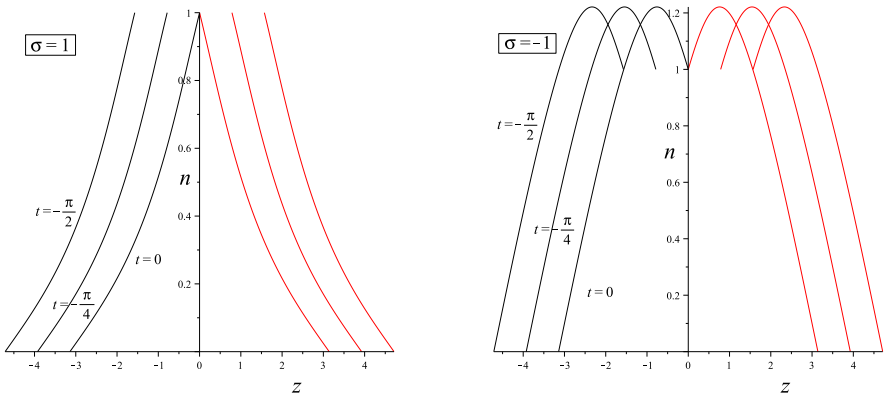


(a) (b)

*Fig. 8.2:* The behavior of the refraction index (8.13) is shown as a function of $z$ for a given direction on the wave front $e_1 = 1/\sqrt{2} = e_2$, $e_3 = 0$ for different values of $t = [-\pi/2, -\pi/4, 0]$ before collision (and at the time of collision $t = 0$) in both cases $\sigma = \pm 1$.

that the refraction index (8.13) becomes

$$n = \sqrt{\frac{2\epsilon_2\epsilon_3}{1+\epsilon_2}} = n_x n_y \sqrt{\frac{2}{n_x^2 + n_y^2}}\,, \tag{8.18}$$

or, equivalently,

$$\frac{1}{n^2} = \frac{1}{2}\left(\frac{1}{n_x^2} + \frac{1}{n_y^2}\right)\,. \tag{8.19}$$

It turns out that in the case of solutions with horizon $n$ assumes practically constant values all over the interaction region after collision.

## 8.3 Light propagation in all spacetime regions of the extended metric

Let us study how an incoming light ray propagating along a straight line in the flat spacetime region IV is deflected when passing through the single wave region II (or to its symmetric counterpart, Region III) and finally enters the collision region I before reaching the singularity.

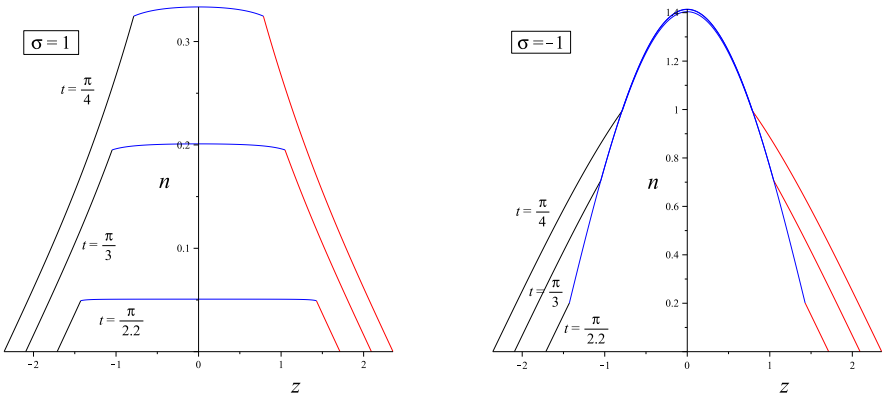


(a) (b)

*Fig. 8.3:* The behavior of the refraction index (8.13) is shown as a function of $z$ for a given direction on the wave front $e_1 = 1/\sqrt{2} = e_2$, $e_3 = 0$ for different values of $t = [\pi/4, \pi/3, \pi/2.2]$ after collision in both cases $\sigma = \pm 1$.

We solve the null geodesic equations in every spacetime region and impose proper matching conditions at the boundaries so that the photon momentum $P^\alpha = \mathrm{d}x^\alpha/\mathrm{d}\lambda$ is continuous everywhere. We limit our analysis to the $t - z$ (or, equivalently, $u - v$) plane, where the most important differences between the horizon-forming and singularity-developing solutions appear, especially concerning the behavior of the geodesics approaching the hypersurface $t = \pi/2$ (or $u + v = \pi/2$).

The constant photon four-momentum $P_{IV}$ of the incoming photon (Region IV) can be parametrized in terms of the conserved specific momenta $p_v$, $p_x$ and $p_y$ associated with the three Killing vectors $\partial_v$, $\partial_x$, $\partial_y$ as

$$\begin{aligned} P_{IV} &= -\frac{p_v}{2}\left(\partial_u + \frac{p_\perp^2}{p_v^2}\partial_v\right) + p_\perp \\ &= -\frac{p_v}{2}\left(1 + \frac{p_\perp^2}{p_v^2}\right)\partial_t + p_\perp - \frac{p_v}{2}\left(-1 + \frac{p_\perp^2}{p_v^2}\right)\partial_z\,, \end{aligned} \tag{8.20}$$

where $p_\perp = p_x\partial_x + p_y\partial_y$ (with $p_\perp^2 = p_x^2 + p_y^2$ using the flat spacetime notation for convenience) and $p_v < 0$ to ensure that $P_{IV}$ is future-pointing. We have made use of the relations $\partial_t = (\partial_u + \partial_v)/2$ and $\partial_z = (\partial_v - \partial_u)/2$, as follows from (8.5).

In the single $u-$wave region II the conservation of $p_v$, $p_x$ and $p_y$ still holds ($\partial_v$, $\partial_x$, $\partial_y$ are Killing fields), permitting the parametrization of the geodesic photon four-momentum as

$$\begin{aligned} P_{II} &= -\frac{p_v}{2F_+^2(u)}\left[\partial_u + \frac{1}{p_v^2}\left(p_x^2\frac{F_+^3(u)}{F_-(u)} + \frac{p_y^2}{\cos^2 u}\right)\partial_v\right] \\ &\quad + p_x\frac{F_+(u)}{F_-(u)}\partial_x + \frac{p_y}{\cos^2 u F_+^2(u)}\partial_y\,. \end{aligned} \tag{8.21}$$

(In the single $v-$wave region III, the Killing fields are $\partial_u$, $\partial_x$, $\partial_y$ instead.)

In the collision region I only $\partial_x$ and $\partial_y$ are Killing vectors, implying that only the specific momenta $p_x$ and $p_y$ are conserved. Nevertheless, there exists a further constant of motion (here denoted by $K$) related to the separation of the Hamilton-Jacobi equation [54]. Even though the metric (8.6) depends on both $u$ and $v$, we still find two additional Killing vectors

$$\xi^{\,\mathrm{I}}_{(3)} = \cos y\ \partial_z + \sin y\ \tan z\ \partial_y \tag{8.22}$$

$$\xi^{\,\mathrm{I}}_{(4)} = -\sin y\ \partial_z + \cos y\ \tan z\ \partial_y \tag{8.23}$$

The third constant that is needed to fully parametrize the equations of motion is denoted by $K$ and given by

$$K = \sqrt{K_3^2 + K_4^2}\,, \tag{8.24}$$

where the constants $K_1 = P\cdot\xi^{\,\mathrm{I}}_{(3)}$ and $K_2 = U\cdot\xi^{\,\mathrm{I}}_{(4)}$ are associated with the Killing vectors (8.22). The photon four-momentum in the collision region turn out to be given by

$$\begin{aligned} P_I &= \frac{1}{F_+^2(t)}\sqrt{p_x^2\frac{F_+^3(t)}{F_-(t)} + p_y^2 + K^2}\partial_t \pm \frac{1}{F_+^2(t)}\sqrt{K^2 - p_y^2\,\tan^2 z}\partial_z \\ &\quad + p_x\,\frac{F_+(t)}{F_-(t)}\partial_x + \frac{p_y}{\cos^2 z\,F_+^2(t)}\partial_y\,, \end{aligned} \tag{8.25}$$

where the $\pm$ signs account for orbits with either increasing $(+)$ or decreasing $(-)$ values of $z$.

| | region IV | | Region II | | Region I | | Region III | |
|---|---|---|---|---|---|---|---|---|
| | coord. | const. | coord. | const. | coord. | const. | coord. | const. |
| $\xi_{(1)}$ | $x$ | $p_x$ | $x$ | $p_x$ | $x$ | $p_x$ | $x$ | $p_x$ |
| $\xi_{(2)}$ | $y$ | $p_y$ | $y$ | $p_y$ | $y$ | $p_y$ | $y$ | $p_y$ |
| $\xi_{(3)}$ | $v$ | $p_v$ | $v$ | $p_v$ | $-$ | $K_3$ | $u$ | $p_u$ |
| $\xi_{(4)}$ | $-$ | $-$ | $-$ | $-$ | $-$ | $K_4$ | $-$ | $-$ |

*Tab. 8.1: The Killing vectors in the different spacetime regions and the associated coordinates and constants there.*

The Killing symmetries for all spacetime regions are summarized in Table 1.

In order to extend a geodesic from Region II to Region I, the value of $K$ must be selected properly, so that the continuity of the $t$ and $z$ (or, equivalently, the $u$ and $v$) components of the four-momentum is guaranteed at the boundary II-I, where $v = 0$. The features of motion are very different depending on whether the four-momentum $P_{IV}$ of the incoming photon has a nonvanishing component along the $y$ direction or not.

Let us consider first the case $p_y = 0$. At the boundary II-I where $t = u$ (hereafter, we suppress the dependence of the various functions on $u$, for a simplified notation) we have

$$\begin{aligned} P_{II} &= -\frac{p_v}{2F_+^2}\left(\partial_u + \frac{p_x^2}{n_x^2 p_v^2}\partial_v\right) + \frac{p_x}{n_x^2 F_+^2}\partial_x\,, \\ P_I &= \frac{1}{2F_+^2}\left(\sqrt{\frac{p_x^2}{n_x^2} + K^2} - K\right)\partial_u \\ &\quad + \frac{1}{2F_+^2}\left(\sqrt{\frac{p_x^2}{n_x^2} + K^2} + K\right)\partial_v + \frac{p_x}{n_x^2 F_+^2}\partial_x\,, \end{aligned} \tag{8.26}$$

where the refraction index along the $x$ axis, $n_x$, follows from (8.13) with $\mathbf{e} = (1, 0, 0)$ and it is such that $F_- = n_x^2 F_+^3$. Note that here we use $\pm\sqrt{K^2} = K$, permitting both sign choices of $K$. It is easy to recognize that the $x$ components already agree, whereas continuity for the $u$ and $v$ components

implies

$$\begin{aligned} -p_v &= \sqrt{\frac{p_x^2}{n_x^2} + K^2} - K\,, \\ -\frac{p_x^2}{p_v n_x^2} &= \sqrt{\frac{p_x^2}{n_x^2} + K^2} + K\,, \end{aligned} \tag{8.27}$$

and both equations are satisfied by

$$K = \frac{p_v}{2} - \frac{p_x^2}{2p_v n_x^2}\,. \tag{8.28}$$

The previous equation then yields the proper value of $K$ allowing for the geodesic path to be continued in Region I. Integrating the geodesic equations in Region II for a given set of initial conditions and selected values of the constants $p_v$ and $p_x$ identifies the value of $u$ at which the photon enters the interaction region.

An example for the integration of the orbits for $p_y = 0$ is shown in Fig. 8.4.

The behavior of null geodesics turns out to be different depending on whether the solution is horizon-forming or singularity-developing. In the former case the motion has a global homogeneity for all values of $p_v$. Only positive values of $K$ are allowed. The limit $p_v \to -\infty$ gives the so-called fold singularities at the points of the horizon $(u = \pi/2, v = 0)$ and $(u = 0, v = \pi/2)$, already discussed by Dorca and Verdaguer [54]. The presence of such singularities is the origin of an accumulation of the null geodesics on the surface $v = 0$ for $u \to \pi/2$, as shown in Fig. 8.4 (a). As follows from the analysis of the refraction index, the geodesics approach the horizon always perpendicularly. In fact, let us examine the slope of the trajectories

$$\frac{\mathrm{d}u}{\mathrm{d}v} = \frac{\sqrt{\frac{p_x^2}{n_x^2} + K^2} - K}{\sqrt{\frac{p_x^2}{n_x^2} + K^2} + K}\,, \tag{8.29}$$

by using (8.26), as the horizon is approached. Notice that the family of

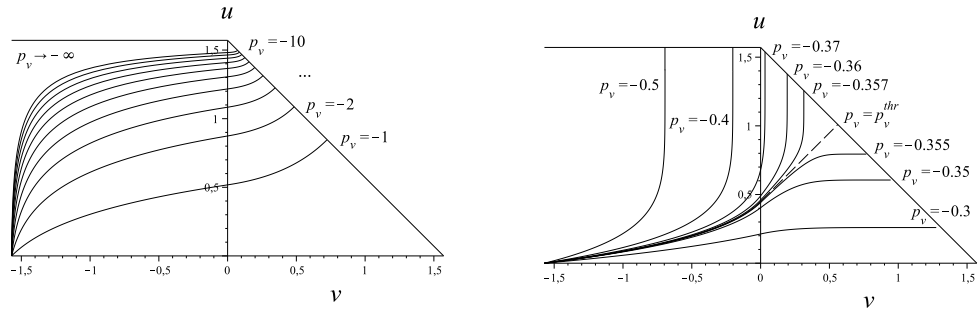


(a) (b)

*Fig. 8.4:* The features of geodesic motion in the $u - v$ plane are shown in panels (a) and (b) in the case $\sigma = 1$ (horizon) and $\sigma = -1$ (singularity), respectively. The geodesics equations $\mathrm{d}u/\mathrm{d}\lambda = P^u$ and $\mathrm{d}v/\mathrm{d}\lambda = P^v$ have been integrated in the single $u$-wave region II with initial conditions $u(0) = 0$, $v(0) = -\pi/2$ and the choice of parameters $p_x = 1$, $p_y = 0$. The curves correspond to different values of $p_v$. The numerical integration of the orbits has then been continued in the collision region I by imposing the matching at the boundary II-I, i.e., $v = 0$. For $\sigma = 1$ the point ($u = \pi/2$, $v = 0$) represents an accumulation point for the null geodesics leading to a fold singularity. The critical value of $p_v$ discriminating among the two kinds of orbits in the case $\sigma = -1$ is $p_v^{\mathrm{thr}} \approx -0.35578$.

curves in the $u - v$ plane which are solutions of (8.29) are symmetric with respect to the symmetry curve $K = 0$. In fact, if $K \to -K$ then $u \leftrightarrow v$. Moreover, the symmetry curve represents then an attractor (when $\sigma = 1$) or a repeller (when $\sigma = -1$) for the other curves of the family, according to the chosen metric (see Fig. 8.5).

In this limit, i.e., $t = u+v \to \pi/2$, the refraction index behaves as $n_x \to 0$, implying that

$$\left.\frac{\mathrm{d}u}{\mathrm{d}v}\right|_{t\to\pi/2} \to 1\,. \tag{8.30}$$

In the case of solutions with a singularity the geodesics exhibit a typical twofold behavior for $p_y = 0$ (see Fig. 8.4 (b)). This is due to the existence of a critical value of $p_v$ in the single wave region, implying $K = 0$ for a given choice of $p_x$ as well as initial conditions. We thus identify those geodesics that propagate through the collision region at a constant value of $z$, irrespective of the presence of the waves, i.e., see (8.28),

$$p_v^{\mathrm{thr}} = -\frac{|p_x|}{n_x}\,. \tag{8.31}$$

In contrast to the case of the horizon-forming solution, every value of $K$ is now allowed. The null geodesics approach the singularity in a way which depends on the sign of $K$. In fact, since here the refraction index $n_x \to \infty$, the slope of the trajectories (8.29) in the limit $t \to \pi/2$ is

$$\left.\frac{\mathrm{d}u}{\mathrm{d}v}\right|_{t\to\pi/2} \to \frac{|K| - K}{|K| + K}\,. \tag{8.32}$$

Therefore, if $K > 0$ (i.e., the value of $p_v$ of the incoming photon is greater than the threshold value (8.31)), the slope turns out to be $\mathrm{d}u/\mathrm{d}v\big|_{t\to\pi/2} \to 0$ (the orbit is parallel to the $v$ axis). On the other hand, if $K < 0$ (i.e., $p_v < p_v^{\mathrm{thr}}$) the slope grows indefinitely, namely $\mathrm{d}u/\mathrm{d}v\big|_{t\to\pi/2} \to \infty$ (the orbit is parallel to the $u$ axis). There also exists a limiting value of $p_v$ below which the photon does not enter the interaction region at all. The case $K = 0$ represents a separatrix, in the sense that in this case the orbit will approach

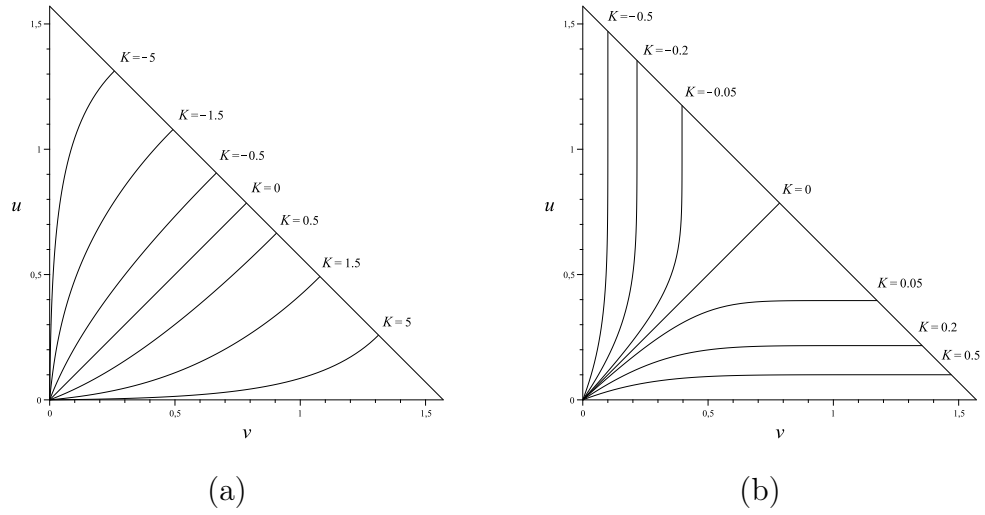


(a) (b)

*Fig. 8.5:* Null geodesics with $p_x = 1$, $p_y = 0$ entering the interaction region from the origin for both (a) horizon-forming ($\sigma = 1$) and (b) singularity-developing ($\sigma = -1$) solutions. The curves correspond to different values of $K$. If $p_y \neq 0$, the situation is similar to panel (a) in both cases. This figure elucidates the property of the curve $K = 0$ of being an attractor or a repeller for other curves in the same family associated with values $K \neq 0$, according to the considered type of background solution. In the case of horizon-forming metric the plot shows in fact a focusing effect around the symmetry curve for $K = 0$; in the singularity forming metric instead we have a defocusing effect around the same curve.

the singularity perpendicularly at a fixed value of $z$, as discussed above.

The different behavior of null orbits approaching the hypersurface $t = \pi/2$ for either horizon-forming or singularity-developing metrics is even more evident if the incoming photon enters the collision region directly from the flat spacetime region IV without passing through the single wave regions, i.e., at the origin $u = 0 = v$, as shown in Fig. 8.5. In this case there is no restriction on the values of $K$, because no matching conditions are required. The constant $K$ can be used to parametrize the orbits for fixed values of $p_x$.

A similar discussion can be made in the case of nonvanishing $p_y \neq 0$ for the incoming photon. The continuity conditions at the boundary II-I for the

momentum components now imply

$$\begin{aligned} -p_v &= \sqrt{\frac{p_x^2}{n_x^2}+p_y^2+K^2}\mp\sqrt{K^2+p_y^2-\frac{p_y^2}{n_y^2}}\,, \\ -\frac{1}{p_v}\left(\frac{p_x^2}{n_x^2}+\frac{p_y^2}{n_y^2}\right) &= \sqrt{\frac{p_x^2}{n_x^2}+p_y^2+K^2}\pm\sqrt{K^2+p_y^2-\frac{p_y^2}{n_y^2}}\,, \end{aligned} \tag{8.33}$$

where $n_y=\cos z=\cos u$, as given by (8.13) with $\mathbf{e}=(0,1,0)$. Solving the system of equations (8.33) for $K^2$ gives

$$K^2=\frac{1}{4p_v^2}\left(p_v^2+\frac{p_x^2}{n_x^2}+\frac{p_y^2}{n_y^2}\right)^2-\frac{p_x^2}{n_x^2}-p_y^2\,. \tag{8.34}$$

Back-substitution into (8.33) implies that the upper sign only is allowed in order to fulfill the matching conditions for both cases $\sigma=\pm1$, i.e., if $p_y\neq0$ only those orbits of photons having a four-momentum (8.25) with a positive $z$ component can be continued across the boundary II-I. The threshold disappears and the geodesic motion exhibits a common behavior for both horizon-forming and singularity-developing solutions, including the way to reach the hypersurface $t=\pi/2$.

This peculiar asymmetry characterizing the behavior of null geodesics depending on the presence/absence of a $y$ component in the incoming four-momentum can be associated with a different role played by the $x$ and $y$ coordinates spanning the surface of the wavefront in these (Petrov-type D) spacetimes, as discussed in Ref. [56] in the case of timelike geodesics.

The case $p_y\neq0$ is so different from $p_y=0$ because of a sort of "broken symmetry" between $x$ and $y$ coordinates, which is associated with the plane symmetry of these (Petrov type D) spacetimes.

In vacuum spacetimes a Killing vector field $\xi$ can be considered as a vector potential generating an electromagnetic field, the so-called Papapetrou field $F$ [57], which satisfies Maxwell's equations in the absence of electromagnetic sources. The Papapetrou field associated with the Killing vector field $\xi_{(1)}=\partial_x$, namely

$$F_{\alpha\beta}=\xi_{(1)\alpha;\beta}\,, \tag{8.35}$$

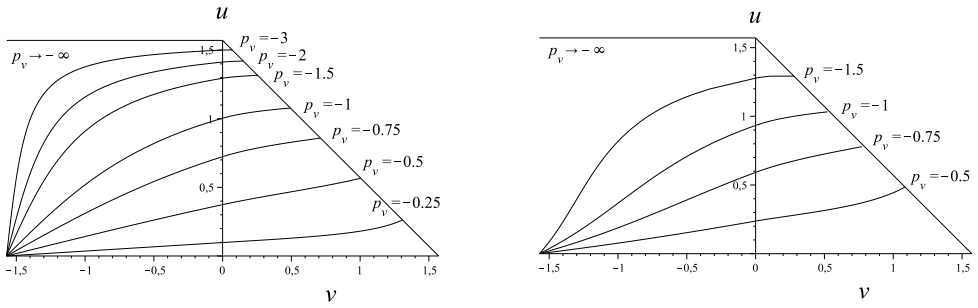


(a) (b)

*Fig. 8.6:* The typical behavior of null geodesics with $p_y \neq 0$ in shown for both kinds of solutions ($\sigma = \pm 1$). The choice of initial conditions in the single $u-$wave region II is the same as in Fig. 8.4, whereas the parameters $p_x$ and $p_y$ have been set to $p_x = 0$, $p_y = 1$ in the case of a horizon-forming metric shown in panel (a) and to $p_x = 1$, $p_y = 1$ in the case of a singularity-developing metric shown in panel (b). The curves correspond to different values of $p_v$. The fold singularity at the point ($u = \pi/2$, $v = 0$) arises for $p_v \to -\infty$ in both cases.

has the two independent principal null directions [56]

$$l = \frac{1}{2\,\cos t}\left[\partial_t + \frac{(1+\sigma\sin t)^2}{\cos t}\,\partial_x\right]$$
$$n = \frac{\cos t}{(1+\sigma\sin t)^2}\,\partial_t - \partial_x\ , \tag{8.36}$$

which are affinely parametrized and normalized so that $l\cdot n = -1$. It is evident that the Killing vector $\xi_{(1)}$ is aligned with the 2-plane that is spanned by the principal null directions of the generated Papapetrou field. This property distinguishes the Killing vector $\xi_{(1)}$ from the one associated with $y$, $\xi_{(2)} = \partial_y$, and leads to a difference between the $x$ and $y$ coordinates in the metric (at least from a purely geometrical point of view).

An example of numerical integration of the orbits with $p_y \neq 0$ is shown in Fig. 8.6.

## 8.4 Closed rectangular paths on the wave front

Since we have chosen the wave to propagate along the $z$ axis, optical effects in that direction turn out to be trivial, as is evident also from the resulting effective refraction index along such a direction, $n_z = 1$. We want to investigate the optical properties of the equivalent medium on the wave front, i.e. on the $x-y$ plane. To this end, let us imagine a square optical path, centered at the origin of the $x-y$ plane, and let $L$ be the length of each side, obtained for instance by using optical guides. Photons moving along the $x$ direction will travel the time $T_x$ along each side of the square which is parallel to the $x$ axis, such that

$$\int_0^{T_x} \frac{\mathrm{d}t}{n_x(t)} = L \tag{8.37}$$

and the time $T_y$

$$T_y = L n_y(z) = L \cos z \tag{8.38}$$

along each side of the square which is parallel to the $y$ axis. Solving for $T_x$, equation (8.37) then gives

$$T_x = \sigma \arcsin \left[ 2\mathrm{LambertW}\left( -\frac{1}{2} e^{-\frac{1+\sigma L}{2}} \right) + 1 \right] . \tag{8.39}$$

where $W(\xi)$ denotes the Lambert $W$ function, i.e. the special function satisfying the equation $W(\xi)e^{W(\xi)} = \xi$. It has an infinite number of solutions for each (non-zero) value of $\xi$, i.e., it has an infinite number of branches. Let us denote by $W_k(\xi)$ the $k-$branch of the Lambert $W$ function, where $k$ is any non-zero integer [58]. If the variable $\xi$ is real, then there are two possible real values of $W(\xi)$ in the interval $-1/e \leq \xi < 0$. The branch satisfying $W(\xi) \geq -1$ is denoted by $W_0(\xi)$ and is referred to as the principal branch of the $W$ function, whereas the branch satisfying $W(\xi) \leq -1$ is denoted by $W_{-1}(\xi)$. The specification of $L$ selects then the branch.

A full path will then correspond to the elapsed time

$$\Delta T = 2T_x + 2T_y . \tag{8.40}$$

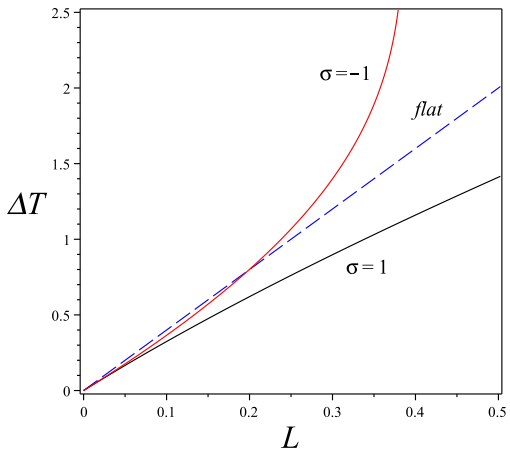


*Fig. 8.7:* The elapsed time corresponding to photons making a square path on the wave front in the collision region (for horizon-forming as well as singularity-developing colliding gravitational waves) is plotted as a function of the length of the square side $L$. Here we have set $z = \pi/4$, but the behavior is similar for a different choice of $z$. The case of a flat spacetime is also shown for comparison.

Its behavior as a function of $L$ for a fixed value of $z$ is shown in Fig. 8.7. The explicit value of $\Delta T$ strongly depends on the spacetime region where it is evaluated. In the flat spacetime, one would simply have

$$\Delta T_{(\text{flat})} = 4L\,. \tag{8.41}$$

Note that $L$ in equations (8.37)–(8.41) is a dimensionless quantity just as $T_x$ and $T_y$. Apart from the manifest difference from the flat spacetime case, the measurement of $\Delta T$ by a simple interferometric device would allow us to clearly distinguish among the horizon-forming and the singularity-forming metrics and would also provide information about the distinct spacetime region where it is evaluated, i.e., inbound flat, single wave or collision region.

# 9. SUMMARY

We consider the propagation of electromagnetic waves and massive neutral test particles in the background of a radiation field that is generated by either an exact gravitational plane wave with a single (+) polarization state or an exact electromagnetic wave in the framework of general relativity. Both types of wave are chosen to be traveling in the positive $z$ direction, orthogonal to the symmetry planes. The spacetime metric of the radiation field is generally described by

$$\mathrm{d}s^2 = -2\mathrm{d}u\mathrm{d}v + F(u)^2\mathrm{d}x^2 + G(u)^2\mathrm{d}y^2\,, \tag{9.1}$$

where the null coordinates $u$ and $v$ are related to the standard temporal and spatial coordinates by $u = (t-z)/\sqrt{2}$ and $v = (t+z)/\sqrt{2}$, and where $\partial_v$, $\partial_x$, $\partial_y$ are all Killing vectors. The metric functions are given by $F = \cos(b_{gw}u)$, $G = \cosh(b_{gw}u)$ in the case of a gravitational wave, or by $F = G = \cos(b_{em}u)$ in the case of an electromagnetic wave. The parameter $b$ is the frequency of the wave under consideration. Let the radiation field be sandwiched between two flat spacetime regions $u \in (-\infty, 0)\cup(u_1, \infty)$ and let us extend the metric (9.1) to all values of $u$ by requiring $C^1$ regularity conditions at the boundary, i.e., $F = G = 1$ in the in zone and $F = \alpha + \beta u$, $G = \gamma + \delta u$ in the out zone. Even though the metric functions in the out zone do not have the value 1 associated with flat coordinates, standard Cartesian coordinates can be restored by a specific coordinate transformation $(u, v, x, y) \to (U, V, X, Y)$.

We first considered the propagation of electromagnetic waves in the radiation field of an exact gravitational plane wave, obtaining null geodesics of the photons in all spacetime regions. Solving Maxwell's equation for the vector potential, we found that the electromagnetic field is a plane wave in the in zone, whereas the nonsingular field emerging after the interaction is not exactly a plane wave but is dominated by plane wave behavior with the wave

vector aligned with the null geodesics of the background. We have been able to identify the physical effects of the exact gravitational wave on the electromagnetic field by choosing a suitable photon round trip in a Michelson interferometer, with the phase shift between the ingoing electromagnetic wave and the dominant part of the outgoing field as the most significant interferometer response. In addition, we have calculated the change of the polarization vector, as well as the angular deflection and delay of photon beams making the round trip.

We then investigated the interaction of massive particles with radiation fields generated by either exact gravitational or exact electromagnetic waves. In the case of a gravitational wave, the test particle motion is geodesic. The incoming particle's conserved specific momenta $p_v$, $p_x$, $p_y$ (associated with the Killing vectors) allow the complete integration of the geodesic equations in all spacetime regions. In the case of an electromagnetic wave, the spacetime region of interaction is nonvacuum, resulting in an accelerated motion of test particles. Following the approach of Poynting and Robertson, the particles are assumed to interact with the radiation field by absorbing and re-emitting radiation, causing a drag force that deflects them from geodesic motion. (Explicitly, the interaction is modeled by a force term entering the equations of motion proportional to the four-momentum density of radiation observed in the particle's rest frame.)
The features of the scattering in both cases have been analyzed and compared by computing the boost relating the initial four-momentum of the particle and the four-momentum with which it emerges from the interaction. (The final state has been obtained by imposing matching conditions on the particle's four-momentum and trajectory at the boundary between the interaction region and the flat out zone.) We find that in the gravitational wave case the change of momentum in the transverse $x - y$ plane involves a rotation due to the deformation of the plane wave directions by the wave, while in the electromagnetic wave case only an overall scaling is involved. For the changes of momentum in the longitudinal $u - v$ plane, the gravitational case lacks a component along $\partial_u$ because the motion is geodesic and $\partial_v$ is a Killing vector field, while in the electromagnetic case a component along $\partial_u$ exists because

the force responsible for the change in momentum itself has a covariant component along $\partial_v$. Thus the scattering of massive particles by radiation fields of different kinds is strongly influenced by the nature of the interaction, in principle leading to detectable observational consequences.

We have employed the optical medium analogy to study light propagation in the radiation fields introduced above. In the optical medium analogy, an electromagnetic field in any gravitational background associated with the metric (9.1) can be thought of as propagating in the presence of a medium whose properties are constructed by the metric tensor. In particular we have analyzed the deflection of light rays by a radiation field in terms of the associated optical properties of the equivalent optical medium. (Here we have treated the scattering process as a series of successive refractions through media with approximately constant refraction indices and were thus able to adopt standard tools of ordinary wave optics.) We have found that the most relevant physics involves the transverse $x-y$ plane: there the equivalent medium of a gravitational wave is inhomogeneous and anisotropic, whereas that of an electromagnetic wave is inhomogeneous but isotropic. In both cases the medium is optically active in the sense that the refraction index depends on time. Moreover, there exist directions in which the effective refraction index of the medium is $< 1$ (so that the coordinate components of the velocity of light become $> 1$). This realizes an interesting and novel point of view for looking at the photon scattering by electromagnetic as well as gravitational waves in the exact theory of general relativity, which may also have a counterpart in experiments. For instance, by means of nonlinear optical materials, one can arrange for an analogue material of the above mentioned radiation field spacetimes and compare the geometrization of physical interactions with experimental data.

Finally we have applied the optical medium analogy to light propagation in colliding gravitational wave spacetimes, namely those characterized by the Ferrari-Ibañez-metric where the collision of two exact gravitational waves with a single polarization state (propagating along the same direction but in opposite senses) leads to the formation of either a horizon or a singularity, depending on the properties of the metric. This particular colliding

gravitational wave spacetime was chosen for its mathematical simplicity and the possibility to easily switch between the horizon-forming and singularity-developing solution (by changing the signs of certain metric functions). Standard tools of ordinary wave optics were used to study the properties of the equivalent optical medium, allowing for a simple discussion of some interesting physical effects (despite the complexity of the nonlinear interaction upon collision).

In the plane transverse to the direction of propagation of the gravitational waves, the equivalent optical medium of the interaction region was found to be homogeneous and optically active along one axis (optically active in the sense that the associated refraction index is time-dependent), but inhomogeneous and optically inactive along the other. An analysis of the effective refraction index of the medium along the direction of gravitational wave propagation at different times (before and after the time of collision) illustrated the different optical properties of the equivalent media in the two scenarios with either a horizon or a singularity.

The continuation of null geodesic orbits from one of the single-wave regions into the collision region was discussed in detail. The distinction between the horizon-forming and singularity-developing backgrounds was characterized by the different behavior of null orbits approaching the hypersurface where the horizon or the singularity is located, with the most important differences appearing in the plane of the direction of the gravitational waves. The different behavior for the two cases with either horizon or singularity was also found to depend on the properties of the incoming photons' geodesic motion in the flat spacetime region before the arrival of the gravitational waves.

Furthermore it was illustrated how the optical properties of the medium (namely the time-dependency of the refraction index along one coordinate axis) would affect the elapsed time for photons traveling a closed rectangular path in an optical guide on the wave front in the collision region, and how an interferometric could potentially provide information about the spacetime region under consideration and the nature of the nonlinear interaction.

# 10. LIST OF PUBLICATIONS

- Donato Bini, Pierluigi Fortini, Maria Haney, and Antonello Ortolan
  *Electromagnetic waves in gravitational wave spacetimes*
  Class. Quantum Grav. **28**, 235007 (2011)

- Donato Bini, Andrea Geralico, Maria Haney, and Robert T. Jantzen
  *Scattering of particles by radiation fields: A comparative scenario*
  Phys. Rev. D **86**, 064016 (2012)

- Donato Bini, Pierluigi Fortini, Andrea Geralico, Maria Haney, and Antonello Ortolan
  *Light scattering by radiation fields: The optical medium analogy*
  Europhys. Lett. **102**, 20006 (2013)

- Donato Bini, Andrea Geralico, and Maria Haney
  *Refraction index analysis of light propagation in a colliding gravitational wave spacetime*
  submitted for publication in Gen. Relat. Grav.

# ACKNOWLEDGMENTS

For their invaluable support and advice throughout my time as a PhD student at Università di Roma "Sapienza" I would like to thank

Prof. Remo Ruffini,
Donato Bini,
Andrea Geralico, Antonello Ortolan and Bob Jantzen,
everyone at ICRAnet in Rome and Pescara, and
Prof. Gerhard Schäfer and Achamveedu Gopakumar.

# BIBLIOGRAPHY


[1] Griffiths J. B., *Colliding Plane Waves in General Relativity* (Clarendon Press, Oxford, 1991).

[2] Tsagas C. G., *Phys. Rev. D* **84**, 043524 (2011).

[3] Misner C. W., Thorne K. S., and Wheeler J. A., *Gravitation* (W.H. Freeman, San Francisco, 1973).

[4] Rindler W., *Relativity: Special, General, and Cosmological* (Oxford University Press, Oxford, 2001).

[5] Stephani H., Kramer D., MacCallum M., Hoenselaers C., and Herlt E., *Exact Solutions of Einstein's Field Equations* 2nd ed. (Cambridge University Press, Cambridge, 2003).

[6] Belinski V., and Verdaguer E., *Gravitational Solitons* (Cambridge University Press, Cambridge, 2005).

[7] Maggiore M., *Gravitational Waves Vol. 1: Theory and Experiments* (Oxford University Press, Oxford, 2007).

[8] Brinkmann H. W., *Math. Ann.* **18**, 119 (1925).

[9] Penrose R., in *General Relativity*, ed. O'Raifeartaigh L. (Clarendon Press, Oxford, 1972).

[10] Podolský J., and Veselý K., *Czech. J. Phys.* **48**, 871 (1998).

[11] Rindler W., *Essential Relativity* (Springer, New York, 1977).

[12] Bondi H., Pirani F. A. E., and Robinson I., *Proc. R. Soc. A* **251**, 519 (1959).

[13] Ehlers J., and Kundt W., *Exact Solutions of the Gravitational Field Equations*, Chap. 2 in *The Theory of Gravitation*, ed. Witten L. (John Wiley & Sons, New York), 49-101 (1962).

[14] Bondi H., and Pirani F. A. E., *Proc. R. Soc.* **421**, 395 (1989).

[15] J. B. Griffiths, *Phys. Lett.* **54A**, 269 (1975).

[16] Poynting J. H., *Phil. Trans. R. Soc. A* **202**, 525 (1904).

[17] Robertson H. P., *Mon. Not. R. Astron. Soc.* **97**, 423 (1937).

[18] Eddington A. S., *The Internal Constitution of Stars* (Cambridge University Press, Cambridge, 1926).

[19] Wyatt S. P., and Whipple F. L., *Astrophys. J.* **111**, 134 (1950).

[20] Guess A. W., *Astrophys. J.* **135**, 855 (1962).

[21] Abramowicz M. A., Ellis G. F. R., and Lanza A., *Astrophys. J.* **361**, 470 (1990).

[22] Bini D., Jantzen R. T., and Stella L., *Class. Quantum Grav.* **26**, 055009 (2009).

[23] Bini D., Geralico A., Jantzen R. T., Semerák O., and Stella L., *Class. Quantum Grav.* **28**, 035008 (2011).

[24] Bini D., Geralico A., Jantzen R. T., and Semerák O., *Class. Quantum Grav.* **28**, 245019 (2011).

[25] Vaidya P. C., *Curr. Sci.* **12**, 183 (1943).

[26] Bini D., Gregoris D., and Rosquist K., *Gen. Relat. Grav.* **44**, 2669 (2012).

[27] Bini D., and Geralico A., *Phys. Rev. D* **85**, 044001 (2012).

[28] De Felice F., *Gen. Rel. Grav.* **2**, 347 (1971).

[29] Mashhoon B., *Phys. Rev. D* **7**, 2807 (1973).

[30] Mashhoon B., *Phys. Rev. D* **10**, 1059 (1974).

[31] Mashhoon B., *Phys. Rev. D* **11**, 2679 (1975).

[32] Mashhoon B., and Grishchuk L. P., *Astrophys. J.* **236**, 990 (1980).

[33] Plebanski J., *Phys. Rev.* **118**, 1396 (1960).

[34] Volkov A. M., Izmest'ev A. A., and Skrotskii G. V., *Zh. Eksp. Teor. Fiz.* **59**, 1254 (1970).

[35] Volkov A. M., Izmest'ev A. A., and Skrotskii G. V., *Sov. Phys. JETP* **32**, 686 (1971).

[36] Finn L., *Phys. Rev. D* **79**, 022002 (2009).

[37] Rakhmanov M., *Class. Quantum Grav.* **26**, 155010 (2009).

[38] Braginsky V. B., Kardashev N. S., Polnarev A. G., and Novikov I. D., *Nuovo Cimento* **105 B**, 1141 (1990).

[39] Bini D., Fortini P., Haney M., and Ortolan A., *Class. Quantum Grav.* **28**, 235007 (2011).

[40] Faraoni V., *Gen. Relat. Grav.* **23**, 583 (1991).

[41] Fortini P., and Ortolan A., *Nuovo Cimento* **106 B**, 101 (1991).

[42] Garriga J., and Verdaguer E., *Phys. Rev. D* **43**, 391 (1991).

[43] Bini D., Geralico A., Haney M., and Jantzen R. T., *Phys. Rev. D* **86**, 064016 (2012).

[44] Griffiths J. B., *Ann. Phys. (N.Y.)* **102**, 388 (1976).

[45] Bini D., Fortini P., Geralico A., Haney M., and Ortolan A., *Europhys. Lett.* **102**, 20006 (2013).

[46] Mashhoon B., *Phys. Lett.* **122A**, 299 (1987).

[47] Hizhnyakov V. V., *Quantum Opt.* **4**, 227 (1992).

[48] Philbin T. G., Kuklewicz C., Robertson S., Hill S., König F., and Leonhardt U., *Science* **319**, 1367 (2008).

[49] Khan K., Penrose R., *Nature (London)* **229**, 185 (1971).

[50] Ferrari V., Ibañez J., *Gen. Relat. Grav.* **19**, 385 (1987).

[51] Ferrari V., and Ibañez J., *Gen. Relat. Grav.* **19**, 405 (1987).

[52] Ferrari V., and Ibañez J., *Proc. R. Soc. Lond. A* **417**, 417 (1988).

[53] Szekeres P., *J. Math. Phys.* **13**, 286 (1972).

[54] Dorca M., and Verdaguer E., *Nucl. Phys. B* **403**, 770 (1993).

[55] Liu Y. M., and Zhang, X., *Chem. Soc. Rev.* **40**, 2494 (2011).

[56] Bini D., Cruciani G., Lunari A., *Class. Quantum Grav.* **20**, 341 (2003).

[57] Fayos F., and C. F. Sopuerta, *Class. Quant. Grav.*, **16**, 2965, (1999).

[58] See e.g. http://mathworld.wolfram.com/LambertW-Function.html